The Pennsylvania State University

The Graduate School

Department Microbiology and Immunology

THE EFFECT OF HPV16 INFECTION ON THE CELLULAR TRANSCRIPTOME AND METHYLOME

A Dissertation in

Biomedical Sciences

by

Sa Do Kang

Submitted in Partial Fulfillment
of the Requirements
for the Degree of

Doctor of Philosophy

May 2019

The dissertation of Sa Do Kang was reviewed and approved* by the following:

Craig Meyers
Distinguished Professor, Department of Microbiology & Immunology
Director of the Training Program in Viruses and Cancer
Dissertation Advisor
Chair of Committee

Neil Christensen
Professor, Department of Pathology
Professor, Department of Microbiology & Immunology

Jianming Hu
Professor, Department of Microbiology & Immunology

Lisa Shantz
Associate Professor, Department of Cellular and Molecular Physiology

Diane Thiboutot
Professor of Dermatology

Ralph Keil
Associate Professor, College of Medicine, Biochemistry and Molecular Biology
Chair, Biomedical Sciences Graduate Program

*Signatures are on file in the Graduate School

ABSTRACT

HPV infection is the world's most common sexually transmitted infection, and can cause various cancers including cervical cancer, anal cancer, penile cancer, and head and neck cancer. Overall, the virus is responsible for approximately 5% of all cancers worldwide, and therefore, its burden on public health and health economics is significant even with the recent introduction of effective vaccines against HPV. For this reason, numerous studies have investigated the epidemiology and biology of HPV infection and how it can lead to tumorigenesis.

Of all the cancers caused by HPV infection, cervical cancer has been at the center of scientific research because of its widespread prevalence and the fact that practically all cases of cervical cancer are attributed to HPV infection. Previously, most studies of global gene expression changes in cervical have focused on the cancerous stages of HPV infection, which is often characterized by integration of the viral genome into the host genome and a subsequent drop in progeny virion production. Therefore, not much is known about global gene expression changes at early pre-neoplastic stages of infection when the virus establishes persistent infection and progeny virions are produced at high levels. In this study we show for the first time, global gene expression changes of early stage HPV16 infection in cervical tissue using 3-dimensional organotypic raft cultures that produce high levels of progeny virions. We used oligonucleotide microarrays to measure global gene expression changes in early passage HPV16-immortalized human cervical keratinocytes, and organotypic raft cultures were used in order to allow the virus to go through its full life-cycle. A total of 649 and 769 genes were at least 1.5-fold upregulated and downregulated, respectively. Gene ontology analysis of upregulated genes identified biological processes that were significantly represented including cell cycle process and DNA metabolism. In contrast, biological processes that were significantly represented with downregulated genes included epidermis development, extracellular matrix disassembly, and regulation of NF-kappaB signaling. Individual genes were selected for validation at the transcriptional and translational levels including UBC, which was central to the protein association network of immune response genes, and top downregulated genes RPTN, SERPINB4, KRT23, and KLK8. In particular, we identified a group of genes that are typically overexpressed in cancerous stages to be significantly downregulated in our model of precancerous infection including KLK8 and SERPINB4. This study shows that persistent and productive infection of cervical keratinocytes with HPV16 significantly affects the expression of genes in various biological pathways including the cell cycle, epidermis development, and immune response. Additionally, opposing trends of gene expression suggests that early (precancerous) stages and cancerous stages of infection are two distinct disease states that may require different therapeutic approaches.

The prevalence of HPV-positive head and neck squamous cell carcinomas (HNSCCs) have been increasing in the past few decades. Interestingly, the overwhelming majority of HPV-positive HNSCCs, which typically present in the oropharyngeal region (tonsils and base of tongue), occur in males and this sex-gap in HNSCC incidence is widening over time. Currently, not much is known about the biology that gives rise to this sex-bias in HPV-positive HNSCCs.

A recently emerging area of genomics research is epigenetics, and in particular, analysis of the methylome. DNA methylation of CpG sites is one of the most abundant forms of epigenetic modifications, and is considered to have great potential in cancer research and therapy development since DNA methylation can be reversed. As with previous studies of global gene expression changes in HPV infection, most previous studies of DNA methylation in HPV infection have focused on the cancerous stages. In this study, we measure methylome changes that occur with productive HPV16 infection in human tonsil tissue using the organotypic raft culture system. In particular, we separated our analysis by sex in order to understand the different patterns of methylation between males and females, and raft tissue samples were harvested at d4, d10, d20 in order to capture different stages of the HPV life-cycle. Bisulfite conversion method was used to analyze the methylome in genomic contexts including CpG islands, shores, and shelves, and promoter, intron, exon, and intergenic regions. Our analysis showed a significant degree of sex-specific methylation patterns throughout the time course including a large number of CpG sites that had methylation patterns in the opposite direction (hypomethylation vs. hypermethylation) between males and females. Of note, the X chromosome in females was consistently hypomethylated over the time course, while the X chromosome was consistently hypermethylated in males. Additionally, analysis of the methylation pattern over the time course showed that the methylome is very dynamic, and there are great numbers of differentially methylated CpG sites that are specific to each time point. This could indicate that the host methylome is greatly affected by the different states of tissue differentiation and/or different stages of the HPV life-cycle. Overall, our study shows that the sex-specific methylomes of HPV16-infected tonsil tissue could be associated with the sex bias in HNSCC incidence.

The risk of developing HPV-associated malignancies is significantly higher in individuals infected with HIV compared to the general population. Although some studies have linked the expression of HIV proteins Tat and GP120 to increased susceptibility to HPV infection, the exact mechanism of increased HPV infection in HIV patients is largely unknown. Epidemiological studies have linked drugs used to treat HIV, also known as antiretroviral treatment (ART) drugs, with increased risk of HPV-associated oral warts and anal cancer, but actual mechanistic evidence is lacking. A series of previous studies of non-infected organotypic raft tissue showed that use of ART drugs dysregulates proliferation and disrupts the integrity of oral tissue, which could increase the susceptibility to HPV infection. In this study, we examine the effect of two ART drugs, Amprenavir and Kaletra, on human keratinocytes persistently infected with HPV16 using

the organotypic raft culture system. In order to examine the effect of these drugs on various anatomical sites associated with HPV-positive cancers, cervical, tonsillar, and anal keratinocytes were used for the experiments. The results showed that the viral titer decreased with drug treatment in HPV16-infected cervical keratinocytes. Also, viral genome replication was affected to a greater degree than virion production. In contrast, treatment with Kaletra increased the viral titer in HPV16-infected anal tissue. In the context of epidemiological studies that have identified anal cancer to be the only type of HPV-associated cancer linked to ART drug use, our results suggest that increased virion production with Kaletra treatment may contribute to increased cancer risk specifically in anal tissue.

TABLE OF CONTENTS

LIST OF FIGURES

LIST OF TABLES

Abbreviations

HPV	Human papillomavirus
HIV	Human immunodeficiency virus
DNA	deoxyribonucleic acid
RNA	ribonucleic acid
HCK	Human cervical keratinocytes
HAK	Human anal keratinocytes
HTLK	Human tonsil keratinocytes
16HCK	HPV16 infected human cervical keratinocytes
16HAK	HPV16 infected human anal keratinocytes
16HTLK	HPV16 infected human tonsil keratinocytes
HDMCG	HPV16 differentially methylated CpG site
CGI	CpG island
ml	milliliter
mg	milligram
ug	microgram
uM	micromolar
M	Molar
H&E	hematoxylin and eosin

ACKNOWLEDGEMENTS

I would like to begin by thanking my dissertation advisor and mentor, Dr. Craig Meyers. Thank you for the opportunity to work with you and learn from you. You are not only a pioneer and leader in HPV research, but also a kind, patient, and generous mentor. I thoroughly enjoyed my time under your guidance and I feel extremely blessed to have joined your lab for my thesis work.

Next, I would like to thank all the members of my committee for their guidance and support over the years. Your constructive criticism and feedback allowed me to grow as a scientist.

I would also like to thank lab members Dr. Samina Alam, Dr. Sreejata Chatterjee, and Janice Milici. Thank you for all your help and training, and also for your friendship. I will always cherish the laughs and memories we shared.

We would like to thank funding support by National Institutes of Health grants R01CA225268 and R01DE018305-03S1 (NIDCR-ARRA Supplement). The findings and conclusions of this thesis do not necessarily reflect the view of the funding agency.

CHAPTER 1: Literature Review

Introduction to HPV

Epidemiology

Human papillomavirus infections are predicted to be the most common sexually transmitted infection worldwide with approximately 291 million women infected with the virus at any given point in time (1, 2). Up to date, there has been more than 200 types of HPV that have been identified. Most HPV types cause benign lesions in various parts of the human body including the anogenital area and are classified as low-risk HPV types. In contrast, only a small subset of 12 HPV types have been identified as having the potential to cause cancers, and therefore, are classified as high-risk HPV types. The burden of these high-risk HPV types on the worldwide incidence of cancers is quite significant, accounting for approximately 630,000 new cases each year (3, 4). This amounts to approximately 4.5% of all cancers worldwide: 8.6% in women and 0.8% in men (3). Notably, HPV16 and HPV18 are responsible for the majority of anogenital, and head and neck cancers (Table 1.1). Cervical cancer is the most common cancer caused by HPV infection in the US, while the second most common HPV attributed cancer occurs in the oropharyngeal area with the majority of cases affecting men (Figure 1.1). Development of vaccinations against HPV infection in recent years have allowed effective prevention of HPV-associated cancers. However, vaccination rates are below 50% in most countries including the US where the vaccines were developed (5).

Table 1.1. Obtained from (3). Prevalence of HPV-associated cancers.

HPV-related cancer site (ICD-10 code)	Number attributable to HPV[1]	Relative contribution of HPV16/18[2]		Relative contribution of HPV6/11/16/18/31/33/45/52/58[2]	
		Percent	Number	Percent	Number
Cervix uteri (C53)	530,000	70.8	370,000	89.5	470,000
Anus (C21)	35,000	87.0	30,000	95.9	33,000
Vulva (C51)	8,500	72.6	6,200	87.1	7,400
Vagina (C52)	12,000	63.7	7,400	85.3	9,900
Penis (C60)	13,000	70.2	9,100	84.6	11,000
Head and neck (C01-06, C09-10, C32)	38,000	84.9	32,000	89.7	34,000
Total HPV-related sites in women	570,000	71.4	410,000	89.6	510,000
Total HPV-related sites in men	60,000	82.3	50,000	90.4	55,000
Total HPV-related sites	630,000	72.4	460,000	89.7	570,000

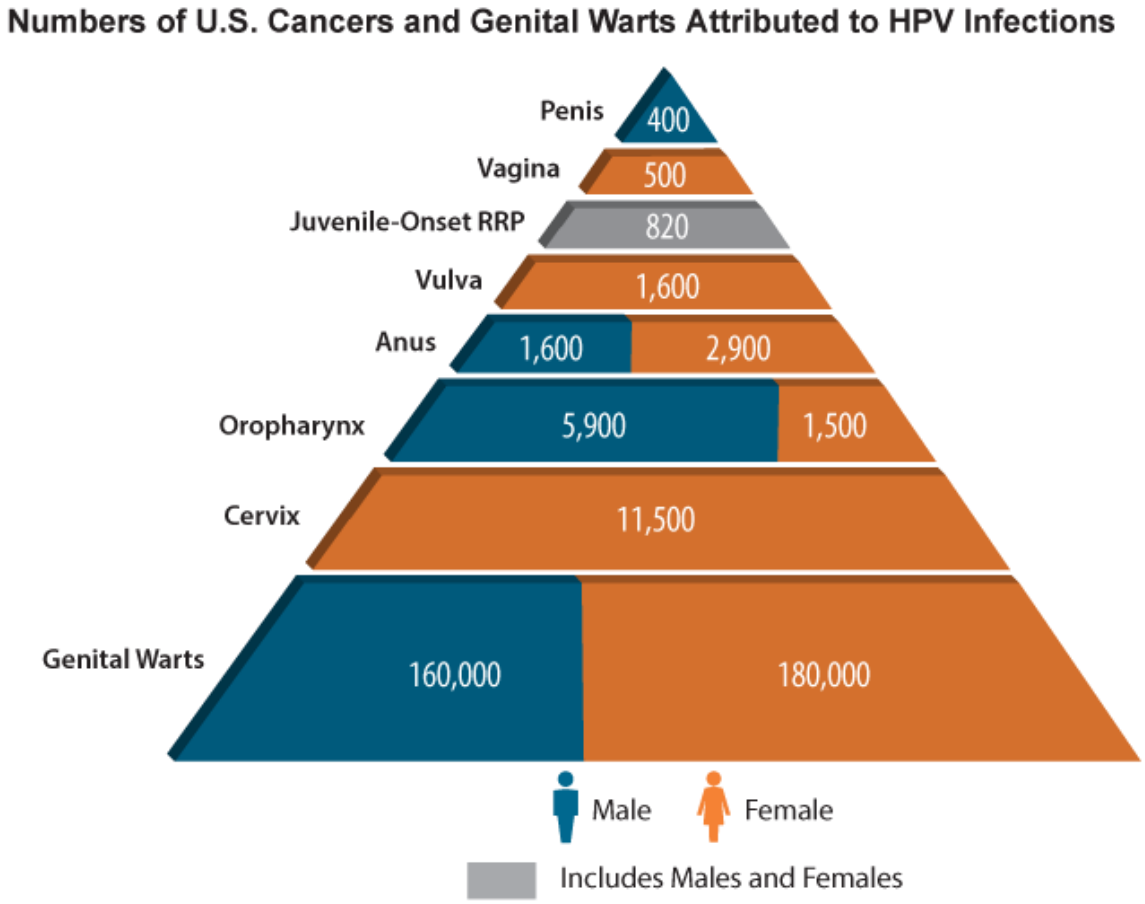

Figure 1.1. Obtained from (6). Incidence of HPV-associated warts and cancers in the US.

HPV genome and structure

HPV is a nonenveloped virus that is a member of the Papillomaviridae family (7). It is approximately 55 nm in diameter and the icosahedral capsid encloses a double-stranded circular DNA that is approximately 7900 base pairs (7). The HPV capsids consists of 72 pentamers that are supported by interpentameric and intrapentameric disulfide bonds (8). A typical high-risk HPV genome consists of six early genes, two late genes, and an upstream regulatory region (URR). There are six early genes that are involved in various processes including replication, transcription, viral release, immune evasion (Figure 1.2). In particular, early genes E6 and E7 are well established oncogenes that promotes transformation and tumorigenesis (9–16). The two late genes encode structural proteins that comprise the viral capsid: L1 major capsid protein and L2 minor capsid

protein. In addition to contributing to the capsid structure, the L2 capsid protein is heavily involved in the intracellular trafficking of the viral genome into the nucleus (17–19). The URR contains the viral origin of replication, and promoter and enhancer elements that controls the transcription and replication of early genes.

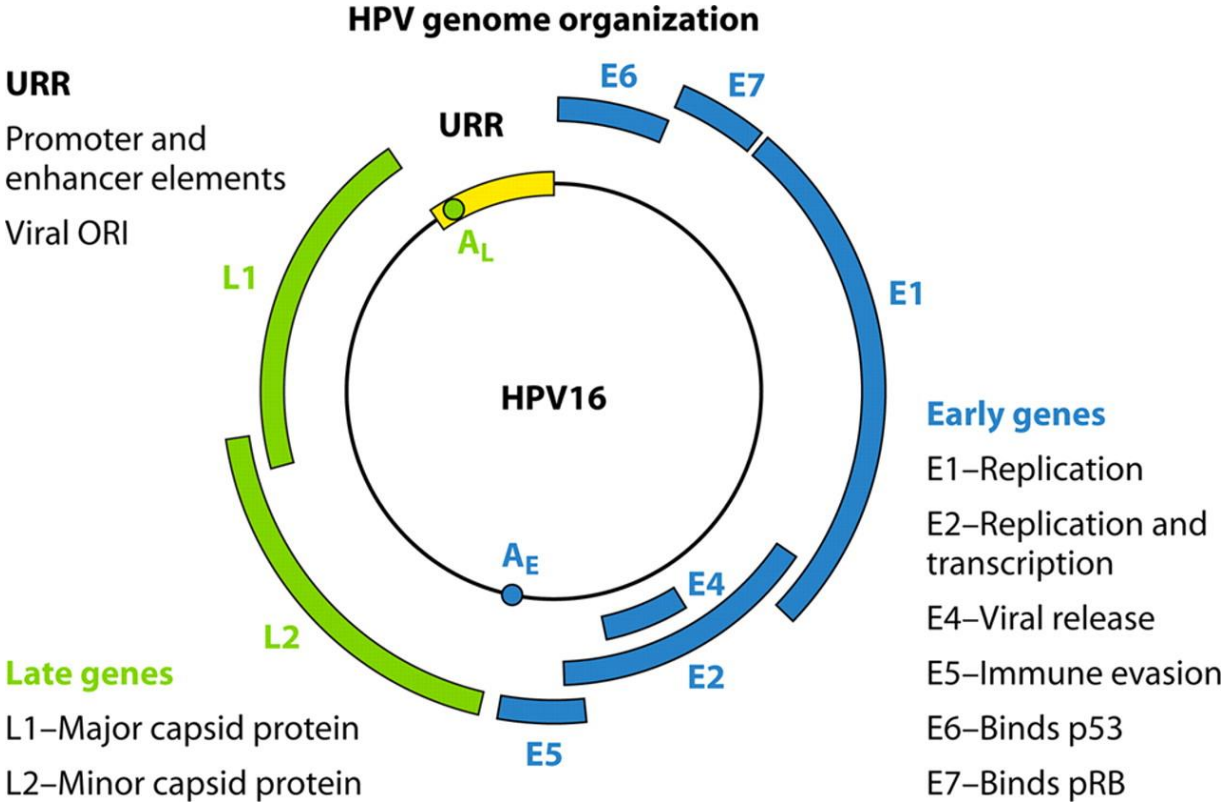

Figure 1.2. Obtained from (20). The genomic organization of a typical high-risk HPV. There are six early genes that are involved in replication, transcription, viral release, immune evasion, and binding of p53, pRB proteins. There are two late genes that encode the viral capsid proteins L1 and L2. The upper regulatory region (URR) contains promoters, enhancers, and viral origin of replication.

HPV life-cycle and progression to cancer

HPV infection initially occurs by microabrasion in the skin that allows the virus to access and infect the basal cells of the epidermis where viral genome is maintained episomally in low copy numbers (Figure 1.3). As the basal cells divide and are pushed towards the surface of the skin, the epithelial cells gradually differentiate. Throughout the various stages of epithelial differentiation from the basal cell layer to the cornified stratum,

different sets of viral genes are expressed in a tightly regulated manner (Figure 1.3) (21). In the mid layers of the epidermis, proteins, such as E4, required for viral genome replication are expressed while in the top cornified layers the two capsid proteins L1 and L2 are expressed, allowing the progeny virions to assemble. The assembly of the virus has been shown to be dependent on the tissue-spanning redox gradient (8). For the release of progeny virions, HPV does not utilize lytic pathways or bud off of the host cell membrane. Rather, HPV progeny virion release occurs by natural sloughing off of the skin at the outer surface of the epidermis in the cornified layers. Since the life-cycle spans all strata of the epidermis and is also dependent on the redox gradient across the tissue, HPV cannot be cultured in the traditional monolayer cell culture system.

Initial infection with high-risk HPV can lead to low-grade squamous intraepithelial lesions (LSILs). LSILs are largely inconspicuous and most of these lesions are naturally cleared within 18 months (22–24). However, in a fraction of cases, the infection persists for years and eventually develop into cancer. During earlier stages of infection (LSIL or cervical intraepithelial neoplasia grade 1), the virus continues to replicate and produce high levels of progeny virions. However, as the lesions progress and develop into cancer, the viral genome often integrates into the host genome, which disrupts the viral life-cycle and results in significantly reduced production of progeny virions (Figure 1.4). The integration of the viral genome often results in the disruption of the E2 gene, which transcriptionally inhibits E6 and E7 oncogenes. As a result, the integration leads to persistent upregulation of E6 and E7 expression. Since E6 and E7 were identified as oncogenes that play a critical role in tumorigenesis, many studies have investigated the mechanism through which they promote cancer. Although studies have shown that the role E6 and E7 are multifaceted, the main oncogenic driving force of these two oncogenes come from their ability to inhibit tumor suppressor genes TP53 and RB1, respectively as shown in Figure 1.5 (9–16).

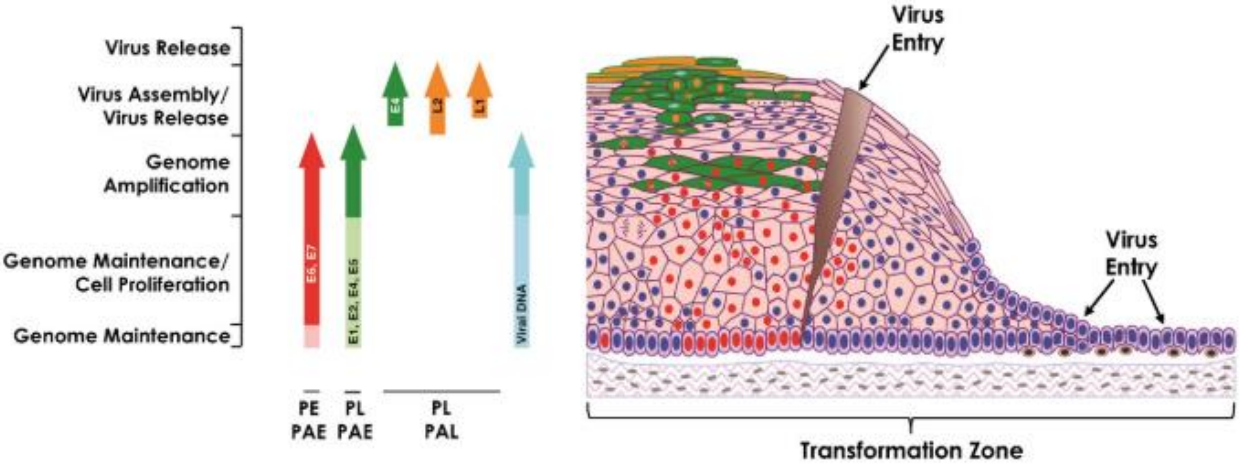

Figure 1.3. Obtained from (21). Life Cycle of High-Risk HPVs in Cervical Epithelium. Initial infection of HPV is thought to occur through micro-abrasions of the epidermis that allows the virus to access and infect the basal lamina. As the infected cells divide and are pushed towards the surface of the skin, the tissue gradually differentiates, and different sets of viral proteins are expressed at different stages of epidermal differentiation in a tightly regulated manner.

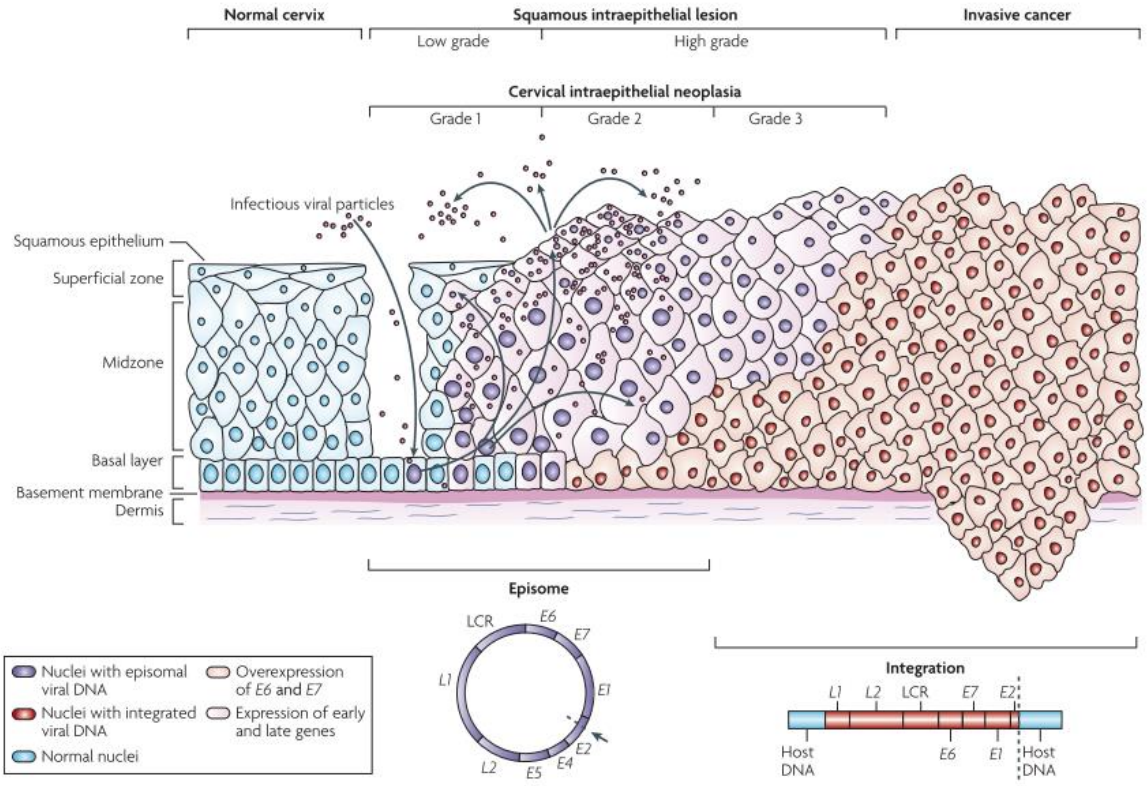

Figure 1.4. Obtained from (25). HPV-mediated progression to cervical cancer. Early stage persistent infections and low- grade intraepithelial lesions allow the virus to complete its life cycle by producing high levels of progeny virions. Once the lesions progress to invasive cancer, the HPV genome typically integrates into the host genome, which disrupts the E2 gene and subsequent upregulation of E6 and E7.

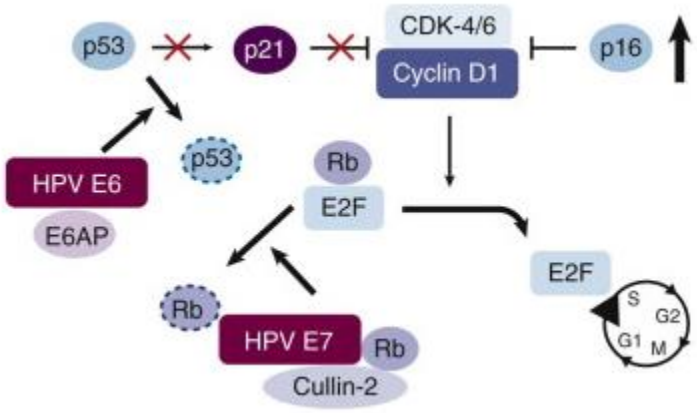

Figure 1.5. Obtained from (26). Mechanisms of E6 and E7 oncogenes. The HPV E6 oncoprotein interacts with E6 -associated protein (E6AP) to mediate degradation of p53. The E7 oncoprotein mediates degradation of the Rb protein, which results in the release of transcription factor E2F, allowing unchecked G1 to S phase progression. HPV-associated malignancies are typically characterized by upregulation of p16 expression.

Culturing HPV in organotypic rafts

The HPV life-cycle is tightly associated with keratinocyte differentiation and spans all strata of the epidermis including the stratum basal, stratum spinosum, stratum granulosum, stratum lucidum, and stratum corneum (21). Therefore, HPV cannot be cultured in the traditional monolayer cell culture system. Currently, the only method to produce native HPV virions *in vitro* is via the organotypic raft culture system that mimics the microenvironment of the skin (Figure 1.6) (27–29). In the organotypic raft culture system, a collagen matrix containing fibroblasts are created to act as the dermal equivalent. Keratinocytes that stably maintain HPV genomes are then seeded on top of the collagen matrix and lifted up onto a support grid to create an air-liquid interface. The collagen matrix comes into direct contact with the culture medium underneath while the keratinocytes on top are exposed to the air and supplied with nutrients and growth factors by diffusion. The organotypic raft culture allows the keratinocytes to differentiate. This mimics the in vivo environment where the epidermis exposed to air and does not come into direct contact with the vascular supply (Figure 1.7) (30).

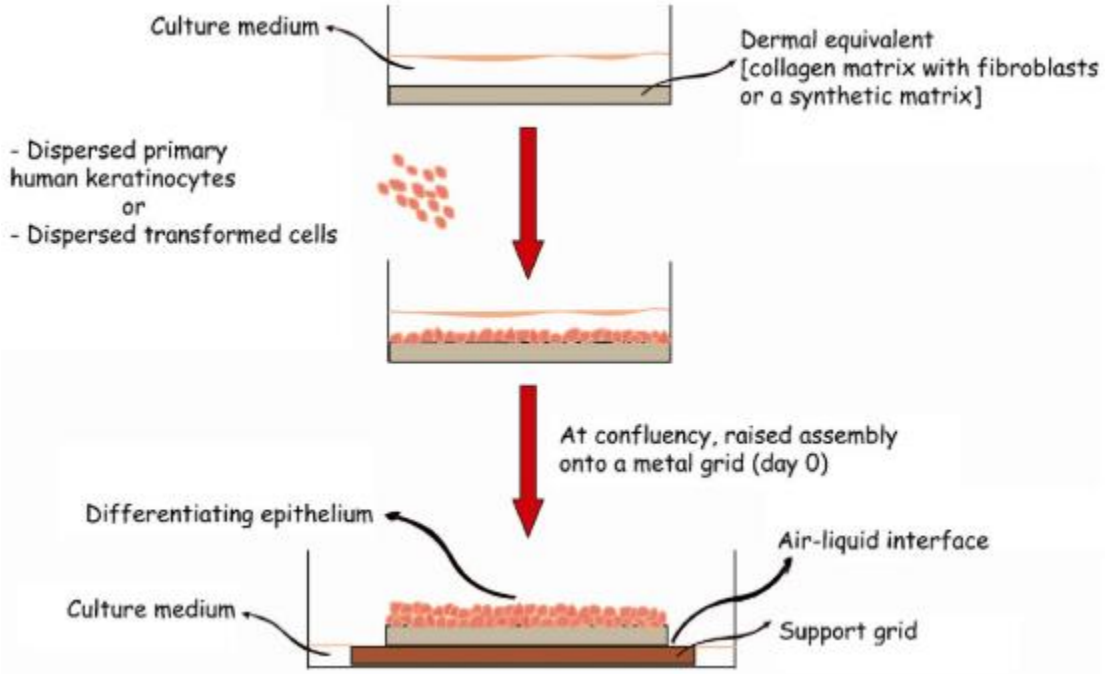

Figure 1.6. Obtained from (31). The organotypic raft culture system.

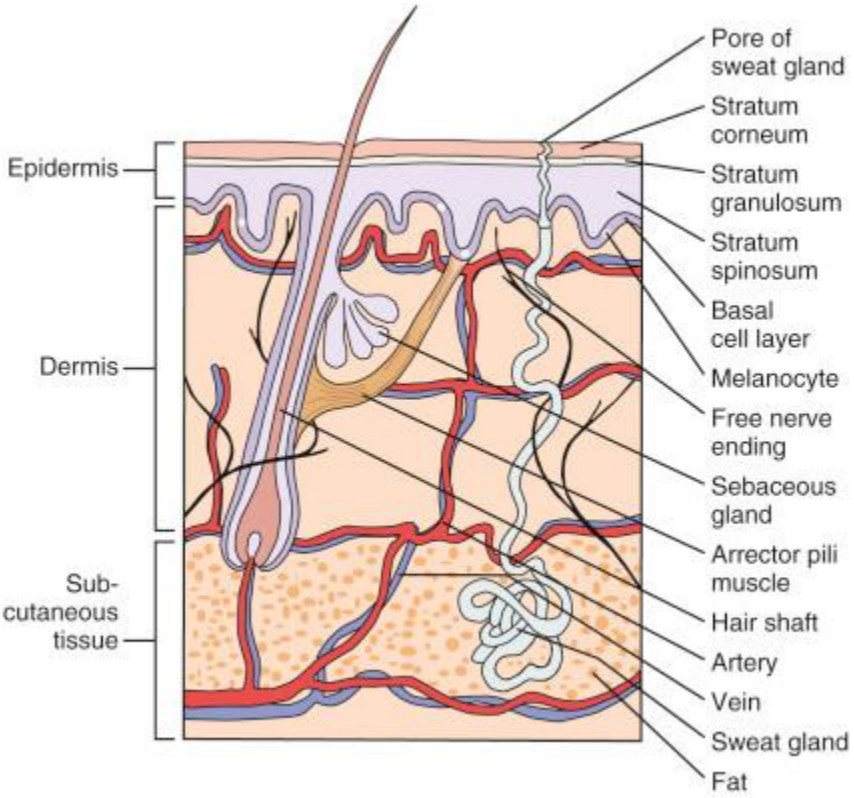

Figure 1.7. Obtained from (32). The structure of skin.

Global gene expression changes in HPV infection in cervical epithelium

HPV is responsible for most cases of cervical cancer, which is the third most common cancer in women worldwide and the most common cancer in women in developing countries (33). In persistently infected cervical tissue with normal or low-grade dysplasia the HPV genome is maintained episomally and infectious viral particles are produced. In contrast, progression to severe dysplasia and invasive cancer is marked by integration of viral genome into the host genome that typically results in disruption of the E2 gene, subsequent upregulation of oncogenes E6 and E7, and abrogation of virion production (34, 35).

In the past, many studies have looked into changes in whole genome expression profiles of precancerous and cancerous lesions in order to better understand the progression of persistent HPV infection to cervical cancer. However, most of these studies focus on neoplastic lesions and cancerous lesions (36–44) because it is difficult to acquire clinical samples at earlier stages of infection when patients are largely asymptomatic. Therefore, there is a gap in knowledge of global gene expression in earlier pre-neoplastic stages of the disease when HPV establishes productive infection in the host. In two recent studies, human keratinocytes persistently infected with HPV16 were used to measure global gene expression changes (45, 46), but they used keratinocytes derived from foreskin, which may not be appropriate for modeling infection in cervical tissue since HPV may have tissue-specific effects (47). Furthermore, these studies used monolayer cell cultures that do not produce virions by disallowing the virus to progress through its differentiation-dependent replication life-cycle (29, 48). In other studies, overexpression tools were used to examine the effect of specific HPV oncoproteins on global gene expression (49, 50). Since these studies only examine the effect of individual viral proteins, they do not account for the full picture of HPV infection in the natural environment.

Epigenetic changes in tonsil tissue with HPV infection

HPV infection and Head and Neck Cancers

Head and neck squamous cell carcinoma (HNSCC) is the sixth most common cancer worldwide with approximately 563,000 new cases and 300,000 deaths each year (51). HNSCCs are categorized by the specific area in the head and neck in which they arise from including the nasal cavity, paranasal sinuses, salivary glands, oral cavity, pharynx, and larynx (Figure 1.8). The pharynx region can be further subdivided into three parts (Figure 1.8): nasopharynx (upper part, behind the nose), oropharynx (middle part including soft palate, base of the tongue, and tonsils), and hypopharynx (lower part) (52). Traditionally, the main causes of HNSCCs were tobacco and alcohol use, poor oral hygiene, and genetics. With a significant decrease in tobacco use in the US in recent decades, the overall incidence of HNSCCs has been decreasing in the US (53). However, in recent years HPV-associated HNSCCs have been steadily increasing, and therefore, the proportion of HNSCCs attributed to HPV infection has increased over the years. Interestingly, more than 90% of HPV-positive HNSCCs are caused by a single HPV type, HPV16 (53). HNSCCs caused by HPV infection mainly occur in the oropharyngeal region (base of the tongue and tonsils) (54) whereas HNSCCs unrelated to HPV mainly occur in the other regions of the head and neck (53). This difference in specificity of anatomical sites between HPV-negative and HPV-positive HNSCCs was reflected in a recent study of HNSCCs in the US: the incidence of oropharyngeal cancers increased by 1.3% in the base of the tongue, and 0.6% in the tonsils each year between 1973 and 2004. In contrast, the incidence of cancers in the oral cavity, which are mostly HPV-negative, decreased by 1.9% each year during the same time period (53, 55). The overall prevalence of HPV in oropharyngeal cancers worldwide has significantly increased from 40.5% before 2000 to 64.3% between 2000 and 2004, and 72.2% between 2005 and 2009 (56). A recent study reported that in the US, approximately 63.5% of oropharyngeal cancers are attributed to HPV infection (57).

The biology of HPV-negative and HPV-positive oropharyngeal cancers have shown to be distinct with HPV-positive cancers characterized by p53 and Rb inhibition and p16 upregulation. In contrast, HPV-negative oropharyngeal cancers have been characterized by p53 mutation and p16 downregulation. Moreover, HPV-positive oropharyngeal cancers are more responsive to chemotherapy and radiation treatments, and thus, confer a better prognosis than those that are HPV-negative (53, 58–65).

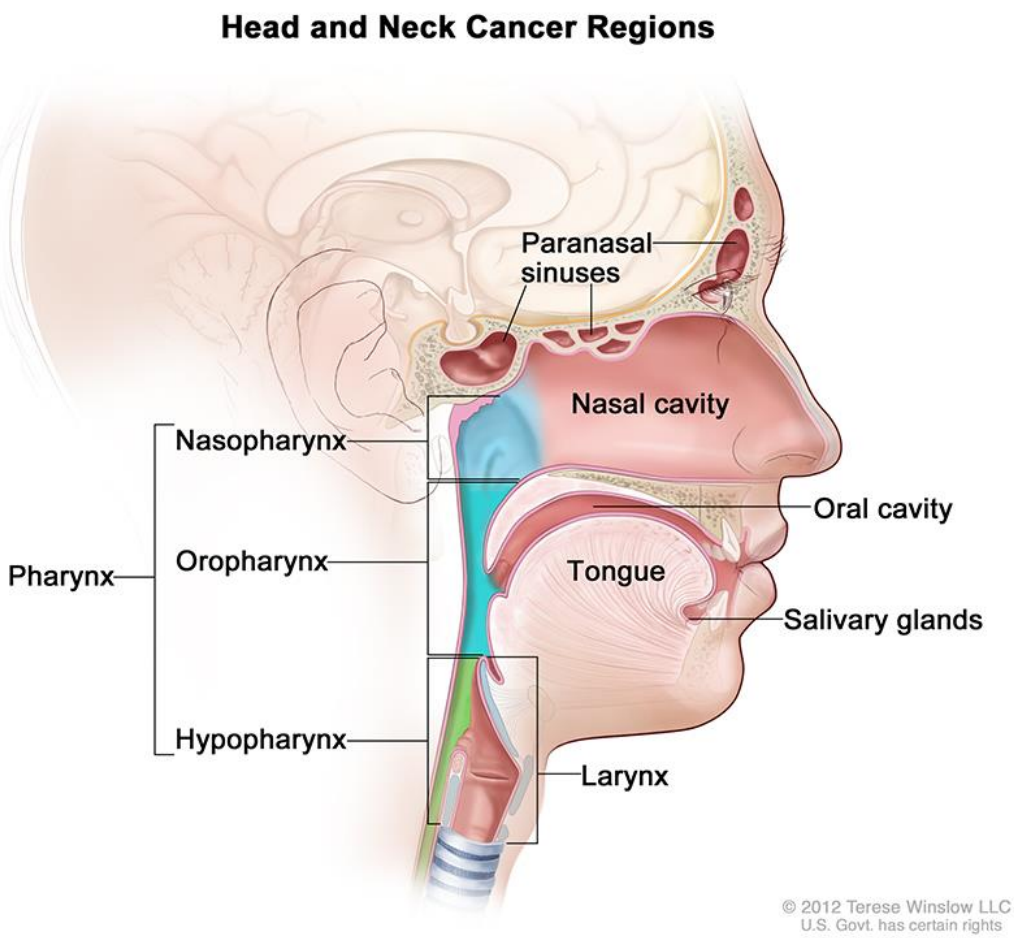

Figure 1.8. Obtained from (66). Head and neck cancer regions.

Epigenetics: DNA methylation

The field of epigenetics refers to the study of inheritance of altered characteristics through mechanisms that do not involve changes in the DNA sequence. The mechanisms that through which epigenetic changes occur include DNA methylation, histone modification, regulatory RNA, and structural continuity (67). Of these mechanisms, DNA methylation is the most commonly occurring, and most extensively studied form of epigenetic modification. In DNA methylation, a methyl group is covalently added to DNA by a group of enzymes called DNA methylases or DNA

methyltransferases (DNMTs) (67). DNA methylation in plants and animals mostly occur on the fifth carbon of cytosine bases, which results in a 5-methylcytosine (5mC). These cytosines are often followed by a guanine base. Since they are linked by a phosphate group, these dinucleotides are referred to as CpG methylation sites (68). The methyl group of a CpG site is located in the major groove of the DNA double helix and can prevent binding of transcription factors, resulting in inhibition of gene expression. Moreover, a class of proteins that specifically bind to methylated DNA, such as MECP2 and the MBD family of proteins, can inhibit gene expression by binding to methylated DNA and blocking transcription factors (68).

There are two groups of DNMTs: maintenance methylases and de novo methylases. Maintenance methylases add methyl groups to newly synthesized DNA during replication at locations opposite to the methylated bases of the parental DNA strand. This ensures that the methylation patterns are passed on to the next generation of an organism or progeny cells. In contrast, a change in methylation pattern occurs when de novo methylases add methyl groups at new locations of the DNA (67). In humans, there is one maintenance DNMT (DNMT1) and two de novo DNMTs (DNMT3a and DNMT3b) (68).

S-adenosyl methionine (SAM) is used by DNMTs as a methyl donor, resulting in S-adenosyl homocysteine (SAH) as shown in Figure 1.8. For demethylation, 5mC is first converted to several intermediates by the ten-eleven translocation (TET) family of proteins. Two of the intermediates, 5-formyl cytosine and 5-carboxy cytosine, can be excised from the DNA by thymine DNA glycosylase (TDG). The excised site is then filled in with a new cytosine nucleotide via the base excision repair mechanism (Figure 1.9).

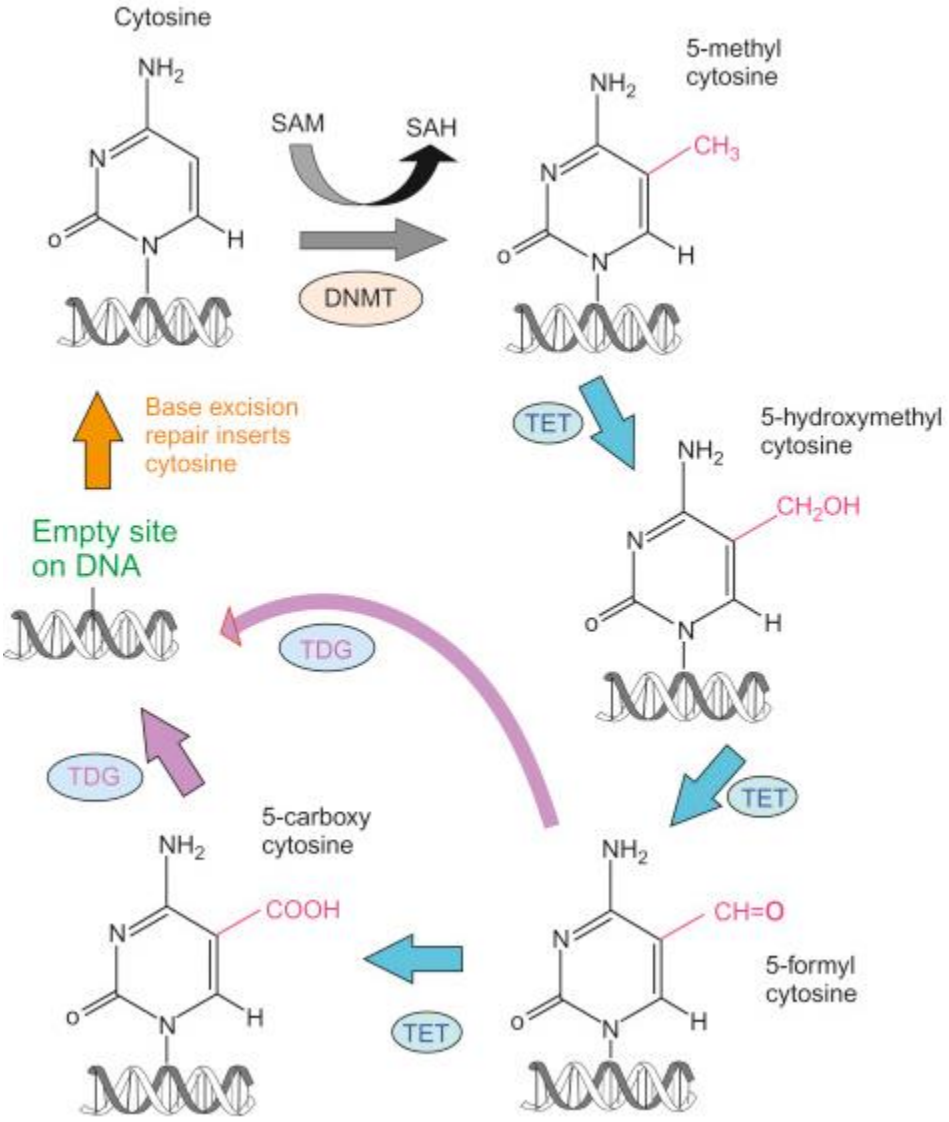

Figure 1.9. Obtained from (67). Methylation and Demethylation of DNA. Cytosine is methylated by DNA methyltransferase (DNMT) to 5-methyl cytosine (5mC) with the use of S-adenosyl methionine (SAM) as a methyl donor. The ten-eleven translocation (TET) family of proteins can initiate demethylation by converting 5mc to several intermediates (5-hydroxymethyl cytosine, 5-formyl cytosine, 5-carboxy cytosine). Thymine DNA glycosylase (TDG) can excise both 5-formyl cytosine and 5-carboxy cytosine, which leaves an empty site on the DNA. This is filled with a new cytosine by the base excision repair system.

CpG methylation patterns in genomic regions

CpG dinucleotides are significantly underrepresented in the mammal genome than expected (20% of expected level), which is due to the hypermutability of methylated cytosine bases (69, 70). CpG sites are unevenly distributed throughout the genome and cluster in regions called CpG islands (CGIs), which are flanked by CGI shores (0–2 kb up- and downstream of CGIs) and CGI shelves (2–4 kb up- and downstream of CGIs, Figure 1.9).

Although there is no strict definition, CGIs are generally defined as a 1000-kb stretch of DNA with GC content greater than 50% (68). Approximately 60% of human gene promoters have CGIs (Figure 1.10), and most of them are constitutively expressed genes (68, 71). In other words, CGIs are normally hypomethylated, which is a trend that can be seen across different tissue types (68, 72, 73). This suggests that CGI methylation is not a typical mechanism through which normal cells regulate gene expression (73). In contrast, while CpG shores and shelves have significantly less CpG content than CGIs, the percent methylation is much higher (Figures 1.10 and 1.11). Since the majority of gene promoters contain CGIs, a sudden drop in methylation levels are observed around the transcription start site (TSS) of genes, while methylation levels dramatically increase downstream of the TSS (and overlapping CGI) as shown in Figure 1.11. The methylation levels are then maintained at a plateau across the gene body. Increased gene expression is associated with decreased CGI (or promoter) methylation and increased gene body methylation. Therefore, in decreased gene expression, methylation levels drop to a lesser degree at the TSS (the trough at the TSS is raised) while, at the same time, the methylation percentage plateaus at a decreased level throughout the gene body (Figure 1.11). An example of this methylation trend can be observed in samples Y1 (red line) and C4 (yellow line) in Figure 1.11.

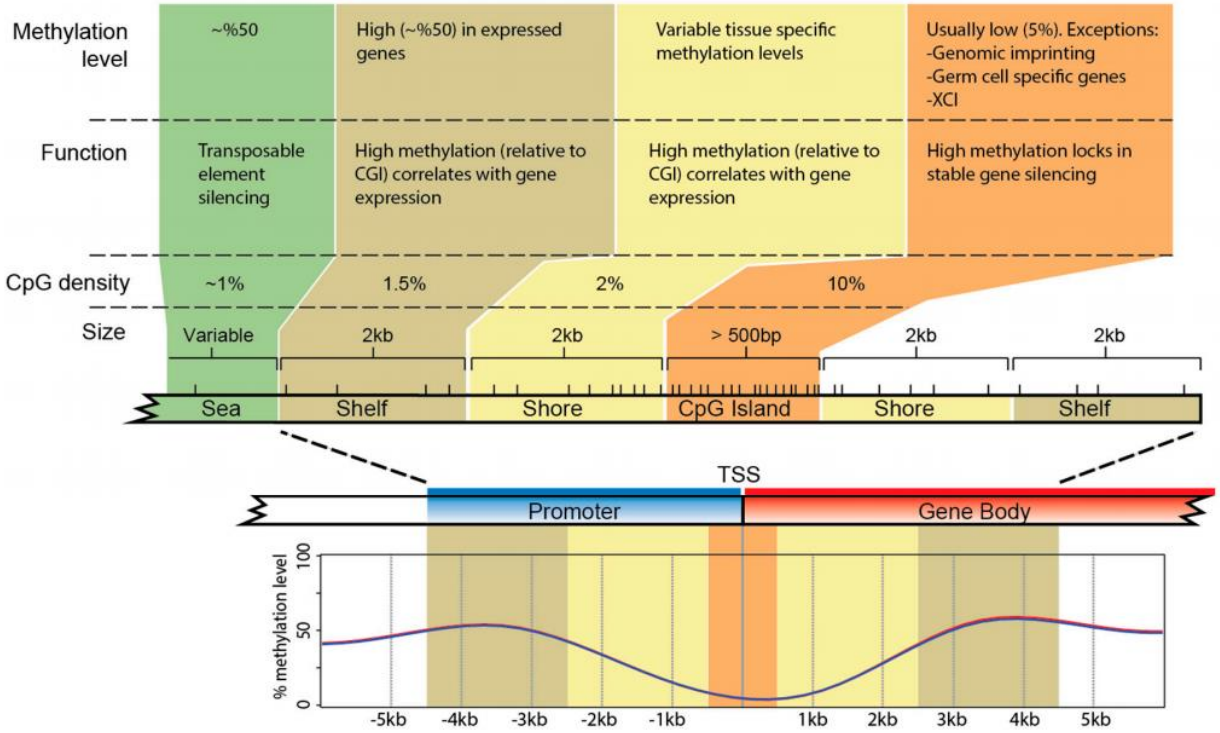

Figure 1.10. Obtained from (69). CpG site distribution and methylation levels. Typical CpG island structure in the promoter (blue) and gene body (red). DNA methylation levels are shown for expressed genes, along with how methylation levels correlate with gene expression. The DNA methylation level across TSSs of expressed genes in mouse liver is shown below the gene. Dashes immediately above CGIs, shores, and shelves represent CpG dinucleotides, with highest density in the CGI near the TSS. Statements about the upstream shore and shelf apply also to gene body shore and shelf.

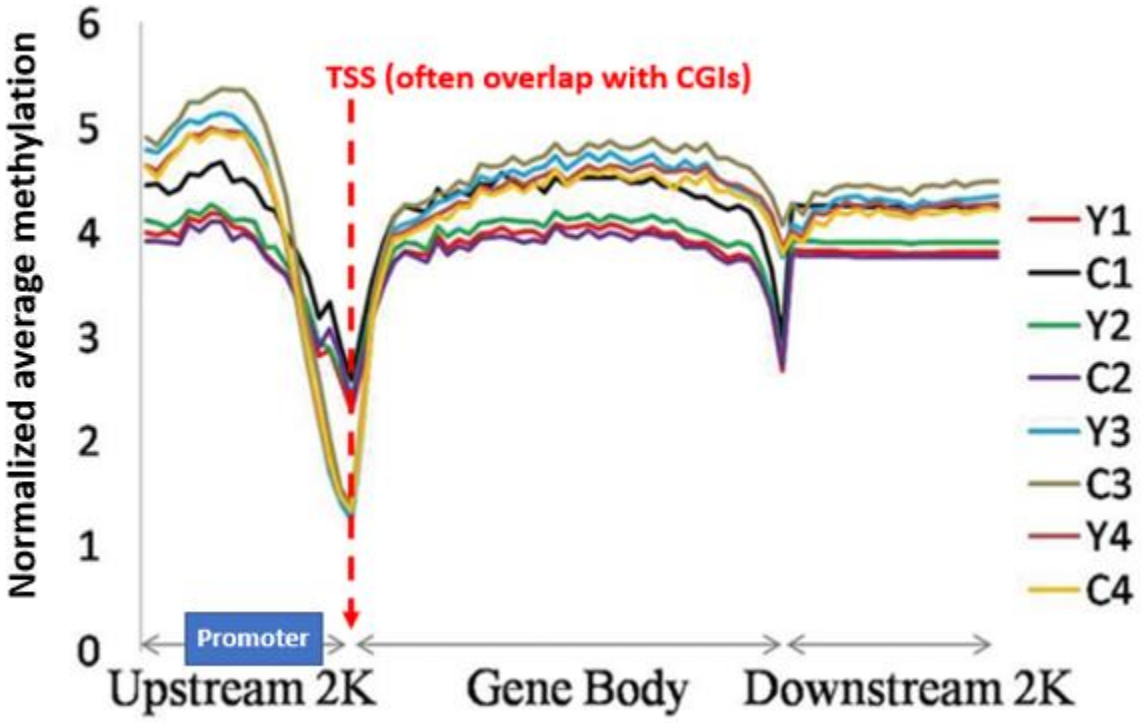

Figure 1.11. Obtained and modified from (74). Relative methylation levels of different human genomic sequences in the centenarians and controls. Y and C represent the younger control and centenarian samples, respectively**.**

Bisulfite sequencing of the methylome

A commonly used technique for analyzing the methylation status of a genome, also referred to as methylome, is bisulfite sequencing (67). When DNA is treated with sodium bisulfite, only unmethylated cytosine bases are converted to uracil bases while methylated cytosine bases are left intact. The uracil bases are then converted to thymine bases with PCR amplification. Finally, sequencing the sodium bisulfite-treated DNA and comparing it to the original DNA sequence allows identification of the cytosine bases that were methylated (Figure 1.12).

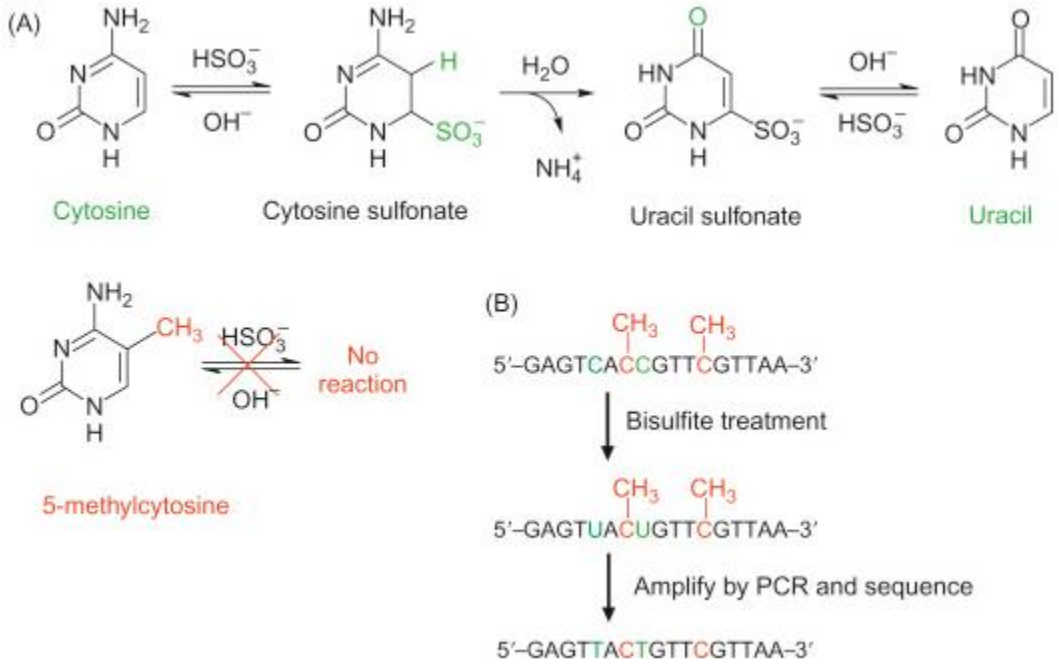

Figure 1.12. Obtained from (67). Bisulfite conversion of cytosine to uracil.

DNA methylation in cancer

CpG islands are typically hypomethylated in normal tissue (68, 72, 73). In contrast, many cancer cell genomes are characterized by hypermethylation of CpG islands, especially those that are located in the promoter regions of tumor suppressor genes (68, 72, 75, 76). Hypomethylation patterns are also observed in cancer genomes, but they are typically in promoter regions of oncogenes (77, 78).

While genetic modifications, or mutations, are mostly considered to be irreversible, epigenetic modifications are considered to be reversible. Therefore, many studies have focused on epigenetic changes in cancer as it could reveal novel therapeutic targets (68).

DNA methylation of viral genome in cervical cancer

Both the viral and host genome can be targeted by methylation in HPV infection with the HPV16 genome containing 110 CpG sites (79, 80). However, it is unclear whether methylation of the viral genome is orchestrated by the virus itself through hijacking of

the host's DNMTs to establish a successful infection, or if it is a result of the host defense mechanism to suppress viral gene expression (77).

HPV early gene E2 is involved in viral transcription, replication, and maintenance. One of its function is to repress expression of E6 and E7, which is mediated through binding of E2 to E2 binding sites (E2BS) located in the LCR of the HPV genome. A previous study showed that E2's ability to bind E2BSs is inhibited by methylation of CpG sites within E2BSs (81). Moreover, LCR (including E2BSs) methylation status was dependent on the level of differentiation of the infected keratinocyte (81). Since the virus life-cycle is closely associated with the differentiation of keratinocytes, this result suggests that the methylation pattern of the HPV genome may vary at different stages of its life-cycle.

Progression from persistent HPV infection to cervical cancer has classically been associated with the integration of viral genome into the host genome in a manner that disrupts the E2 gene (Figure 1.4). This inactivation of the E2 gene results in E6 and E7 upregulation, which is important for cancer progression and maintenance. However, a study reported that there are cases of cervical carcinoma in which the E2 gene is intact and expressed, with E6 and E7 levels that were still high (82). In these cases, the E2BSs were hypermethylated, and therefore, E2 was not able to bind them. Methylation of E2BSs was observed in 75% of primary cervical tumors that did not present disruption in the E2 gene. This study showed that epigenetic modifications can contribute to tumorigenesis in HPV infection through a different mechanism that does not involve viral genome integration (82).

Methylome analysis of the HPV genome has revealed that the HPV genome gets progressively methylated throughout the progression of the disease. In primary human foreskin keratinocytes transfected with the HPV16 genome, viral genomes from pre-immortal keratinocytes were mostly unmethylated whereas viral genomes from immortalized keratinocytes were highly methylated (82). A similar trend was shown in clinical samples: the HPV16 genome had gradually increasing levels of methylation from tissue samples of asymptomatic carriers of the virus, through pre-neoplastic lesions, to primary cervical carcinomas (Figure 1.13).

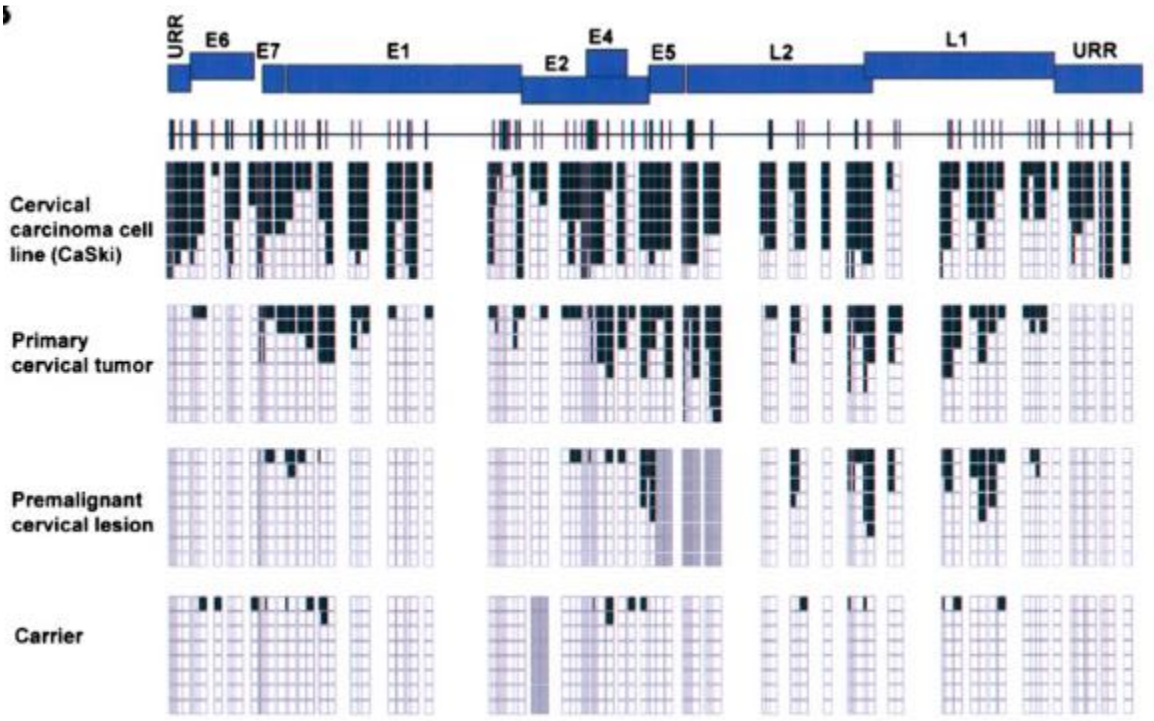

Figure 1.13. Obtained from (82). Example of bisulfite genomic sequencing analysis of multiple clones for the HPV16 genome. (Black squares) Methylated and (white squares) unmethylated CpG dinucleotides; (gray squares) deleted genome sequences.

DNA methylation of host genome in cervical cancer

It has been shown that DNMT1 expression is increased in cervical cancer cell lines compared to primary cervical keratinocyte cultures, suggesting that HPV infection may affect the methylome of the host (83). Other studies showed that E7 increases DNMT1 expression, and that E7 directly binds DNMT1 to increase its activity (84, 85). Additionally, an increased copy number of DNMT3B has been observed in cervical cancer samples that correlated with increased mRNA expression of the enzyme (86). As expected, numerous host genes have been shown to be increasingly methylated throughout the progression of the disease as shown in Table 1.2. Genes that are hypermethylated in cervical carcinoma include putative tumor suppressor genes including SOCS1, PTEN, BLU, and RASSF1 (87–90).

Table 1.2. Obtained from (79). List of genes that are hypermethylated in precancerous lesions and cancers of the cervix.

No.	Gene	Disease-free controls	LG CIN	HG CIN	Squamous cell carcinoma	Cervical carcinoma	Adeno-carcinoma
1	*APC*	18% (90; 4)	32% (37; 1)	34% (38; 1)	24% (238; 5)	32%* (88; 1)	54%* (65; 4)
2	*CCNA1*	0% (25; 1)	0% (13; 1)	36%* (11; 1)		93%* (30; 1)	
3	*CDH1*	0% (53; 4)	7% (42; 3)	22%* (60; 3)	61%* (170(3)	47%* (135; 4)	33%* (57; 3)
4	*CDKN2A*	3% (254; 7)	12%* (120; 6)	29%* (237; 9)	32%* (407; 8)	22%* (372; 7)	20%* (110; 7)
5	*DAPK1*	1% (184; 5)	6% (69; 3)	30%* (88; 3)	64%* (299; 6)	52%* (180; 3)	39%* (89; 5)
6	*HIC1*	2% (43; 3)	52%* (54; 2)	70%* (91; 3)	20%* (108; 2)	71%* (79; 1)	63%* (27; 2)
7	*IGSF4*	0% (25; 3)	0% (29; 2)	39%* (31; 2)	58%* (52; 1)	65%* (23; 1)	
8	*RARB*	0% (47; 4)	5% (83; 3)	15%* (61; 3)	30%* (117; 3)	40%* (121; 3)	15%* (13; 2)
9	*ROBO1*	0% (51; 1)	7% (62; 1)	8%* (48; 1)		46%* (119; 1)	
10	*SLIT1*	0% (40; 1)	0% (48; 1)	10%* (39; 1)		53%* (119; 1)	
11	*SLIT2*	0% (51; 1)	2% (62; 1)	25%* (48; 1)		64%* (119; 1)	
12	*FANCF*	0% (18; 1)		0% (37; 1)		30%* (91; 1)	
13	*FHIT*	0% (50; 4)	3% (76; 2)	2% (63; 2)	12%* (77; 1)	24%* (189; 4)	0% (5; 1)
14	*MGMT*	3% (206; 6)	4% (93; 3)	7% (74; 3)	11%* (217; 4)	14%* (109; 2)	12%* (51; 3)
15	*PTEN*	0% (11(1)	15% (27; 2)	0% (11(1)	58%* (62; 1)		
16	*RASSF1*	3% (29; 3)	3% (58; 3)	1% (73; 3)	17%* (299; 7)	5% (110; 3)	26%* (132; 6)
17	*SLIT3*	0% (40; 1)	4% (48; 1)	2% (42; 1)		49%* (118; 1)	
18	*TERT*	0% (14; 1)	0% (13; 1)	0% (31; 1)		62%* (76; 2)	0% (9; 1)
19	*TIMP3*	0% (8; 1)	0% (13; 1)	16% (31; 1)		11% (171; 3)	55%* (38; 2)
20	*C15orf48*	0% (21; 1)				36%* (22; 1)	
21	*MT1G*	5% (21; 1)				55%* (22; 1)	
22	*POU2F3*	0% (7; 1)			41%* (32; 1)		36% (14; 1)
23	*SFRP1*	5% (21; 1)				58%* (22; 1)	
24	*SPARC*	5% (21; 1)				91%* (22; 1)	
25	*TFPI2*	38% (21; 1)				82%* (22; 1)	
26	*TNFRSF10C*	0% (12; 1)				100%* (50; 1)	
27	*HSPA2*		0% (13; 1)	3% (31; 1)		73%* (11(1)	
28	*SOCS1*		0% (13; 1)	7% (31; 1)		50%* (11; 1)	
29	*TWIST1*		0% (23; 1)	14% (22; 1)		43%* (56; 1)	
30	*SOCS2*		23% (13; 1)	45% (31; 1)		64%* (11; 1)	
31	*CDH13*		5% (41; 2)	14% (63; 2)		46%* (89; 1)	

DNA methylation of viral genome in HPV+ HNSCC

Not many studies have investigated the viral methylome in HPV-associated HNSCCs. One study that analyzed HPV methylomes in advanced stage HPV+ HNSCCs showed that the viral genome is mostly hypomethylated, including the LCR. Another study analyzed the methylation status of E2BSs in HPV+ oropharyngeal cancers and identified three subgroups of the cancer depending on the level of methylation: 1) complete methylation (>80%) of the E2BSs was associated with integrated HPV genomes with an intact E2 gene; 2) intermediate methylation levels (20% - 80%) was associated with mostly episomal HPV genomes with intact E2 gene; and 3) no methylation (<20%) with a disrupted E2 gene.

DNA methylation of host genome in HPV+ HNSCC

A study that analyzed the methylation of host genes in oropharyngeal cancer samples reported an overall hypermethylation signature in HPV+ cancers compared to HPV- cancers. When E6 and E7 were ectopically expressed in a HPV- oropharayngeal cancer cell line, the host methylome partially changed to a hypermethylation pattern similar to that observed in HPV+ oropharyngeal tumors. The study concluded that E6 was the main effector gene that caused the hypermethylation pattern in HPV+ oropharyngeal cancers (91). Based on these observations, it can be speculated that the better prognosis of HPV+ oropharyngeal cancers compared to HPV- ones is due to the fact that HPV+ cancers are more epigenetically driven—a mechanism that is reversible (77).

In another study that systematically reviewed different methylation patterns between HPV- and HPV+ oropharyngeal cancers, genes involved in cell proliferation, invasion and metastasis, evasion of growth suppressors, and resisting cell death were significantly associated with HPV status, suggesting that HPV induces a specific methylation pattern in the host genome. Interestingly, even within HPV+ oropharyngeal cancers, tumors with integrated copies of HPV and tumors without integrants displayed distinct DNA methylation patterns (77).

Sex-differences in HPV+ HNSCCs

Sex differences in oral HPV infection

The sex bias in prevalence and virulence of or HPV16 infection has been reported in many studies. The prevalence of oral HPV16 is five-fold higher in men than in women (92). In a cohort study of 409 individuals, the risk of HPV infection significantly increased with increasing number of recent oral sex partners for men, but not for women (93). Additionally, the median time to clearance was significantly longer in men (5.3 months) than in women (3 months), and in an adjusted analysis, men were 37% less likely to clear an oral HPV infection than women (92, 93).

Sex differences in other infectious diseases

Sex differences in infectious diseases is not limited to HPV, but rather widespread across various pathogens. Overall, disease intensity (pathogen load) and prevalence are predominantly worse in males for viral, bacterial, parasitic, and fungal infections in general (Figure 1.14). As an example, women have approximately 40% less human immunodeficiency virus (HIV) RNA in circulation than men (94), and tuberculosis incidence is twice as high in men than in women in most countries (95). Also, hepatitis B virus (HBV) titer and risk of development of hepatocellular carcinoma is higher in men than in women (96).

The higher prevalence of infections in males can be partially explained by differences in immune response between males and females. The activity of innate immune cells including macrophages and dendritic cells are higher in females than males, and the induction of antiviral genes in females are 10-fold greater than in males (97–100). Moreover, both the humoral and cell-mediated immune response to antigens are significantly higher in females than in males (100).

	Intensity	Prevalence or Incidence	Severity
Viruses			
HIV			
Influenza virus (avian H7N9)	N.D.		
Influenza virus (2009 H1N1)	N.D.		
MERS-CoV	N.D.		
Hepatitis B Virus			
Bacteria			
Mycobacterium tuberculosis	N.D.		
Legionella pneumophila	N.D.		
Campylobacter jejuni	N.D.		
Leptospira spp.	N.D.		
Parasites			
Plasmodium falciparum			
Toxoplasma gondii	N.D.		
Schistosoma mansoni			
Entamoeba histolytica	N.D.		
Fungi			
Paracoccidioides brasilliensis			
Aspergillosis fumigatus	N.D.		
Crptococcus neoformans	N.D.		

= **Male Bias**
= **No Observed Bias**
= **Female Bias**
N.D. = **Not Determined**

Figure 1.14. Obtained from (101). Sex differences in infectious diseases. Sex differences in the intensity (i.e., pathogen load), prevalence (i.e., proportion of population with disease), incidence (i.e., new cases of disease), and severity (i.e., hospitalization or progression of disease state) of disease following microbial infections in humans.

Sex differences in HNSCC

As shown in Figure 1.1, the incidence rate of oropharyngeal cancer is significantly higher in men than in women. Between 1973 and 2006, the incidence of HPV-negative HNSCCs in the US has steadily decreased in both women and men, which is consistent with the decreasing rates of tobacco use over the years. In contrast, the incidence of HPV-positive HNSCCs have steadily increased over the same time period only in men, while

the incidence in women have remained relatively unchanged (Figure 1.15). This trend can also be seen in Figure 1.16 that shows increasing male-female incidence rate ratios for oropharyngeal cancers between 1977 and 2011 in age groups 40-69 years old (102).

Currently, it is unclear whether the significantly higher incidence rate in men can be attributed to sexual behaviors alone, or whether there are biological differences between men and women that make men more susceptible to oral HPV infection. It is possible that the higher incidence of HPV infection in cervical than penile tissue may expose more men to the virus performing oral sex on women, than in women performing oral sex on men. However, 8-40% of HPV-positive HNSCC patients report never having oral sex (53, 103, 104), and therefore, sexual behavior alone may not explain the sex bias in HPV-positive oropharyngeal cancer.

One possible biological explanation for sex differences in HNSCC involves a receptor of the female sex hormone estrogen, ERβ. A study showed that increased ERβ expression or stimulation with an ERβ agonist promotes differentiation by promoting NOTCH1 transcription in HNSCC cells (105). Since estrogen expression, and therefore, ERβ stimulation is higher in females, females may have greater protection from tumorigenesis through promotion of tissue differentiation via the ERβ-NOTCH1 pathway.

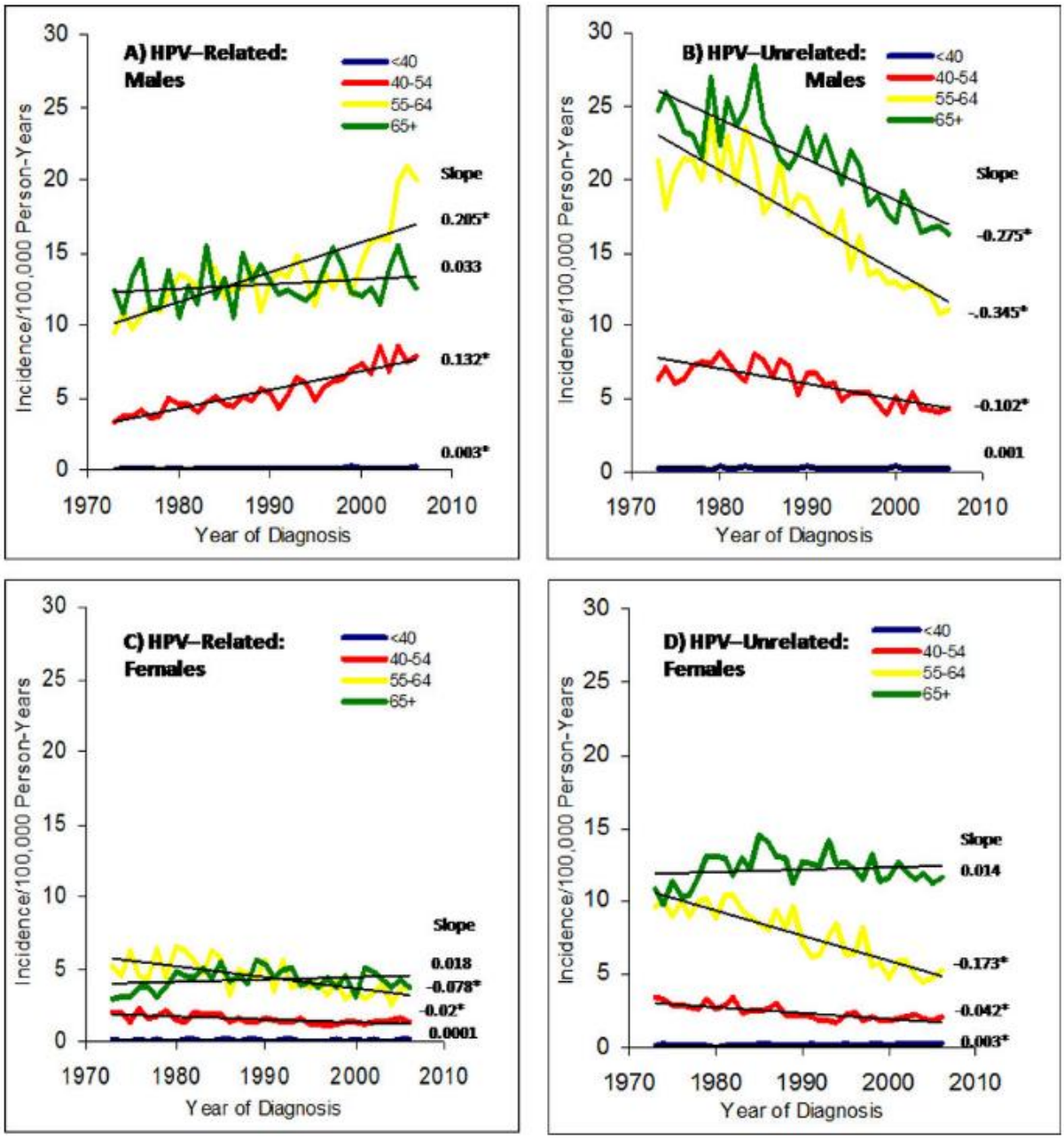

Figure 1.15. Obtained from (53). Incidence rates of HPV-related and HPV-unrelated HNSCCs. Incidence rates of HPV-related and HPV-unrelated HNSCCs in the US between 1973 and 2006, stratified by age at diagnosis.

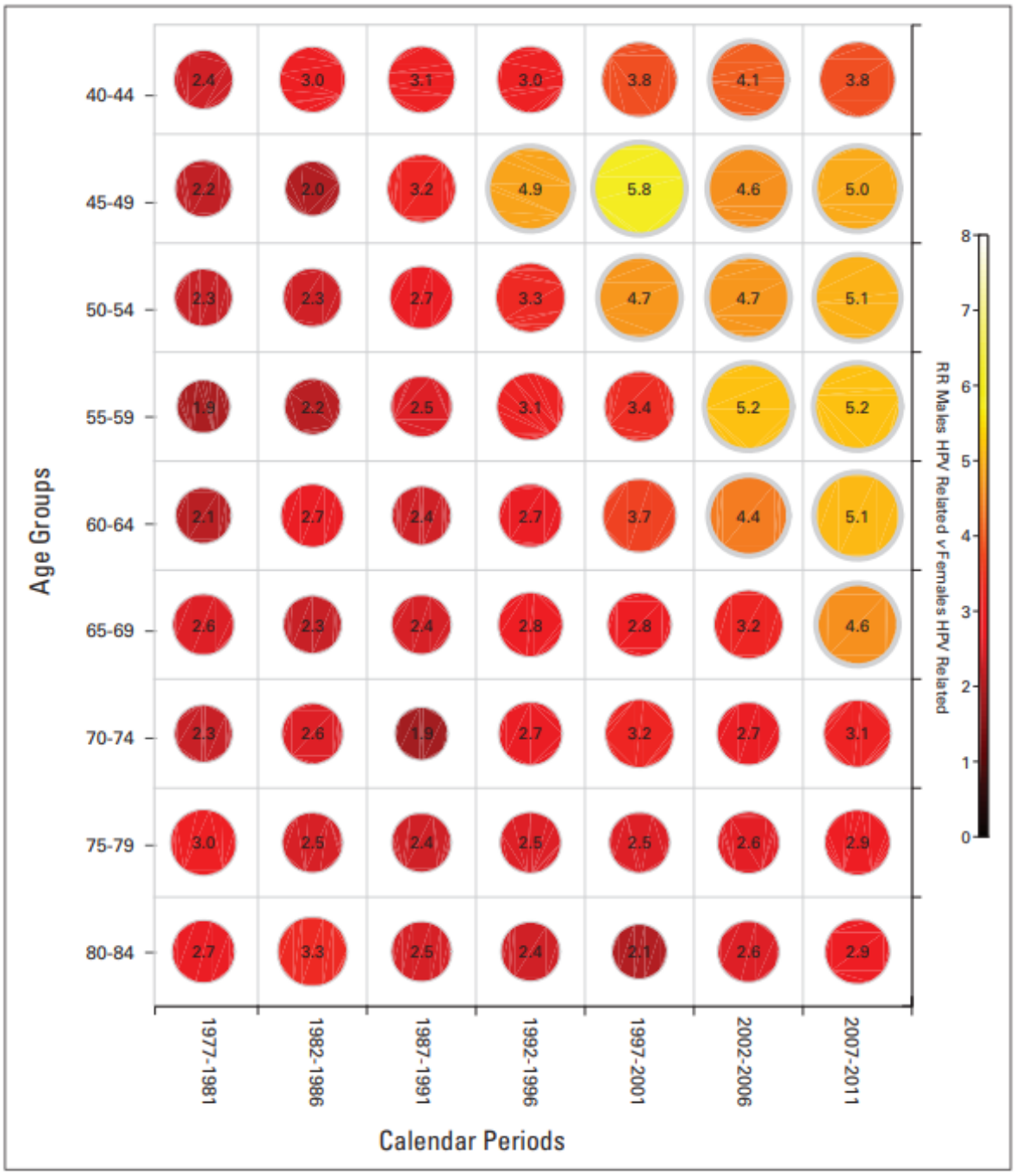

Figure 1.16. Obtained from (102). Male-female incidence rate ratios for oropharyngeal cancers. Shown are male-female incidence rate ratios (RRs) for oropharynx cancers, stratified by age in rows (5-year groups) and calendar periods in columns (5-year groups).

Sex differences in cancer

The incidence of many types of cancers in non-reproductive organs is significantly higher in males than in females including cancers of the colon, skin, head and neck, esophagus, lung, and liver (Figure 1.17) (106). Previously, these sex differences were attributed to environmental and behavioral factors such as exposure to carcinogens, smoking, and alcohol consumption. However, studies have shown that even when adjusted for these factors, males have an overall higher prevalence in various types of cancers (107, 108). Moreover, sex differences exist in childhood malignancies that are mostly not affected by environmental and behavioral factors (109).

It is thought that higher immune surveillance in women, which in some cases result in higher rates of autoimmune diseases, may also help detect and fight against various types of cancer (106). The effect of sex-related hormones and their receptors has been extensively studied in the context of cancers of non-reproductive organs. Androgen receptor (AR) activity increases neutrophil production while decreasing T cell proliferation. A high neutrophil/lymphocyte ratio is a biomarker of poor prognosis in various types of cancers, and since androgen expression is higher in males, this mechanism may have a contribution to sex differences in cancer (110, 111). In contrast, estrogen receptor beta (ERβ) has been shown to protect against several types of cancer including colon cancer, HNSCC, glioma, mesothelioma, renal cell carcinoma, and T cell lymphoma (105, 112–117).

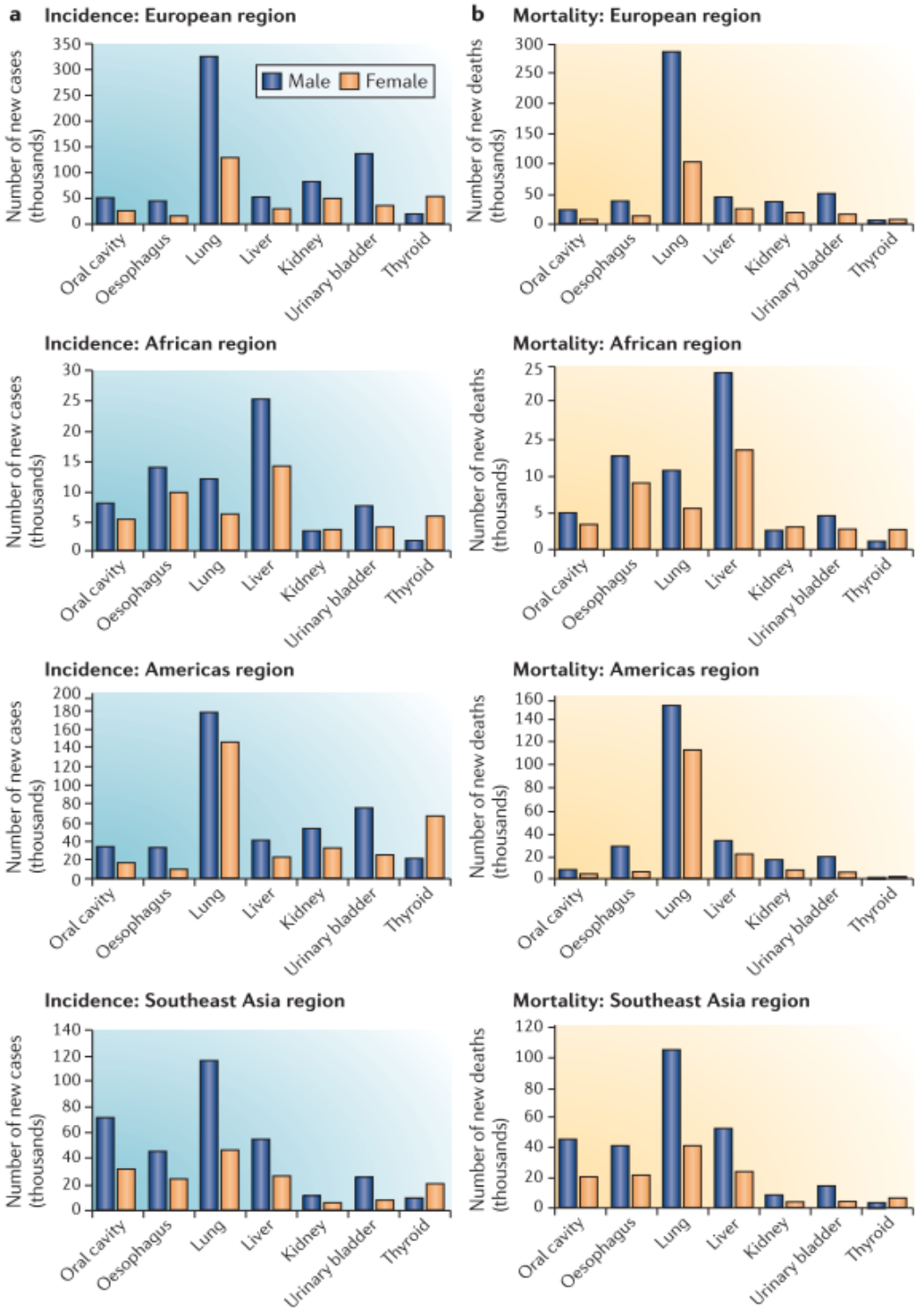

Figure 1.17. Obtained from (106). Sex differences in various cancers. Major cancer types, in organs unrelated to reproductive function, with sex differences in incidence and mortality

HPV in the context of HIV infection

Epidemiology of HPV infection and associated diseases in HIV patients

Previous studies have reported increased rates of HPV infection and HPV-associated diseases in HIV-positive individuals compared to the general population. In a cross-sectional study of female commercial sex workers in Senegal, infection with both HIV-1 and HIV-2 were associated with detection of HPV (118). In another prospective cohort study of homosexual men, HPV-associated high grade anal squamous intraepithelial neoplasia (HG-AIN) incidence was approximately three-fold higher in HIV-positive individuals compared to HIV-negative individuals (119). Increased rates of HPV infection in HIV-positive individuals may also lead to increased risk of HPV-associated cancers. Several studies have reported increased risk of HPV-associated cancers in HIV-positive populations, including cervical cancer, oropharyngeal cancer, and anal cancer (120–124).

The biology of HPV infection in the context of HIV infection

Although higher risk of HPV infection and associated diseases amongst HIV-positive individuals is well-established by numerous studies, not much is known about the biology of HPV infection in the context of HIV infection. One study suggested that the HIV proteins Tat and GP120 may increase initial infection of HPV by disrupting epithelial tight junctions to facilitate HPV pseudovirion infection of the basal cells (120). Another study showed that HIV-1 Tat protein increased the expression of HPV oncoproteins E6 and E7 in human oral keratinocytes, and also significantly increased the proliferation of these cells (125). Similarly, expression of Tat protein in a human cervical carcinoma cell line caused upregulation of E6 expression and subsequent decrease in p53 expression (126). These results suggest that HIV may not only facilitates initial infection, but also the tumorigenesis of HPV-infected cells.

Antiretroviral therapy (ART)

Since its introduction in the late 1980s, antiretroviral therapy (ART) regimens which is used to treat HIV patients have significantly reduced the morbidity and mortality (127). With continued advancements in ART drugs, the life expectancy of HIV patients treated

with ART has reached similar levels of that of the general population (128). In the US, there are currently 28 ART drugs approved by the food and drug administration (FDA) as shown in Table 1.3. The ART drugs can be grouped into five categories depending on the mechanism of action and which step of the HIV life-cycle it inhibits: entry inhibitors (EIs), nucleoside reverse transcriptase inhibitors (NRTIs), non-nucleoside reverse transcriptase inhibitors (NNRTIs), integrase strand transfer inhibitors (INSTIs), and protease inhibitors (PIs) (Table 1.3, Figure 1.17). Entry inhibitors interfere with viral binding to the cellular CCR5 chemokine receptor or fusion of the virus with the host cell membrane. NRTIs and NNRTIs inhibits the reverse transcription of RNA to DNA. INSTIs inhibit the viral integrase enzyme to prevent the integration of viral DNA into the host genome. Lastly, PIs binds to the active site of the viral protease enzyme to prevent cleavage of the precursor protein, which affects viral maturation and infectivity (128) (Figure 1.18).

ART drugs: dermatological side effects of and association with HPV-positive cancers

All groups of ART drugs (PIs, NRTIs, NNRTIs, EIs, INSTIs) have shown to have dermatological adverse reactions, specifically skin rashes (129). Amprenavir and Kaletra are PIs that were approved by the FDA for treating HIV infection in 1999 and 2000, respectively. Kaletra is a coformulation of two drugs, lopinavir and ritonavir. While lopinavir binds to the viral protease to inhibit its activity, ritonavir acts as a pharmacokinetic booster by inhibiting the cytochrome P450 3A4 isoenzyme, which decreases the metabolism of lopinavir and increases its bioavailability (128). In general, the use of ART drugs have been associated various adverse cutaneous reactions (129). The adverse reactions of Amprenavir and Kaletra include dermatological symptoms including skin rashes, toxic epidermal necrolysis, Stevens-Johnson Syndrome, and skin infections, such as cellulitis, folliculitis, and furuncle (130–132). Additionally, both drugs have shown to cause adverse orofacial effects including oral warts, perioral paresthesia, and xerostomia (129, 131, 133–140).

Not much is known on how ART drugs affect epidermal physiology, especially in oral tissue. A few studies have shown that various PIs (Amprenavir and Kaletra) and NRTIs (Efavirenz, Tenofovir, Zidovudine) increase proliferation of suprabasal cells, deregulate differentiation, and affect tissue integrity of primary gingival keratinocytes in organotypic raft cultures (133, 134, 141, 142).

When considering that HPV infects the skin via microabrasion and causes cancer in epithelial tissue, it can be suspected that the dermatological side effects and disruption of epidermal physiology by ART drugs may affect HPV infection. Indeed, epidemiological

studies have shown that HIV patients on ART regimens have significantly increased levels of HPV associated lesions including oral warts and anal cancer (121, 135, 143–147). The effect of ART treatment on cervical cancer is less clear with its incidence remaining stable amongst HIV patients in the post-ART era (121, 148–150). In contrast, use of ART in HIV patients has been associated with a significant decrease in other malignancies and diseases associated with viral and fungal infections including Kaposi sarcoma (Kaposi's sarcoma-associated herpesvirus, KSHV), non-Hodgkin's lymphoma (Epstein-Barr virus, EBV), oral candidosis (Candida albicans), and hairy leucoplakia (EBV) (135, 148–152). This suggests that lowering viral load and restoring immune capacity of the host with ART can generally prevent infection and disease development of a variety of pathogens, but in the case of HPV infection, ART treatment does not have preventative effects and may even contribute to the pathogenesis of HPV-associated lesions and malignancies.

Table 1.3. Obtained from (128). ART drugs. List of FDA-approved ART drugs categorized by mechanism of action.

MECHANISTIC DRUG CLASS	GENERIC NAME	ABBREVIATION(S)	TRADE NAME	YEAR OF U.S. FDA APPROVAL
HIV NUCLEOSIDE ANALOGUE REVERSE TRANSCRIPTASE INHIBITORS (NRTIs)				
	zidovudine	ZDV, AZT	Retrovir	1987
	didanosine	ddI	Videx	1991
	zalcitabine	ddC	Hivid	1992 *
	stavudine	d4T	Zerit	1994
	lamivudine	3TC	Epivir	1995
	abacavir	ABC	Ziagen	1998
	tenofovir	TDF	Viread	2001
	emtricitabine	FTC	Emtriva	2003
HIV NON-NUCLEOSIDE ANALOGUE REVERSE TRANSCRIPTASE INHIBITORS (NNRTIs)				
	nevirapine	NVP	Viramune	1996
	delavirdine	DLV	Rescriptor	1997
	efavirenz	EFV	Sustiva	1998
	etravirine	ETR	Intelence	2008
	rilpivirine	RPV	Edurant	2010
HIV PROTEASE INHIBITORS (PIs)				
	saquinavir	SQV	Invirase	1995
	ritonavir	RTV	Norvir	1996
	indinavir	IDV	Crixivan	1996
	nelfinavir	NFV	Viracept	1997
	amprenavir	APV	Agenerase	1999 *
	lopinavir/ritonavir	LPV/r	Kaletra	2000
	atazanavir	ATV	Reyataz	2003
	fosamprenavir	FPV	Lexiva	2003
	tipranavir	TPV	Aptivus	2005
	darunavir	DRV	Prezista	2006
HIV ENTRY INHIBITORS (EIs)				
Fusion inhibitor	enfuvirtide	ENF, T-20	Fuzeon	2003
CCR5 antagonist	maraviroc	MVC	Selzentry	2007
HIV INTEGRASE INHIBITORS (INSTIs)				
	raltegravir	RAL	Isentress	2007
	elvitegravir	EVG	Viteka	2011
	dolutegravir	DTG	Tivicay	2013

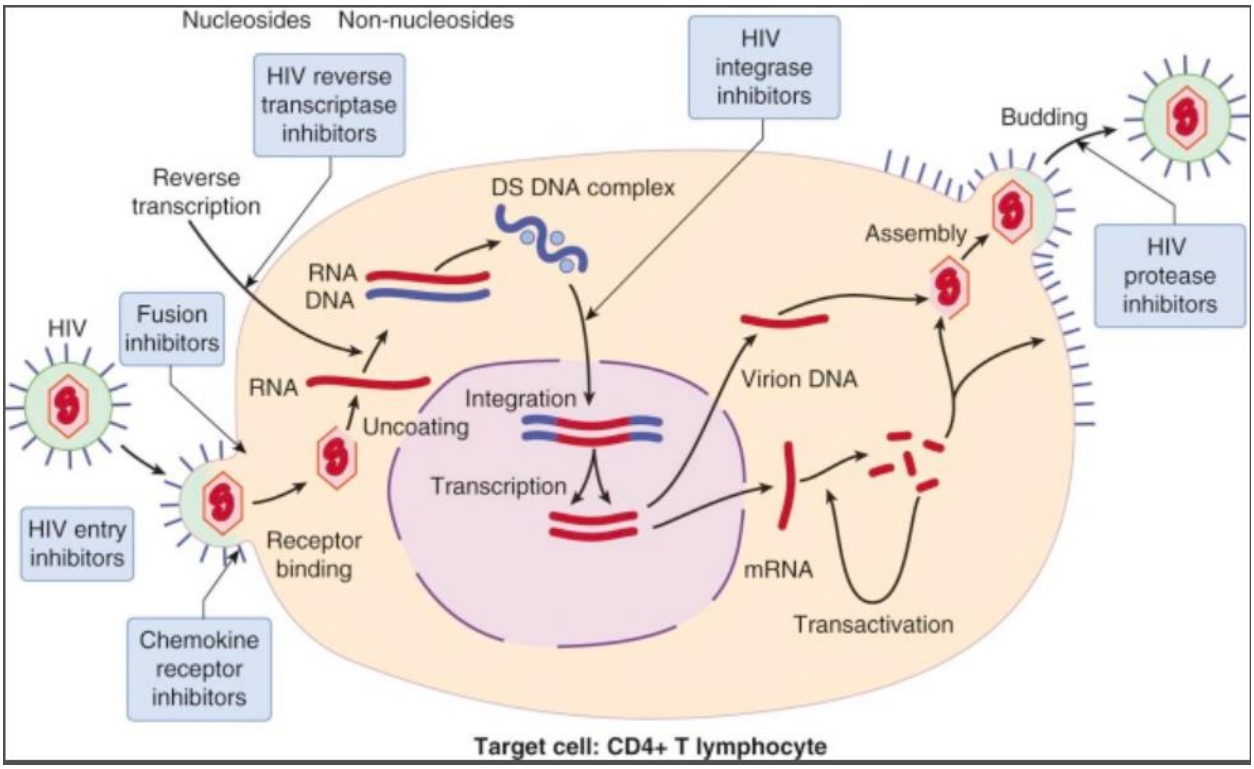

Figure 1.18. Obtained from (128). Life cycle of HIV and mechanisms of action of ART drugs.

CHAPTER 2: Materials and Methods

Creating cervical cell lines and organotypic raft cultures

Primary human cervical keratinocytes (HCK) were isolated from cervical biopsies as previously described (153). The Human Subjects Protection Office of the Institutional Review Board at Penn State University College of Medicine screened our study design for exempt status according to the policies of this institution and the provisions of applicable federal regulations and, as submitted, found not to require formal IRB review because no human participants are involved as defined by the federal regulations.

HCK cell lines persistently infected with HPV16 (16HCK) were produced by electroporating primary HCK with HPV16 plasmid DNA as previously described (27, 154). The electroporated cells were cultured with mitomycin-C-treated (Enzo Life Sciences) J2 3T3 feeder cells as previously described (153).

Organotypic raft cultures were grown as previously described (27, 28) at first or second passage for primary HCK and sixth to ninth passage for 16HCK. The raft tissues were harvested after 10 days for microarray analysis and 20 days for qPCR, Western blot, and immunofluorescence staining. Viral gene expression has been shown to peak between 10 and 12 days (155) while virion maturity reaches maximum stability around 20 days (8).

For microarray analysis, three primary HCK cell lines and three 16HCK cell lines—each representing a different cervical tissue donor—were used to grow raft tissues. These experiments were repeated at separate timepoints to represent a total of six individually grown raft tissues (N=6) for primary HCK and 16HCK each.

For validation experiments (RT-qPCR, Western blots, immunofluorescence staining) we used primary HCK and 16HCK cell lines from new donors in order to increase the rigor of our data. Only one 16HCK cell line that was used for the microarray analysis was also used for the validation experiments, but this raft tissue was grown at a different time point as a separate experiment from tissue grown for the microarray analysis. For experiments with 10 day rafts, three primary HCK cell lines representing three donors (N=3), and three 16HCK cell lines representing three different donors were used to grow raft tissues (N=3). For experiments with 20 day raft tissues, six raft experiments were set up each (N=6) with 16HCK and primary HCK cell lines representing three and six donors, respectively.

Microarray analysis

Raft tissue from primary HCK and 16HCK were harvested at 10 days and RNA was extracted using the RNeasy Fibrous Tissue Midi Kit (Qiagen).Microarray analysis was performed using the Illumina HumanHT-12 v4 Expression Beadchip (Illumina, San Diego,

CA), which targets over 31,000 annotated genes with more than 47,000 probes derived from the National Center for Biotechnology Information (NCBI) RefSeq Release 38 (November 7, 2009) and other sources. RNA quality and concentration were assessed using an Agilent 2100 Bioanalyzer with RNA Nano LabChip (Agilent, Santa Clara, CA). cRNA was synthesized by TotalPrep Amplification (Ambion, Austin, TX) from 500 ng of RNA according to manufacturer's instructions. T7 oligo (dT) primed reverse transcription was used to produce first strand cDNA. cDNA then underwent second strand synthesis and RNA degradation by DNA Polymerase and RNase H, followed by filtration clean up. In vitro transcription (IVT) was employed to generate multiple copies of biotinylated cRNA. The labeled cRNA was purified using filtration, quantified by NanoDrop, and volume-adjusted for a total of 750 ng/sample. Samples were fragmented, and denatured before hybridization for 18 hours at 58°C. Following hybridization, the beadchips were washed and fluorescently labeled. Beadchips were scanned with a BeadArray Reader (Illumina, San Diego, CA).

The CLC Genomics Workbench 4.8 package (https://www.qiagenbioinformatics.com/) was used to determine the significantly differentially expressed genes of the HPV16+ versus primary tissue. For each comparison, quantile normalization of six primary HCK (N=6) and six 16HCK samples (N=6) was performed followed by pairwise homogeneous t-test resulting in normalized fold changes and p-values. Significantly differentially expressed genes were considered to be those with $p < 0.05$ and absolute fold change >= 1.5.

Gene ontology analysis and protein association network

In order to categorize the significant gene expression changes into gene ontology (GO) groups the GOrilla package was used (http://cbl-gorilla.cs.technion.ac.il/) (156). Two unranked lists of genes, target (significantly modulated genes) and background (all genes in the microarray), were used to identify significantly enriched GO terms. We focused on the sub-ontology Biological Processes for our analysis. REVIGO was used to further summarize the redundancy in the GO analysis (http://revigo.irb.hr/) (157). In our analysis, we used the similarity coefficient of 0.7 (medium size list) to summarize the GO list.

In order to identify protein-protein associations amongst the upregulated and downregulated genes, the online tool STRING (https://string-db.org/) was used (158). Genes from similar GO categories were pooled together to form protein association networks of "cell cycle" and "DNA metabolism" for the upregulated genes, and "skin development," "immune response," and "cell death" for the downregulated genes.

Viral Titers (DNA encapsidation assay)

Viral titers of each raft experiment were measured with the qPCR-based DNA encapsidation assay as previously described (8, 159).

RT-qPCR

RT-qPCR was used in order to measure levels of transcription of SERPINB4, KLK8, RPTN, CDK2, and UBC. For *SERPINB4*, forward primer 5'-ATTTCCTGATGGGACTATTGGCAATG-3', reverse primer 5'-CAGCAGCACAATCATGCTTAGA-3', and probe 5'-/56-FAM/ACGACACTG/ZEN/GTTCTTGTGAACGCA/3IABkFQ/-3' was used. For *KLK8*, forward primer 5'-TGGGTCCGAATCAGTAGGT-3', reverse primer 5'-GCAGGAACATCCACGTCTT-3', and probe 5'-/56-FAM/CCCTGGATT/ZEN/CTGGAAGACCTCACC/3IABkFQ/-3' was used. For *RPTN*, forward primer 5'-CCACAAATATGCCAAAGGGAATG-3', reverse primer 5'-GTCATTTGGTCTCTGGAGGATG-3', and probe 5'-/56-FAM/ACTGCTCTT/ZEN/GGCTGAGTTTGGAGA/3IABkFQ/-3' was used. For *CDK2*, forward primer 5'-GCCTGATTACAAGCCAAGTTTC-3', reverse primer 5'-CGCTTGTTAGGGTCGTAGTG-3', and probe 5'-/56-FAM/AGATGGACG/ZEN/GAGCTTGTTATCGCA/3IABkFQ/-3' was used. For *UBC*, forward primer 5'-GGATTTGGGTCGCAGTTCTT-3', reverse primer 5'-TGGATCTTTGCCTTGACATTCT-3', and probe 5'-/56-FAM/AGGTTGAGC/ZEN/CCAGTGACACCATC/3IABkFQ/-3' was used. TATA-binding protein (TBP) was used as control for which forward primer 5'-CACGGCACTGATTTTCAGTTCT-3', reverse primer 5'-TTCTTGC TGCCAGTCTGGACT-3', and probe 5'-HEX-TGTGCACAGGAGCCAAGAGTGAAGA-BHQ-1-3' was used. All primers and probes were synthesized by Integrated DNA Technologies, and QuantiTect Probe RT-PCR Kit (Qiagen) was used for the PCR reactions. All RT-PCR reactions were performed using the C1000 Thermal Cycler (Bio-Rad). The thermal cycler was programmed for 30 minutes at 50 °C, then 15 minutes at 95 °C, then 42 cycles of 15 seconds at 94 °C and 1 minute at 54.5 °C.

Western blot

Raft tissue were harvested at 20 days and used to prepare total protein extracts as previously described (160). Total protein concentrations were measured using the Peterson protein assay as previously described (161). The total protein extracts were applied to sodium dodecyl sulfate polyacrylamide gel (8-10%) and transferred to nitrocellulose membrane, then incubated overnight at 4 °C with antibodies against SERPINB4 (Lifespan Biosciences, LS-C172681, 1:2000 dilution), KLK8 (Abnova, H00011202-M01, 1:2000 dilution), RPTN (Lifespan Biosciences, LS-B17, 1:2000 dilution), KRT23 (Abcam, ab117590, 1:2000 dilution), and ubiquitin (Cell Signaling, 3933S, 1:2000 dilution). GAPDH antibody (Santa Cruz, sc-47724, 1:1000 dilution) was used as control. The membranes were then washed and incubated with horseradish peroxidase-linked secondary antibody (GE Healthcare, NA931VS/NA934VS) and developed using Amersham ECL Prime Western Blotting Detection Reagent (GE Healthcare).

Densitometry analysis was conducted by normalizing the protein expression levels to GAPDH.

Immunohistochemistry and Immunofluorescence Staining

Raft cultures were fixed in 10% buffered formalin, embedded in paraffin, and 4-µm cross-sections were prepared. A section from each sample was stained with hematoxylin and eosin as previously described (29).

For Immunofluorescence staining, the slides were submerged in xylenes for deparaffinization, and then were rehydrated. Antigen retrieval was achieved by submerging the slides in Tris-EDTA buffer (pH 9) in a 90 °C water bath for 10 minutes. The slides were then rinsed with TBS-Tween and blocked with Background Sniper (Biocare Medical). The slides were then stained with the primary antibody overnight at 4 °C. Each sample was stained with antibodies against SERPINB4 (Lifespan Biosciences, LS-C172681, 1:2000 dilution), RPTN (Lifespan Biosciences, LS-B17, 1:1000 dilution), KRT23 (Abcam, ab117590, 1:500 dilution), and Ub (Cell Signaling, 3933S, 1:750 dilution). The slides were then rinsed with TBS-Tween 3 times and stained with secondary antibody (Life Technologies, Alexa Fluor 488) diluted 1:200 for 1 hour at room temperature. Next, the slides were stained with Hoechst nuclear stain (1:5000 dilution) for 15 minutes and rinsed with TBS-Tween twice. All antibodies were diluted in Da Vinci Green diluent (Biocare Medical). The experiment was conducted with three primary HCK and three 16HCK samples in duplicates. A Nikon Eclipse 80i microscope and NIS Elements version 4.4 software was used to acquire images.

Statistical analysis

Microarray data shown in Fig. 1 are quantile normalized means of six primary HCK and six 16HCK samples using the CLC Genomics Workbench 4.8 software package. Statistical significance was determined with the homogeneous t-test, using the CLC Genomics Workbench 4.8 software package.

In order to establish statistical significance in qPCR data and Western blot densitometry analysis, t-test was used with a p-value cutoff of $p < 0.05$.

Bisulfite oligonucleotide-capture sequencing (BOCS)

Genomic DNA (gDNA) was isolated from cultures using silica spin-columns (Zymo Research). gDNA was quantified by fluorescent assay (PicoGreen, Invitrogen). 1 µg of gDNA for each sample was brought up to 50 µl volume with 1X TE and sheared by sonication (Covaris S2) to an average basepair size of 160 using the following settings; intensity of 5, duty cycle of 10%, 200 cycles per burst, 6 cycles of 60 seconds, at 4 °C. The size of sheared products was confirmed by capillary electrophoresis (DNA 1000, Agilent). gDNA libraries (SureSelect XT Methyl-Seq) were then constructed following the

manufacturer's instructions (Agilent). gDNA fragments were end-repaired in 1X XT2 End-Repair Master Mix, and incubated for 30 minutes at 20 °C. End-repaired gDNA fragments were cleaned by magnetic SPRI-bead method (AMPure XP, Beckman-Coulter) and confirmed to be between 140 and 180 basepairs by capillary electrophoresis (DNA 1000). Fragments were then 3' adenylated in 1X XT2 dA-Tailing Master Mix and incubated for 30 minutes at 37 °C. Methylated adapters were ligated on the gDNA fragments in XT2 Ligation Master Mix, incubated for 15 minutes at 20 °C, cleaned, and confirmed to be between 170 and 230 basepairs by capillary electrophoresis (DNA 1000). gDNA libraries were hybridized to the SureSelect Human Methyl-Seq Capture Library (162) (Agilent) for 24 hours at 65 °C. Capture baits were targeted for CGI units [CG Island ± 4kb (shores and shelves)], Gencode promoters, RefSeq promoters, and regulatory features including DNase I hypersensitivity sites and Ensembl regulatory features. Capture Library-hybridized DNA libraries were isolated and eluted using streptavidin beads. Captured DNA libraries were bisulfite converted using the EZ DNA Methylation-Gold method (Zymo Research), PCR amplified for 8 cycles, and bead purified. Libraries were indexed by PCR for 6 cycles, purified, and confirmed to be a library size of approximately 220 bp (High Sensitivity DNA Chip, Agilent). One old female and one young male library failed QC and were not included in the analysis. Libraries were quantified using standard curve qPCR (KAPA Biosystems), diluted to 4nM and pooled at equal volumes. Pooled libraries (12pM) were sequenced using the Illumina HiSeq 2500 and 2x150 Paired-End Rapid and High Output Runs. All raw fastq files are publicly available from the NCBI Sequence Read Archive with the accession number PRJNA290881.

Bioinformatics for methylome analysis

Prior to alignment paired-end reads were adapter trimmed and filtered in CLC Genomics Workbench 8.5.1.; end-trimming removed 3 bp and 4 bp from the 5' and 3' end of each paired-end read, respectively. Only reads with a Q-score >30 were used for mapping, reads which did not meet criteria after trimming were discarded. Alignment of trimmed bisulfite converted sequences was carried out using Bismark Bisulfite Mapper v0.14.4 (163) against the human reference genome (GRCh38). Analysis of methylation was primarily done in R v3.3.0 using the package MethylKit (164).

Total mean methylation levels for CGs and CHs across the whole genome were determined by counts; averaging all per site methylation calls (CGs and CHs separately) which were determined by dividing the methylated counts over total read counts for each site. The mean methylation fraction was then multiplied by 100 (mean methylation call = (methylated counts /total read counts) X 100). Only cytosines in the BOCS targeted regions, covered by at least 10 reads, and that were present in all samples within a comparison were included for statistical analysis.

Differentially methylated cytosines (DMCG and DMCH) were determined from those sites passing coverage criteria. Differentially methylated sites between groups were determined using logistic regression (164). P-values were adjusted using a false-

discovery rate, or FDR (165). Only sites with a q-value < 0.05 and an absolute methylation difference of ≥ 5% were considered significant.
Differentially methylated sites were examined for enrichment in specific genomic elements and annotated using the R package GenomicFeatures. Refseq genes and CGI unit's coordinates were downloaded from UCSC genome browser (GRCh38) (https://genome.ucsc.edu/). Sites were examined for overlap with genic regions: introns, exons and promoters (defined as 3kb upstream and 300bp downstream of the transcription start site) or CGI units [CG Island including shores (± 2kb from islands), and shelves (± 2kb from shores), or CG Island ± 4kb]. Regions to which no overlap with any Refseq annotated genes was found were determined to be present in intergenic regions. Regions with no overlap with CGI units were annotated as 'other'. Two-tailed χ^2 test (alpha = 0.05) was used to determine the statistically significant differences in observed versus expected genomic annotation frequencies of differential methylated sites. Data is presented as fractions related to the total distribution of the sites analyzed.

Accession number.

The GEO accession number for our microarray data is GSE109039.

CHAPTER 3: The Effect of Productive HPV16 Infection on Global Gene Expression of Cervical Epithelium

*This chapter was published in Journal of Virology in 2018 (166).

Microarray analysis of HPV16 infection in cervical tissue

Global gene expression changes in cervical tissue infected with HPV16 at a pre-neoplastic state were measured by conducting cDNA microarray analysis (GEO accession no. GSE109039) on 10-day organotypic raft tissue from early passage human cervical keratinocytes (HCK) persistently infected with HPV16 (16HCK). In order to create 16HCK cell lines, human cervical tissue from biopsies were acquired, processed, and cultured with keratinocyte-selective medium to grow primary HCKs. The HCKs were then electroporated with the HPV16 genome to establish persistent infection and immortalization. We used organotypic raft cultures as previously described, which allows us to observe the full HPV life-cycle in 3-dimensional (3D) tissue at a precancerous stage of infection when HPV particles are maximally produced. The organotypic raft tissue was harvested at 10 days of culture for microarray analysis when particle production is most active (155), and 20 days of culture when particle maturation is at its maximum (8) to measure the viral titer showing that virus particles are produced at high levels (Table 3.1). By infecting each cell line with the same virus and subjecting the raft cultures to the same condition, we are able to minimize variables and observe the specific effect of HPV infection on cervical tissue.

The experiment was conducted in six individually grown raft tissue representing three donor 16HCK cell lines, and raft tissue from uninfected HCKs served as control. Out of the 34,575 genes that were analyzed with cDNA microarray, a total of 1,245 genes were modified at least 1.5-fold ($p<0.05$) and 533 genes were modified at least 2-fold ($p<0.05$) with HPV16 infection as compared to uninfected control. The average of the pairwise Pearson correlation of the primary HCK samples was 0.885, and that of the 16HCK samples was 0.941. Of those genes that were significantly modulated at least 1.5-fold, 594 genes were upregulated and 651 genes were downregulated. Table 3.2 and 3.3 show the 50 most upregulated and downregulated genes in the microarray analysis. Amongst the top 50 upregulated genes are those associated with cell cycle (*CDKN2A*, *CDC7*, *NASP*, *MDC1*, *NFIX*, *FOXQ1*). In contrast, the 50 most downregulated genes span

from those involved in differentiation (*RPTN*, *LCE1D*, *LCE3C*, *LCE1E*, *S100A7*), ECM-modulation (*KLK6, 8, 10, 13* and *MMP 9, 10*), immune regulation (*LCN2*, *SPNS2*, *FAM3D*, *IL1RN*, *PSG4*, *IL1F7*) to antimicrobial response (*RNASE7*, *PRSS3*, *PRSS2*). This suggests that HPV infection is driving the cell cycle, and disrupting epidermal differentiation and ECM homeostasis while evading the immune and antimicrobial responses by downregulating them.

While most previous global gene expression studies have focused on neoplastic and cancerous stages of HPV infection (36–44), two previous studies have modeled pre-neoplastic, early stage HPV infection similar to our study (45, 46). However, most of the modulated genes in the two studies did not overlap with our results. One of these studies reported that 135 genes were modulated with HPV infection, but only 38 (28.1%) of these were modulated in the same direction and 4 of them were modulated in the opposite direction in our microarray analysis (45). In the other study, a total of 966 genes were reported to be modulated with HPV infection, but only 15 (1.6%) of these were modulated in the same direction in our microarray analysis (46). The two major differences between our study and the two previous studies is that we use cervical keratinocytes instead of foreskin keratinocytes, and that we use organotypic raft cultures instead of monolayer cultures that do not allow HPV to complete its life cycle. Using keratinocytes derived from cervical tissue, and organotypic raft cultures that allow the virus to complete its life cycle in 3D tissue enables us to capture the whole picture of an early stage HPV infection in the cervix.

While fold-change of the 50 most upregulated genes ranged between 12.1 to 2.5, that of the 50 most downregulated genes ranged between 57.5 and 6 indicating that a greater degree of gene modulation occurred in the downregulated genes than the upregulated genes. Similarly, when the cutoff for inclusion was increased to at least 5-fold modulation, only 6 genes were upregulated in contrast to 72 genes that were downregulated as shown in Figure 3.1. This suggests that HPV16 is disrupting the host's physiology mostly by dampening many of the normal processes that may interfere with the virus's survival and replication.

Table 3.1. Viral titers of organotypic rafts. Published in (166).

Raft Identification	**Viral particles per raft**
16HCK-1, replicate 1	9.38×10^7
16HCK-1, replicate 2	1.18×10^7
16HCK-2, replicate 1	5.25×10^8
16HCK-2, replicate 2	6.5×10^9

16HCK-3, replicate 1	5.81×10^7
16HCK-3, replicate 2	1.6×10^9

Table 3.2. Top 50 upregulated genes with productive HPV16 infection. Published in (166).

GENE	FUNCTION	FOLD CHANGE
MT1G	Metallothioneins have a high content of cysteine residues that bind various heavy metals; these proteins are transcriptionally regulated by both heavy metals and glucocorticoids.	12.032
MT1H	Mineral absorption/ metabolism	7.679
TGFBR3	Binds to TGF-beta. Could be involved in capturing and retaining TGF-beta for presentation to the signaling receptors	7.295
KLHL35	Kelch-like family member. Kelch-repeat β-propellers are generally involved in protein-protein interactions	5.814
DLK2	Calcium ion binding and protein dimerization activity	5.057
FBLN1	Cell adhesion/ migration/ ECM architecture organization	5.056
ASS1	Arginine biosynthetic pathway	4.446
GPER	G Protein coupled estrogen receptor; cAMP signaling, calcium mobilization	4.446
TDRD9	Probable ATP binding RNA helicase	4.393
TWIST1	Transcription factor, role in cell lineage determination and differentiation	4.208
FANCE	Member of the Fanconi anemia complementation group E	4.183
JAM3	Cell to cell adhesion in epithelial and endothelial cells	4.169
CDKN2A	Cell cycle regulation	4.122
TSPAN4	Cell surface protein that mediate cell development, activation, growth and motility	3.733
LTBP4	Involved in assembly, targeting and activation of TGFB1	3.718
ERAP2	Aminopeptidase involved in peptide trimming, MHC class I presentation	3.551
LOC341230	Similar to argininosuccinate synthetase	3.454
MXRA5	Matrix remodeling associated proteins	3.281
RPS23	Component of the 40S ribosomal subunit	3.23
C14orf132	Putative uncharacterized protein	3.165
CRIP2	Putative transcription factor with two LIM zinc binding domains	3.148

ANGPTL2	Member of the vascular endothelial growth factor family	3.061
GOLPH4	Involved in endosome to Golgi protein trafficking	3.058
DPYSL2	Cytoskeletal remodeling, endocytosis	3.013
CDC7	Checkpoint control kinase critical for G1/S transition	2.981
FAM134B	ER anchored autophagy receptor	2.947
NASP	Histone binding protein with a role in cell division, cell cycle progression and proliferation	2.885
HEG1	Calcium ion binding receptor component, may act through stabilization of endothelial cell junctions	2.866
ZCWPW1	Zinc finger domain containing protein	2.8
MTE	Metallothioneins have a high content of cysteine residues that bind various heavy metals.	2.786
MDC1	Required for checkpoint mediated cell cycle arrest in response to DNA damage	2.783
CDH13	Calcium dependent cell adhesion proteins	2.775
OLFML2A	Extracellular matrix binding protein	2.762
LOC392871	Undetermined gene ortholog	2.728
CYBRD1	Ferric chelate reductase	2.726
RASIP1	Ras interacting protein required for the formation of vascular structures	2.721
LOC729137	Undetermined gene ortholog	2.7
GPNMB	Type 1 transmembrane glycoprotein	2.693
MOBKL2B	May regulate the activity of kinases	2.672
LOC388494	Undetermined gene ortholog	2.645
C10orf54	Putative uncharacterized protein	2.644
E2F2	E2F family of transcription factors	2.572
LFNG	Transferase enzyme	2.571
LOC100133866	Undetermined gene ortholog	2.568
NFIX	DNA binding protein, capable of activating transcription and replication	2.56
P4HTM	Prolyl hydroxylases	2.553
RELL1	Receptor expressed in lymphoid tissue like 1	2.551
FOXQ1	FOX genes involved in gene development, cell proliferation and tissue specific gene expression	2.53
TJAP1	Tight junction associated protein	2.527
HOXA11AS	Non-coding RNA gene	2.525
FN3KRP	Phosphorylates psicosamines and ribulosamines	2.514

Table 3.3. Top 50 downregulated genes with productive HPV16 infection. Published in (166).

GENE	FUNCTION	FOLD CHANGE
RPTN	Involved in the cornified cell envelope formation. Multifunctional epidermal matrix protein. Reversibly binds calcium.	-57.487
SERPINB4	May act as a protease inhibitor to modulate the host immune response against tumor cells	-48.016
TCN1	Binds Vit B12 and protects it from the acidic environment of the stomach	-34.735
CST6	Active cysteine protease inhibitors. Loss of function is associated with progression of primary tumor to a metastatic phenotype	-27.758
KLK8	Serine proteases with diverse physiological function	-25.804
CEACAM6	GPI anchored glycoprotein and plays a role in cell adhesion	-24.469
KLK6	Serine proteases regulated by steroids	-22.088
KLK13	Expression regulated by steroid hormones and important marker for breast cancer	-21.464
RNASE7	Pancreatic ribosomal protein; broad spectrum antimicrobial activity against bacteria and fungi	-20.029
PRSS3	Digestive protease specialized for the degradation of trypsin inhibitors. In the ileum, may be involved in defensin processing, including DEFA5	-19.968
LCE1D	Precursors of the cornified layers of the stratum corneum	-17.868
MMP9	Zinc dependent endopeptidases and major proteases involved in the degradation of the ECM	-17.142
FLJ22662	Weak phospholipase activity. May act as an amidase or peptidase	-14.394
TMEM45B	Transmembrane protein 45B	-13.469
DMKN	Expressed in differentiated layers of the skin. Upregulated in inflammatory disease	-13.186
C6orf15	Uncharacterized protein coding gene	-12.641
TMEM45A	Paralog of TMEM45B	-12.629
PNLIPRP3	Triglyceride lipase activity	-11.232
KRT23	intermediate filament protein	-11.074
ANXA9	Calcium dependent phospholipid binding protein; binds ECM proteins	-10.728

LCE3C	Precursors of the cornified layers of the stratum corneum	-10.044
S100A7	Calcium binding proteins involved in cell cycle progression and cellular differentiation	-9.88
EPS8L1	Substrate for the Epidermal growth factor receptor	-9.659
RORA	Member of NR1 family of nuclear hormone receptors	-9.136
LCN2	Iron trafficking protein involved in apoptosis, innate immunity and renal development	-9.134
LCE1E	Precursors of the cornified layers of the stratum corneum	-9.067
SPNS2	Sphingolipid transporter with critical function in cardiovascular, immunological and neuronal development	-8.787
FAM3D	Related to cytokine activity	-8.734
KLK7	Member of the kallikrein family of serine proteases	-8.61
HMOX1	Heme oxygenase, an essential enzyme in heme catabolism	-8.548
RNF39	Role in early phase of synaptic plasticity	-8.5
SH3BGRL2	Protein disulphide oxidoreductase activity	-8.478
C1orf68	Uncharacterized protein coding gene	-8.417
POF1B	Key role in organization of the epithelial monolayers by regulating the actin cytoskeleton	-8.233
ATP6V1C2	Subunit of the peripheral V1 complex of the vacuolar ATPase	-8.232
MMP10	Zinc dependent endopeptidases and major proteases involved in the degradation of the ECM	-7.953
LOC730833	Undetermined gene ortholog	-7.935
CAPNS2	Calcium regulated thiol protease, role in tissue remodeling and signal transduction	-7.64
KLK10	Member of the kallikrein family of serine proteases	-7.553
IL1RN	Inhibits the activity of Interleukin-1	-7.499
ABCG1	Intracellular lipid transport	-7.408
THEM5	Role in mitochondrial fatty acid metabolism	-7.287
CYP2J2	Role in arachidonic acid metabolism	-7.259
PRSS2	Serine protease involved in defensin processing	-7.239
LOC645869	Undetermined gene ortholog	-6.803
PSG4	May play a role in regulation of innate immune system	-6.559
FAM63A	Role in protein turnover, deubiquitinase activity	-6.52
MAP2	Stabilizing/stiffening of microtubules	-6.474
SLC5A1	Na^+ /glucose cotransporter	-6.468
IL1F7	Interleukin 1 related gene	-6.392
EPB41L3	Tumor suppressor that inhibits cell proliferation and promotes apoptosis	-6.356

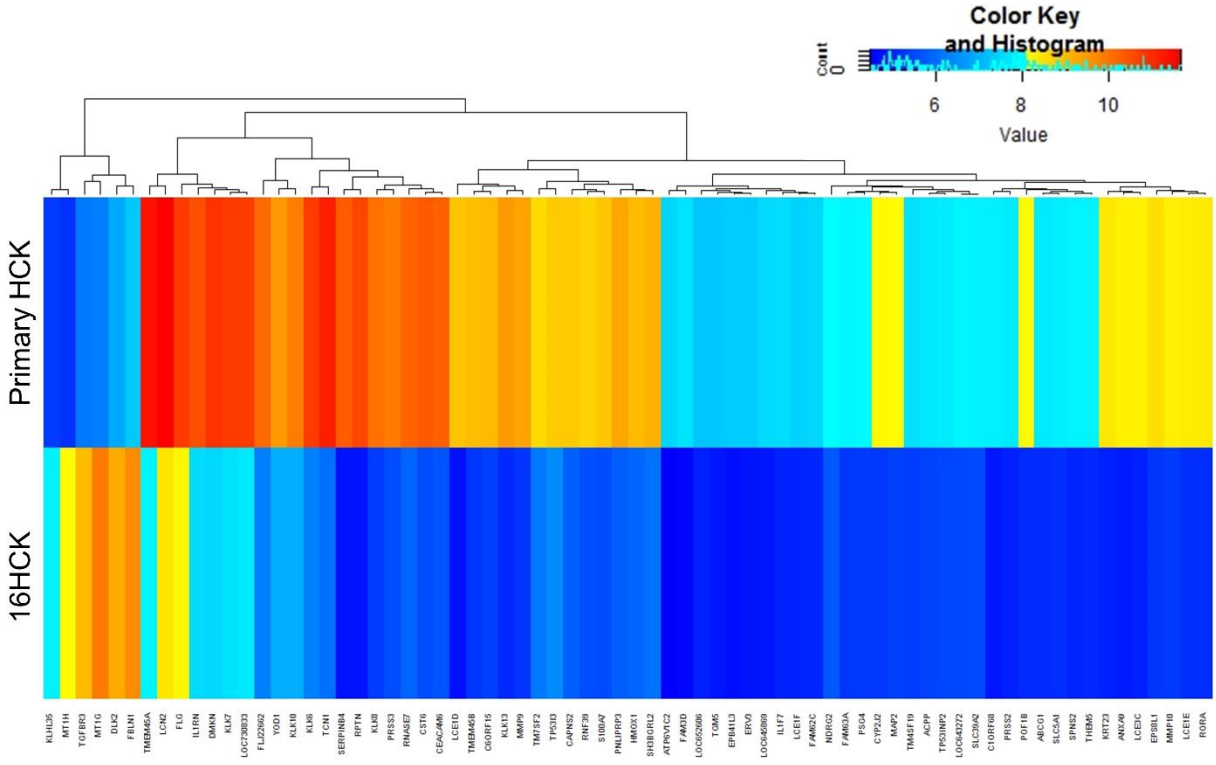

Figure 3.1. Published in (166). Heat map of significantly modified genes. Six raft experiments were set up each with 16HCK and primary HCK cell lines representing three donors each. The tissue were harvested at 10 days of culture for RNA extraction and microarray analysis. The heat map shows genes that were significantly modulated ($p < 0.05$) at least 5-fold with HPV16 infection.

Gene ontology analysis

In order to identify biological pathways that are significantly affected with HPV16 infection, we conducted gene ontology (GO) analysis using the online tool GOrilla (156). The GO analysis result was then summarized using REVIGO to combine similar GO terms for simplified visualization (157). 144 GO terms that were significantly represented in upregulated genes were summarized to 82 GO terms, and 77 GO terms that were significantly represented in downregulated genes were summarized to 52 GO terms using REVIGO.

Amongst the genes that were upregulated with HPV16 infection, many of the represented GO terms are associated with cell cycle progression (cell cycle process, cell division, cell cycle phase transition, regulation of mitotic cell cycle, and cell cycle) and DNA metabolism (DNA metabolic process, DNA repair, cellular response to DNA damage stimulus) as shown in Figure 3.2A. This suggests that persistent infection with HPV16 drives cellular proliferation in cervical tissue as expected due to the presence of viral oncogenes E6/E7 and consistent with previous gene expression studies (39, 42, 49, 167). It is known that HPV oncoproteins E6 and E7 inhibit tumor suppressor genes *TP53* and *RB1* respectively, and that this is the main mechanism through which the virus promotes proliferation and tumorigenesis. "Translesion synthesis," "neuron projection regeneration," and "retina morphogenesis in camera-type eye" were amongst the upregulated DNA metabolism GO terms which have not yet been reported by previous global gene expression studies of HPV16 infection. Translesion synthesis is a cellular DNA damage tolerance process of recovering from stalled replication forks by allowing DNA replication to bypass certain lesions (168, 169). Eight genes of the translesion synthesis GO category were upregulated in our analysis including *POLE2*, *UBA7*, *MAD2L2*, and *RPA2* which have not yet been reported in previous global gene expression studies of HPV infection. So far, not much is known about the exact role of translesion synthesis in HPV infection. One previous study speculated that HPV oncoprotein E6 may have inhibitory effects on translesion synthesis (170) while another study reported that p80, a cellular cofactor of HPV31 replication, may downregulate translesion synthesis (168). Our study shows for the first time that translesion synthesis is upregulated in a productive raft culture model of HPV16, suggesting that this process may facilitate viral replication and production.

Within the genes that were downregulated with HPV16 infection, the GO terms that were significantly represented are associated with skin development (epidermis development, keratinocyte differentiation), immune response (positive regulation of IKK/NF-κB signaling, antimicrobial humoral response), and cell death (cell death, positive regulation of JNK cascade) as shown in Figure 3.2B. Downregulation of genes associated with skin development have also been observed in previous studies of HPV-positive tumors (36, 40, 171). Similarly, downregulation of genes under GO terms associated with immune response and cell death have been shown in previous studies of HPV-positive tumors and E6 transgenic mice (38, 41, 45, 46, 50, 172). Overall, these results suggest that HPV16 perturbs normal epidermal development while having a hyperproliferative and immunosuppressive effect on cervical tissue. Downregulated GO terms that have not yet been reported in previous global gene profiling studies of HPV infection included "positive regulation of cell migration" and "regulation of platelet-derived growth factor production". In contrast to our results, previous studies of global gene expression at cancerous stages of HPV infection have shown upregulation of genes

involved in cell migration, which is an indicator of invasive, or metastatic cancer (38, 43, 173). Specifically, one study showed that *MMP9*, a well-established metastatic gene, is upregulated in cervical carcinoma cell lines and tissue samples, whereas our microarray analysis shows that this gene is downregulated 17.1-fold (173). Moreover, *LCN2*, which is overexpressed in various cancers and prevents degradation of *MMP9*, was downregulated 9.1-fold in our microarray analysis (174–181). These opposing trends in modulation of cell migration genes highlights the fact that our study investigates early productive stages of HPV infection, whereas the other studies focus on the cancerous stages of infection when viral production is significantly decreased. We speculate that cell migration genes interfere with efficient viral replication and assembly and, therefore, are suppressed during the productive stages of infection, whereas these genes are upregulated to facilitate tumor development and metastasis once the infection enters the cancerous stages.

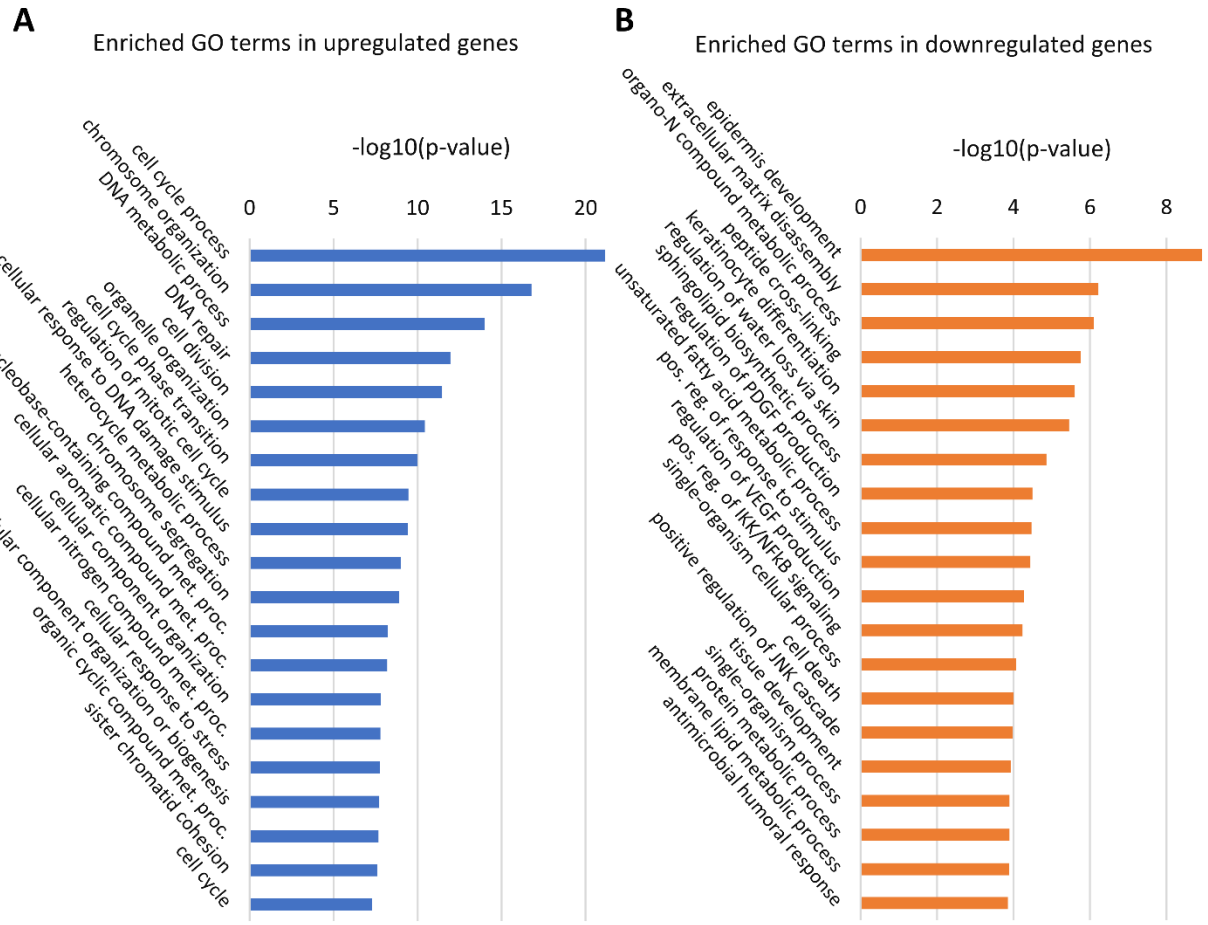

Figure 3.2. Published in (166). Enriched GO terms with lowest p-values. GOrilla was used to perform initial GO analysis of our microarray data, and REVIGO was used to

summarize the enriched GO genesets from the upregulated (A) and downregulated (B) list of genes. Met. proc.: metabolic process.

Upregulation of cell cycle and DNA metabolism

While GO analysis revealed biological processes that are significantly affected by persistent infection of HPV16, it does not provide information on interactions amongst the genes. Therefore, we further examined the interaction amongst individual proteins based on published data using the online tool STRING (158, 182). STRING protein-protein interaction network analysis allows us to identify signaling pathways, interactions amongst signaling pathways, and central proteins that have maximum interactions with other proteins within a category. A protein association network was created for each of the five aforementioned categories of biological processes that were broadly represented in the GO analysis: cell cycle, DNA metabolism, skin development, immune response, and cell death.

From the upregulated genes, a protein association network was created with genes from 32 GO terms related to cell cycle (Figure 3.3A). Genes that are not known to be associated with any other gene in this group were excluded from the figure for simplified visualization. The protein association analysis revealed 15 genes that are central to the network as highlighted in red in Figure 3.3A. These genes include nucleoporins (*NUP 43, 85, 107*), centromere proteins (*CENP E, F, P*), and kinetochore-associated proteins (*KNTC1, SKA2*). This suggests that HPV infection drives the cell cycle and increases the expression of structural proteins involved in cell cycle and cell division. Amongst these genes, *NUP43*, *NUP85*, *NUP107*, *CENPP*, and *SKA2* have not yet been reported to be associated with HPV infection by previous gene expression studies.

Similarly, a protein association network was created with genes from 42 GO terms related to DNA metabolism (Figure 3.3B). Genes in this network include minichromosome maintenance complex components (*MCM 3, 6, 7*), replication factors (*RFC 2, 3, 5*), and DNA polymerase subunits (*POLA1, POLE, POLE2, POLD1*). Amongst these genes, *POLA1*, *POLE*, and *POLE2* have not yet been reported to be associated with HPV infection by previous gene expression studies. Previous studies have shown that overexpression of MCM genes are correlated to cervical carcinogenesis and specifically, *MCM7* has been shown to interact with HPV18 E6 oncoprotein (183, 184). These results are consistent with upregulation of cell cycle genes since cell division requires DNA replication and proteins associated with DNA metabolism. Additionally, our result

suggests that the upregulation of MCM genes is initiated at early stages of HPV infection and sustained throughout carcinogenesis.

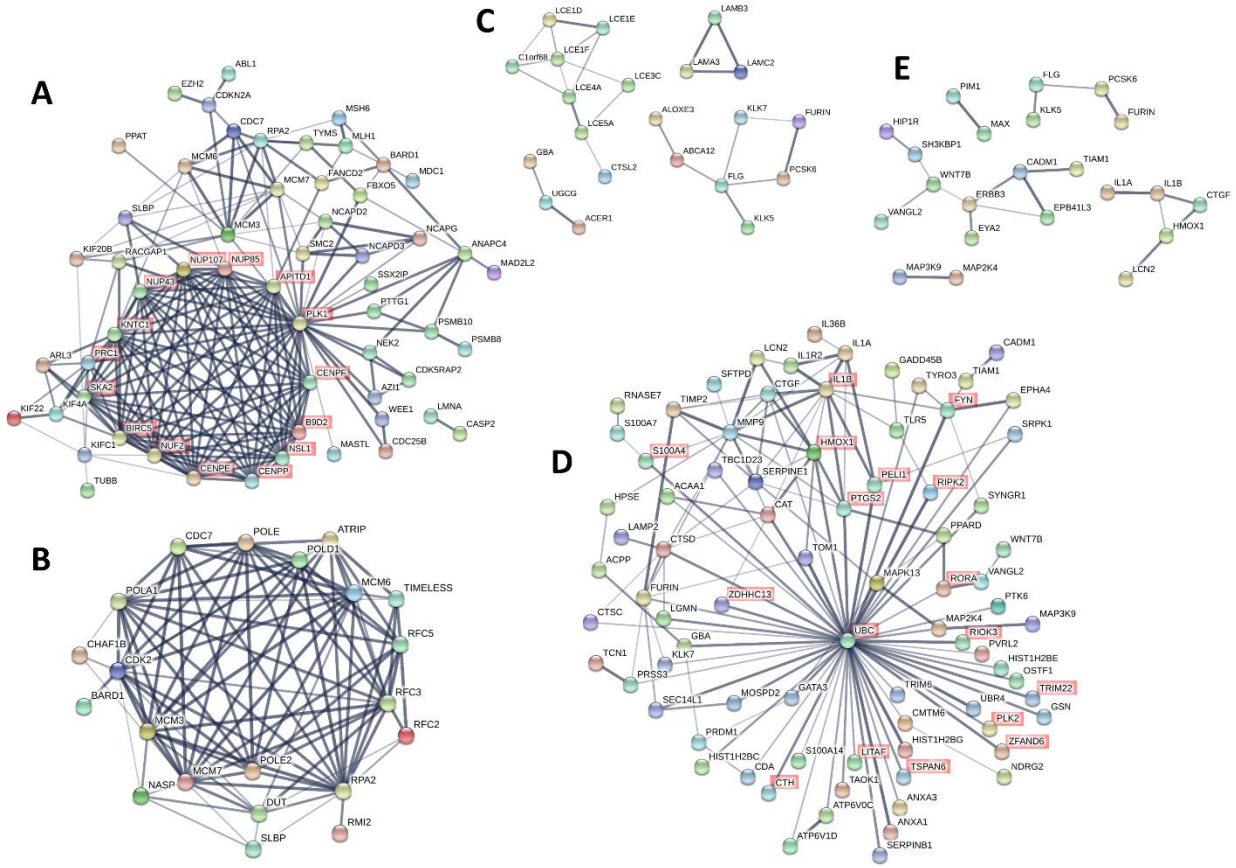

Figure 3.3. Published in (166). Protein association networks. Online tool STRING was used to create protein functional association networks of upregulated (A-B) and downregulated (C-E) genes with >1.5-fold modulation ($p<0.05$). (A) Genes from GO categories related to cell cycle regulation were combined to create the network. (B) Genes from GO categories related to DNA metabolism were combined to create the network. (C) Genes from GO categories related to skin development and differentiation were combined to create the network. (D) Genes from GO categories related to inflammation and immune response were combined to create the network. (E) Genes from GO categories related to apoptosis and cell death were combined to create the network. Thicker and darker lines represent greater confidence in protein interaction based on supporting data. Genes that had no connection to any other gene within the network were excluded from the diagram.

Downregulation of skin development, immune response, and cell death

Within the downregulated gene sets, we combined genes from 7 GO terms in the protein association analysis for skin development, which gave 4 small networks (Figure 3.3C) including a network of late cornified envelope genes (*LCE 1D, 1E, 1F, 3C, 4A, 5A*) and a network of laminins (*LAMA3*, *LAMB3*, *LAMC2*). All eight genes in the network of LCEs were included in the GO term "epithelial cell differentiation" while the three laminin genes were included in the GO term "epidermis development." The LCE genes encode stratum corneum proteins of the epidermis, and are all located in the same region of chromosome 1 (1q21.3) suggesting that epigenetic modifications might be suppressing the expression of this region as a whole. Our study shows for the first time the downregulation of a network of LCE genes in HPV infection. The two previous studies that analyzed global gene expression changes in early stage HPV infection may not have observed changes in LCE genes since they used monolayer cultures that do not allow formation of the four strata of differentiating keratinocytes in the epidermis (45, 46). The three laminin genes *LAMA3*, *LAMB3*, and *LAMC2* encode the three subunits that make up laminin 5, which plays an important role in wound healing, keratinocyte adhesion, motility, and proliferation (185, 186).

Genes from 16 GO terms were included in the protein association analysis for inflammation (Figure 3D). Ubiquitin C (*UBC*), which is downregulated 2.48-fold with HPV16 infection, is at the center of this network with the most associations with other genes related to inflammation. *UBC* is one of the two polyubiquitin genes that are involved in various cellular processes including protein degradation, protein trafficking, cell-cycle regulation, DNA repair, and apoptosis (187). Other ubiquitin-related genes that were significantly downregulated in our microarray analysis includes proteins that are involved in ubiquitin conjugation (*UBE2G1*, *UBE2F*, *UBR4*, *UBTD1*), whereas two of the four ubiquitin-related genes that were significantly upregulated are involved in deubiquitination (*USP1*, *USP13*). This suggests that a decrease in ubiquitination may be important in the HPV16 life-cycle, and that the virus is trying to achieve this by decreasing ubiquitination and increasing deubiquitination. In previous studies, UBR4 has been shown to be a cellular target of HPV16 E7 oncoprotein (188, 189), and we have shown that HPV16 upregulates deubiquitinase UCHL1 in order to escape host immunity (190). Since ubiquitins are involved in many cellular processes, it is hard to identify which specific pathway is being affected by the decrease in ubiquitination. It is possible that the virus is preventing degradation of proteins that are targeted by ubiquitin. Also,

since our results suggest that HPV infection drives cell cycle and downregulates cell death, it is possible that the downregulation of ubiquitination is involved in these processes. The network also included cytokines (*IL1A*, *IL1B*, *IL36B*), MAP kinases (*MAPK13*, *MAP2K4*, *MAP3K9*), proteases (*CTSD*, *CTSC*, *KLK7*, *FURIN*), serine protease inhibitors (*SERPINB1*, *SERPINE1*), and antimicrobial genes (*S100A7*, *RNASE7*, *PRSS3*, *HIST1H2BC*, *HIST1H2BE*, *HIST1H2BG*, *LCN2*). Amongst these genes, *MAP3K9*, *CTSD*, *CTSC*, *SERPINE1*, *HIST1H2BC*, *HIST1H2BE*, and *HIST1H2BG* have not yet been reported to be associated with HPV infection by previous gene expression studies. Of note, RNASE7 is a broad-spectrum antimicrobial protein that we have previously shown to be downregulated by HPV infection (191). In terms of specific signaling pathways, regulation of I-kappaB kinase (IKK) and NF-κB signaling was significantly represented in the network (Figure 3.3D, highlighted in red), which is consistent with our previous study that showed suppression of NF-κB activation by HPV16 (192). Most of these genes were shown to interact with UBC (Figure 3.3D), and it is known that ubiquitination and proteolytic degradation of NF-κB inhibitor IκB can lead to NF-κB activation (193). This suggests that HPV16 is evading the immune system by suppressing the NF-κB pathway, and that this suppression may be mediated by downregulation of UBC.

Lastly, genes from 4 GO terms were included in the protein association analysis for cell death and gave 5 small networks (Figure 3.3E). The networks include genes from the JNK signaling pathway (*TIAM1*, *IL1B*, *VANGL2*, *CTGF*, *WNT7B*) suggesting that HPV16 may be suppressing cell death, and promoting transformation and tumorigenesis through this pathway. This is consistent with our previous study that showed downregulation of cell death with HPV infection (194). Both NF-κB and JNK pathways are downstream of TNF signaling, and TNF ligands and receptors (*TNFRSF19*, *LITAF*, *TNFSF9*) were downregulated in the microarray. This suggests that HPV16 is downregulating NF-κB and JNK pathways via TNF signaling downregulation. Amongst these genes, *TIAM1*, *VANGL2*, *WNT7B*, *TNFRSF19*, and *LITAF* have not yet been reported to be associated with HPV infection by previous gene expression studies.

Gene transcription changes correlate with changes in protein expression

Of the numerous biological processes that were identified with GO analysis, we wanted to focus on processes and pathways that we felt were unique and most relevant to HPV

infection and life-cycle. Therefore, four genes that were modulated at least 10-fold were selected for validation from processes involving epidermal development and differentiation (*KLK8*, *RPTN*, *KRT23*), and immune response (*SERPINB4*). Additionally, *UBC* was selected for validation since it was shown to be central to the protein association network of inflammation (Figure 3.3D), and cyclin-dependent kinase 2 (*CDK2*) was included for analysis as a marker of proliferation. In our microarray analysis *KLK8*, *RPTN*, *KRT23*, *SERPINB4*, and *UBC* were downregulated 25.8, 57.5, 11.1, 48, 2.48-fold, respectively, and *CDK2* was upregulated 1.74-fold with HPV16 infection. KRT23 is a structural protein in epithelial cells, whereas KLK8 and RPTN are involved in skin barrier proteolytic cascade and cornified cell envelope formation, respectively (195, 196). Recently, studies have reported that KRT23 may be involved in other cellular processes including cell cycle regulation and apoptosis (197), which are key processes that are modulated by HPV infection in our study. KRT23 has not yet been reported by any other gene expression studies of HPV infection and, therefore, could be developed into a novel biomarker of productive HPV infection. In a recent gene expression profiling study, SERPINB4 was shown to be downregulated in early stage HPV infection consistent with our analysis (46). SERPINB4 is a serine protease inhibitor that is overexpressed in inflammatory skin diseases and various cancers including squamous cell carcinomas, and may play a critical role in the immune response against HPV replication and virion production as it has been shown that increased SERPINB4 expression can activate NF-κB (198–204). Similarly, KLK8 has been shown to be overexpressed in cervical cancer, ovarian cancer, and oral squamous cell carcinoma (205–208). So far, not much is known about these proteins in the context of pre-neoplastic HPV infections, and therefore, they could potentially become biomarkers or therapeutic targets of HPV infection at its early stages. In particular, overexpression of SERPINB4 and KLK8 in cancers prominently contrasts our microarray data that includes the two genes amongst the top downregulated genes. This contrast highlights the different microenvironments of the precancerous and cancerous states of HPV infection, and understanding the role of SERPINB4 and KLK8 may provide critical insight into the mechanism of HPV-induced carcinogenesis.

In order to increase the rigor of our data, all of the raft cultures for the validation experiments were set up with new cell lines except for one set of 16HCK rafts. Downregulation of *KLK8*, *RPTN*, *SERPINB4*, and upregulation of *CDK2* at the transcriptional level was observed with HPV16 infection in both 10 days and 20 days of culture, consistent with the microarray analysis (Figure 3.4). Transcription of *UBC* was significantly decreased with HPV16 infection at 10 days of culture as expected from our microarray analysis (Figure 3.4A), but was slightly increased at 20 days of culture (Figure 3.4B). We then further validated downregulation of KLK8, RPTN, KRT23, and SERPINB4 at the translational level with Western blot at 10 days (Figure 3.5A,B) and 20 days

(Figure 3.5C,D) of culture. Although KLK8 expression was visibly downregulated with HPV16 infection in Western blot, statistical significance was not reached on both 10 days and 20 days of culture. To measure UBC protein expression, we used an anti-ubiquitin antibody as a proxy for measuring UBC translation since UBC is simply a polyubiquitin protein that accounts for the majority of basal level ubiquitin in cells (187, 209). Western blot against ubiquitin showed differential ubiquitination of various proteins with HPV16 infection (Figure 3.5E,F) and downregulation of monoubiquitin at 20 days of culture (Figure 3.5F). Lastly, downregulation of RPTN, KRT23, SERPINB4, and Ubiquitin were validated with immunofluorescence staining (Figure 3.6). In particular, RPTN, KRT23, and SERPINB4 are minimally expressed in the basal layers of both infected and uninfected controls with no significant difference in expression between the two groups. In contrast, the three proteins are strongly expressed in the upper layers of uninfected tissues and this expression is significantly decreased with HPV16 infection. The downregulation of the proteins may be attributed to the loss of the cornified layer in infected raft tissues.

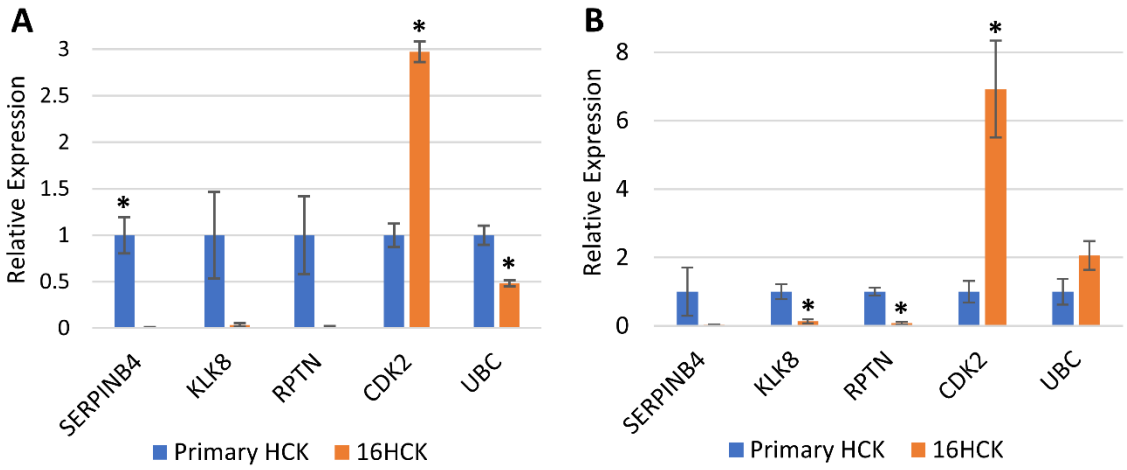

Figure 3.4. Published in (166). RT-PCR of genes of interest. RNA was extracted from (A) day 10 and (B) day 20 raft tissues, and RT-PCR was performed to measure transcription levels of SERPINB4, KLK8, RPTN, CDK2, and UBC. For experiments with 10 day raft tissues (A), three raft experiments were set up each with 16HCK and primary HCK cell lines representing three donors each. For experiments with 20 day raft tissues (B), six raft experiments were set up each with 16HCK and primary HCK cell lines representing three and six donors, respectively. Transcription levels of TATA-binding protein (TBP) was used as control to normalize each measurement (statistical significance $p<0.05$, two-tailed t test). The variance of relative expression ranged from 0.0001 to 0.65 for 10 day tissue and from 0.0012 to 2.96 for 20 day tissue.

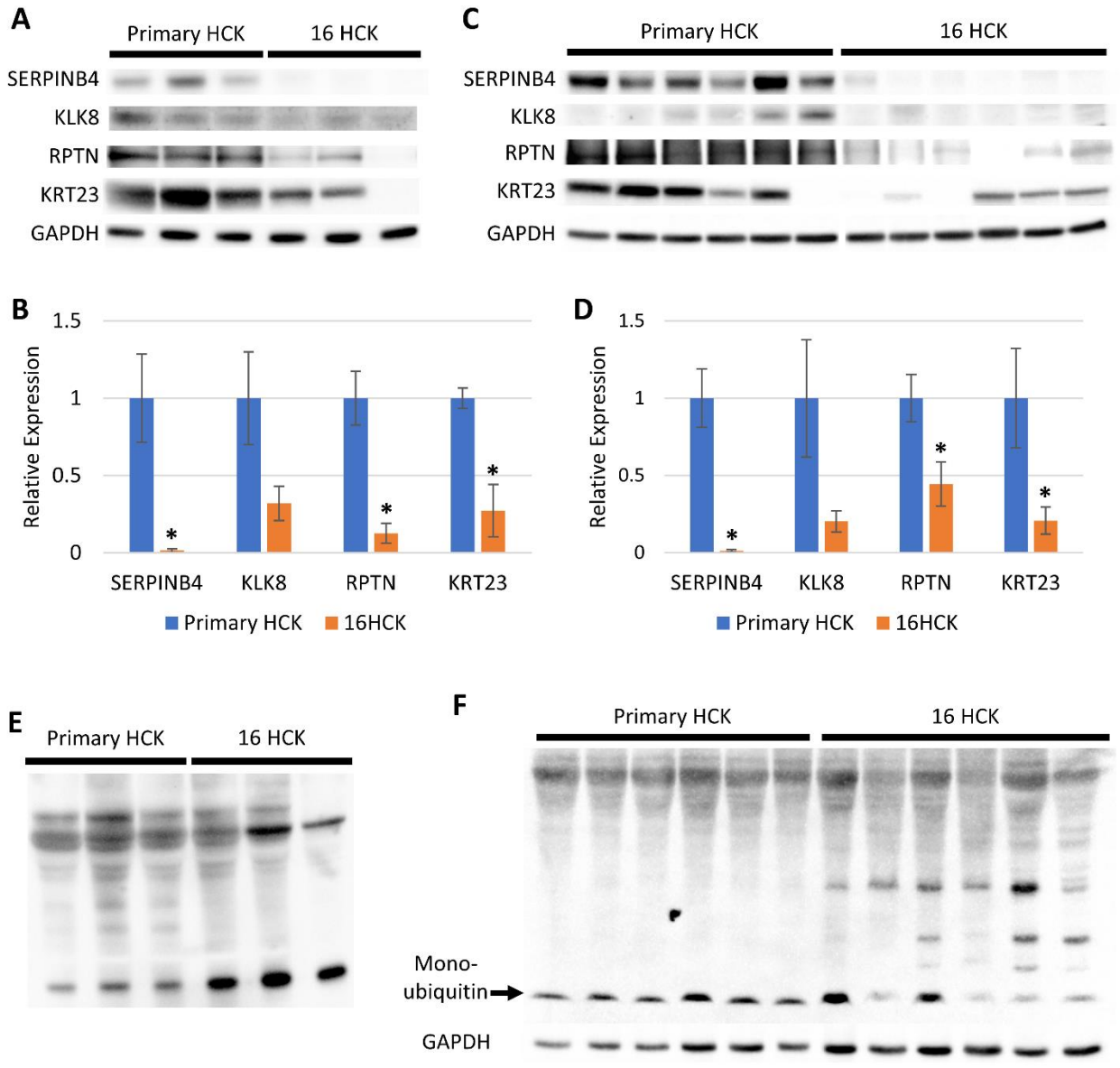

Figure 3.5. Published in (166). Western blot analysis of raft tissue. Protein expression of SERPINB4, KLK8, RPTN, and KRT23 were tested with Western blots in primary HCK and 16HCK raft tissue harvested at (A) day 10 and (C) day 20. Densitometry analysis was conducted on the Western blots at (B) day 10 and (D) day 20 (statistical significance $p<0.05$, two-tailed t test). The variance of relative expression ranged from 0.00037 to 0.27 for 10 day tissue and from 0.00029 to 0.86 for 20 day tissue. Protein expression of Ubiquitin was tested with Western blot in primary HCK and 16HCK raft tissue harvested at (E) 10 days and (F) 20 days of culture. For experiments with 10 day raft tissues (A, B, E), three raft experiments were set up each with 16HCK and primary HCK cell lines

representing three donors each. For experiments with 20 day raft tissues (C, D, F), six raft experiments were set up each with 16HCK and primary HCK cell lines representing three and six donors, respectively. GAPDH was used as control. Images were acquired with Bio-Rad ChemiDoc MP Imaging System and Image Lab Version 6.0.0 software.

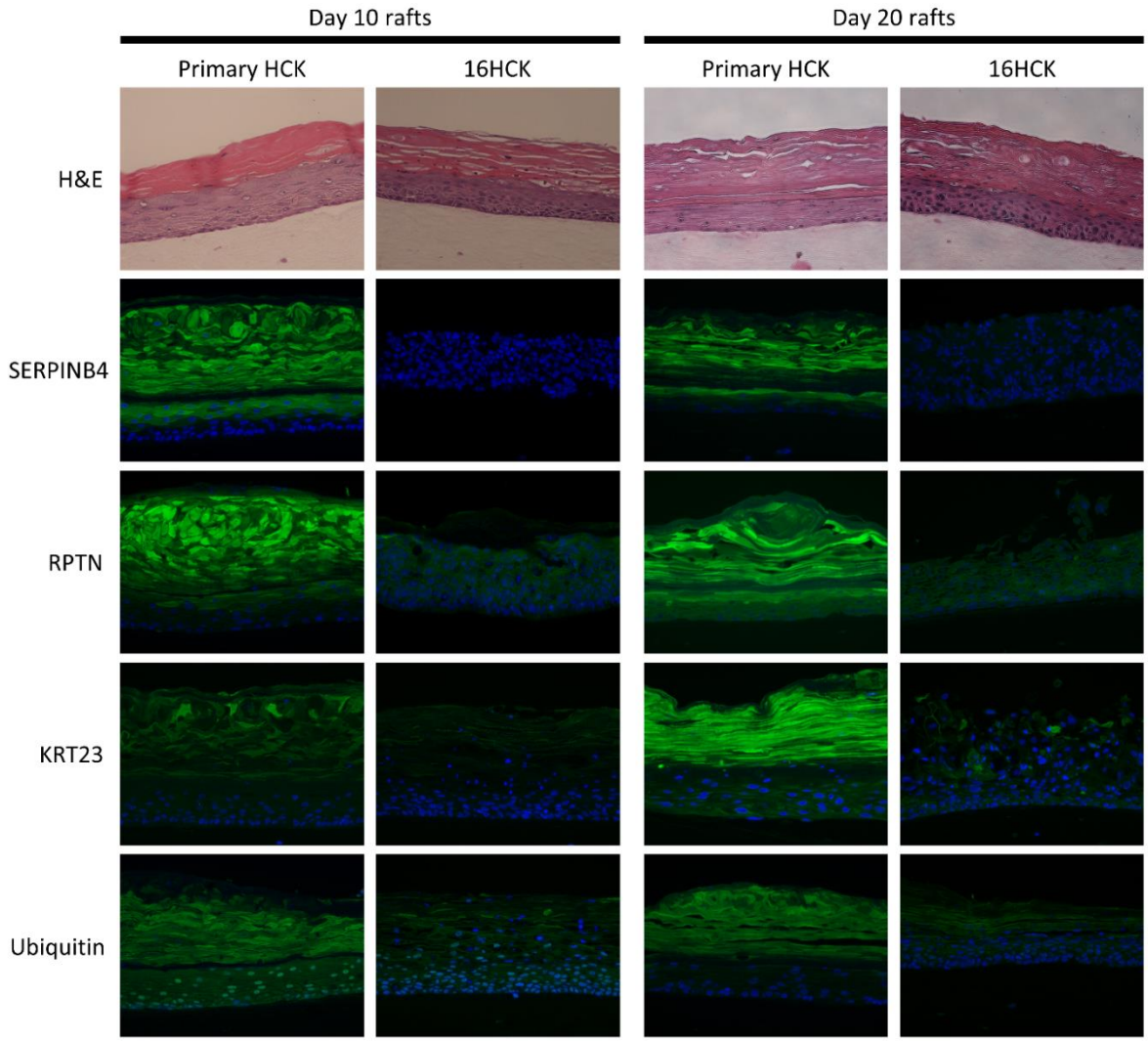

Figure 3.6. Published in (166). Immunofluorescence staining of raft tissue. The spatial protein expression of SERPINB4, RPTN, KRT23, and Ubiquitin was observed by performing immunofluorescence staining of primary HCK and 16HCK raft tissue fixed at 10 days and 20 days of culture (green: target protein, blue: nuclear staining). For experiments with 10 day raft tissues, three raft experiments were set up each with 16HCK and primary HCK cell lines representing three donors each. For experiments with 20 day raft tissues, six raft experiments were set up each with 16HCK and primary HCK

cell lines representing three and six donors, respectively. Magnification 200×. H&E: hematoxylin and eosin staining. Images were acquired with Nikon Eclipse 80i microscope and NIS Elements version 4.4 software.

Discussion

In an attempt to understand HPV infection and its progression to cancer at a holistic level, many studies have investigated global gene expression changes that occur with HPV infection. Most of these studies focus on neoplastic and cancerous lesions (36–44). Two previous studies used early passage HPV16 cell lines, but only 28.1% and 1.6% of the genes reported to be modulated matched our results, and moreover, some of the genes were modulated in the opposite direction (45, 46). The discrepancies between our study and the two previous studies can be attributed to our use of organotypic raft culture system and cervical cells instead of monolayer cell cultures and foreskin cells. Since the HPV life-cycle spans all layers of the epidermis, monolayer cell cultures cannot produce progeny virus particles and, therefore, are limited models of HPV infection. Viral titers were measured on all 16HCK raft tissues to check for high levels of viral particle production (Table 3.1), and confirmed productive infection. Integration of viral genome into the host genome, and subsequent reduction in viral particle production is a hallmark event in the progression of precancerous to cancerous lesions and thus, high levels of viral particle production indicates that the infection is in its earlier precancerous stages. Our study presents for the first time global gene expression changes in cervical tissue with productive HPV infection.

Our microarray data showed that the majority of the modulated genes are downregulated (Figure 3.1). Gene ontology analysis of the microarray data identified gene categories that were significantly represented including cell cycle progression and DNA metabolism in the upregulated genes, and skin development, immune response, cell death in the downregulated genes (Figure 3.2). The upregulation of cell cycle and DNA metabolism genes, and downregulation of cell death genes reflect the proliferative nature of persistent HPV16 infection. Downregulation of immune response and skin development genes can be understood in the context of the virus modulating the host environment to achieve efficient replication and virion production. The trends of modulation in these five gene categories are consistent with previously reported studies of global gene expression (36, 38–42, 45, 46, 49, 50, 167, 171, 172).

Several genes were selected for validation at the transcription and translational levels based on the degree of fold-change, relevance to the HPV life-cycle, and protein association network analysis. *KLK8* and *RPTN* were selected for validation as they were amongst the top downregulated genes and are both involved in epithelium development. It is not surprising to see many genes involved in epithelium development to be affected by HPV infection since the virus infects, replicates, and assembles in the epithelium. In particular, HPV is not a lytic virus and is released from the epidermis via desquamation. Repetin was downregulated 57.5-fold with HPV16 infection in our microarray analysis and this downregulation was validated with qPCR, Western blot, and IF staining. Repetin is a component of the epidermal differentiation complex, and is involved in the formation of the cornified cell envelope (CE) (196). The CE is an insoluble matrix of covalently linked proteins formed beneath the plasma membrane of differentiating keratinocytes and plays an important role in the skin's function as a protective physical barrier against the external environment (210). In the context of HPV infection, the CE may hinder virion release because of its function as a physical barrier. Additionally, a previous study has shown that CEs of epithelial tissue infected with HPV11 are thinner and more fragile compared to those of healthy tissue (211). Therefore, it can be speculated that downregulation of Repetin by HPV may be a strategy to weaken the CE and increase the efficiency of virion release.

KLK8 was downregulated 25.8-fold in our microarray analysis, which was validated with qPCR and Western blot. *KLK8* was the most significantly downregulated gene of the seven KLK genes that were downregulated with HPV16 infection: *KLK3*, *KLK5*, *KLK6*, *KLK7*, *KLK10*, *KLK13* were downregulated 3.6, 4, 22.1, 8.6, 7.5, 21.5-fold, respectively. A previous gene expression study has also identified a cluster of KLK genes (*KLKs 5, 6, 7, 10, 11*) that are downregulated at early stages of HPV16 infection (45). KLKs are a family of 15 serine proteases that are clustered on chromosome 19q13.4 and one of their main functions is cleaving corneodesmosomal adhesion molecules in the cornified layer of the epidermis, which allows regulated desquamation of keratinocytes (195, 212–214). It is counterintuitive that HPV16 infection downregulates KLKs since the virus is released via desquamation. We speculate that the rate at which normal epithelium desquamates is faster than the rate at which HPV virions mature in the cornified layer, and therefore, the virus may be downregulating KLKs in order to impede desquamation and allow virions to adequately mature before being released to the surrounding environment. *KLK8* also plays a role in activation of the antimicrobial peptide LL-37 and thus, HPV16 may be downregulating the protein in order to prevent antimicrobial reaction (195, 215).

SERPINB4, also known as squamous cell carcinoma antigen 2 (SCCA2), is a member of the serpin family of serine protease inhibitors and was downregulated 48-

fold in our microarray analysis. The downregulation in microarray analysis was validated with qPCR, Western blot, and IF staining. SERPINB4 along with SERPINB3 (squamous cell carcinoma antigen 2; SCCA1) have been shown to be overexpressed in various types of cancers including cervical, esophageal, lung, breast, and liver cancers (199, 201–203, 216–218). One of the mechanisms through which SERPINB4 contributes to tumor maintenance is the inhibition of granzyme M-induced cell death(219). Additionally, SERPINB4 overexpression is associated with inflammatory diseases including psoriasis and atopic dermatitis (198, 200, 220–222). Remarkably, *KLK8* shares the same expression pattern in these diseases: while our microarray analysis shows significant downregulation during productive HPV16 infection, the overexpression of *KLK8* has also been associated with both squamous cell carcinomas and inflammatory skin diseases, such as psoriasis and atopic dermatitis (205–208, 223). We speculate that the virus downregulates *SERPINB4* and *KLK8* during productive infection as part of a broad effort to dampen the inflammatory response. Of particular note is that the two genes are overexpressed in various cancers while in our study they are amongst the top downregulated genes during productive HPV infection. Additionally, we have identified nine other genes that are significantly downregulated in our microarray analysis, but have shown to be overexpressed or contribute to disease progression in various types of cancers (Table 3.4). This highlights the fact that early productive stages of HPV infection present a vastly different microenvironment and disease state from the cancerous stages of infection when virion production is significantly decreased. This suggests that KLK8 and SERPINB4 may interfere with the HPV life-cycle or contribute to the immune surveillance against the virus, and therefore, are downregulated during productive infection. In contrast, the two proteins may be necessary for tumor maintenance, and therefore, overexpressed during the cancerous stages of infection. However, since we did not measure levels of expression of these proteins at cancerous stages we cannot definitively compare the protein levels between precancerous and cancerous stages. A direct comparison would require creating organotypic raft cultures with cervical cancer cell lines and measuring SERPINB4 and KLK8 protein levels. In future studies, we aim to investigate the mechanism of *KLK8* and *SERPINB4* downregulation, and how the two genes affect HPV entry, intracellular trafficking, replication, and assembly.

UBC was the central protein in the network of inflammatory genes that were significantly downregulated with persistent HPV16 infection (Figure 3.3D). qPCR showed a statistically significant downregulation of *UBC* expression at 10 days of raft culture (Figure 3.4A), while Western blot of ubiquitin showed downregulation of monoubiquitin at 20 days of culture and differential pattern of protein ubiquitination (Figure 3.5E,F). Additionally, IF staining showed downregulation of the protein with persistent infection at both 10 days and 20 days of culture (Figure 3.6). Since ubiquitin is involved in numerous biological processes it is hard to conclude which specific

pathways are affected with HPV16 infection. However, many proteins that are associated with UBC in the protein association network (Figure 3.3D) are a part of the NFKB pathway, and we speculate that UBC plays a central role in downregulating this pathway especially since it has been shown that ubiquitin-proteasome pathway plays a role in NF-κB activation. In future studies, we would like to investigate the role of *UBC* in relation to top downregulated genes associated with inflammation, such as *SERPINB4* and *KLK8*.

In conclusion, our study shows for the first time global gene expression changes with productive HPV16 infection in an organotypic raft culture model. With gene ontology analysis, broad gene categories were identified that were significantly modulated with persistent HPV16 infection, and these results were largely consistent with what previous studies have reported. However, we identified top downregulated genes that have not yet been extensively studied in the context of HPV infection, and that have potential to be developed as therapeutic targets or biomarkers. Moreover, expression patterns of *SERPINB4* and *KLK8* highlighted that precancerous and cancerous stages of HPV infection are two distinct disease states. We attribute these new findings to our unique model of organotypic raft cultures at early stage HPV16 infection, which allows the virus to go through its complete life-cycle. Future studies investigating how the regulation of *SERPINB4* and *KLK8* changes throughout the different stages of infection may shed light on unidentified mechanisms of HPV persistence and tumorigenesis.

Table 3.4. Differential gene expression between productive HPV16 infection and cancers.

Gene	**Expression fold-change in productive HPV infection**	**Cancers in which gene expression increases and/or promotes disease progression**
SERPINB4	-48.0	HNSCC (199), cervical (201, 203), esophageal (202), lung (224), liver (218), breast (217)
KLK5	-3.2	Bladder (225), ovarian (226), lung (227), breast (228), oral squamous cell carcinoma (OSCC) (207)
KLK6	-22.1	Bladder (225), ovarian (226), colorectal (229), head and neck squamous cell carcinoma (HNSCC) (230), pancreatic (231)

KLK8	-25.8	Bladder (225), ovarian (226), salivary gland (232), cervical (208), OSCC (207), colorectal (231)
KLK10	-7.6	Ovarian (226), OSCC (207), pancreatic (231), colorectal (231)
KLK13	-21.5	Lung (233), ovarian (234)
MMP9	-17.1	Cervical (173), breast (235), HNSCC (236), prostate (237)
MMP10	-8.0	OSCC (238), HNSCC (239), esophageal (240)
LCN2	-9.1	Breast (175, 176), esophageal (177), pancreatic (178), ovarian (179), colorectal (180), thyroid (181)
CTSD	-1.5	Breast (241), ovarian (242)
CTSV	-2.8	Breast (243), colorectal (243)

CHAPTER 4: The effect of productive HPV16 infection on the epigenome of tonsil keratinocytes

Experimental design

In order to investigate the effect of HPV16 infection on the methylome of tonsil tissue, tonsil keratinocytes were isolated from pooled human tonsil tissue and electroporated with the HPV16 genome. Once the electroporated cells immortalized around passage 7, they were put up on raft cultures and the tissue was harvested at d4, d10, and d20 to measure the effect of infection at different stages of the HPV life-cycle. DNA was extracted from the harvested raft tissue and then underwent methylome analysis (Figure 4.1). For both non-infected (primary HTLK) and infected (16HTLK) groups, five male and five female cell lines were used to conduct the experiments. Monolayer cells were also analyzed as control: five male and five female cell lines of 16HTLK, and three male and three females cell lines of primary HTLK were used.

Figure 4.2 shows Hematoxylin and eosin (H&E) stains of primary HTLK and 16HTLK raft tissues of male and female cell lines at d4, d10, and d20. The three time points were chosen to measure changes in the methylome at different stages of tissue differentiation, and therefore, different stages of the differentiation dependent life-cycle of HPV16. At d4 of raft culture, all of the HPV early genes are expressed and there are low levels of viral replication (155, 244–246). At d10 of raft culture, all HPV early and late genes are maximally expressed and viral replication occurs at high levels with formation of unstable infectious virus particles (8, 155, 244–248). Finally, at d20 of raft culture, high levels of fully mature, stable, and infectious virus particles are formed (8, 247–249).

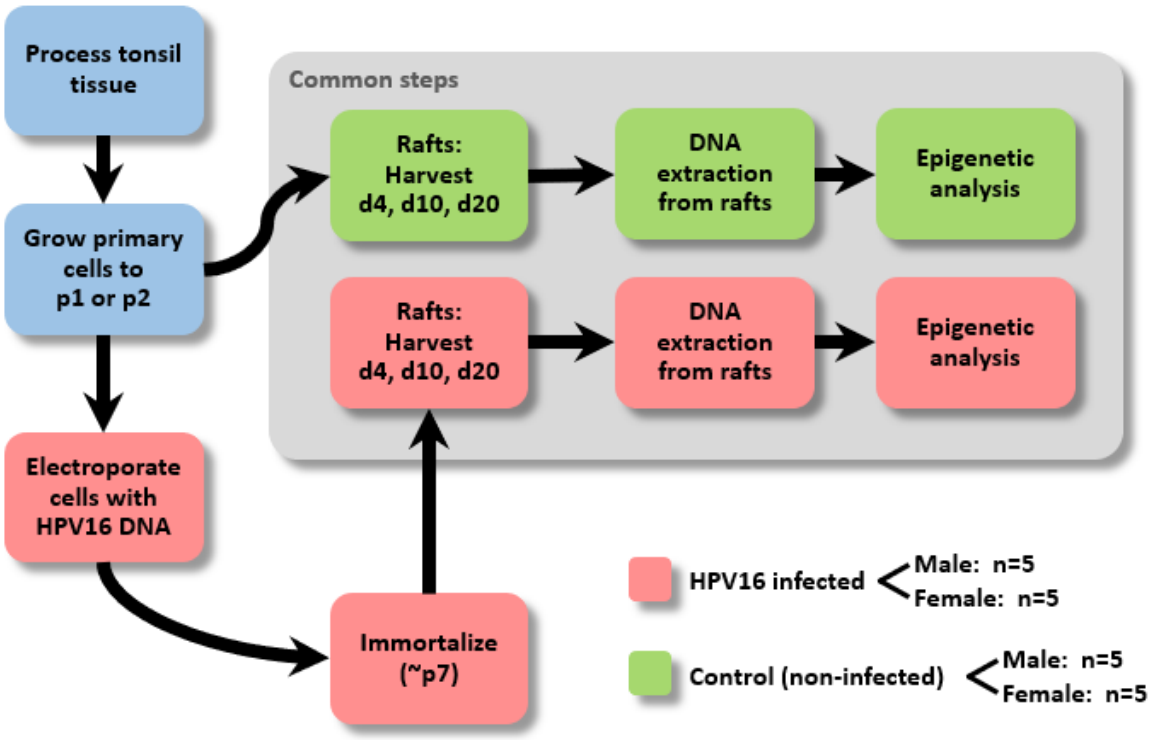

Figure 4.1. Experimental design and workflow. Non-infected (HTLK) and HPV16 infected tonsil keratinocytes (16HTLK) were put up in organotypic raft culture and harvested at d4, d10, d20 for methylome analysis.

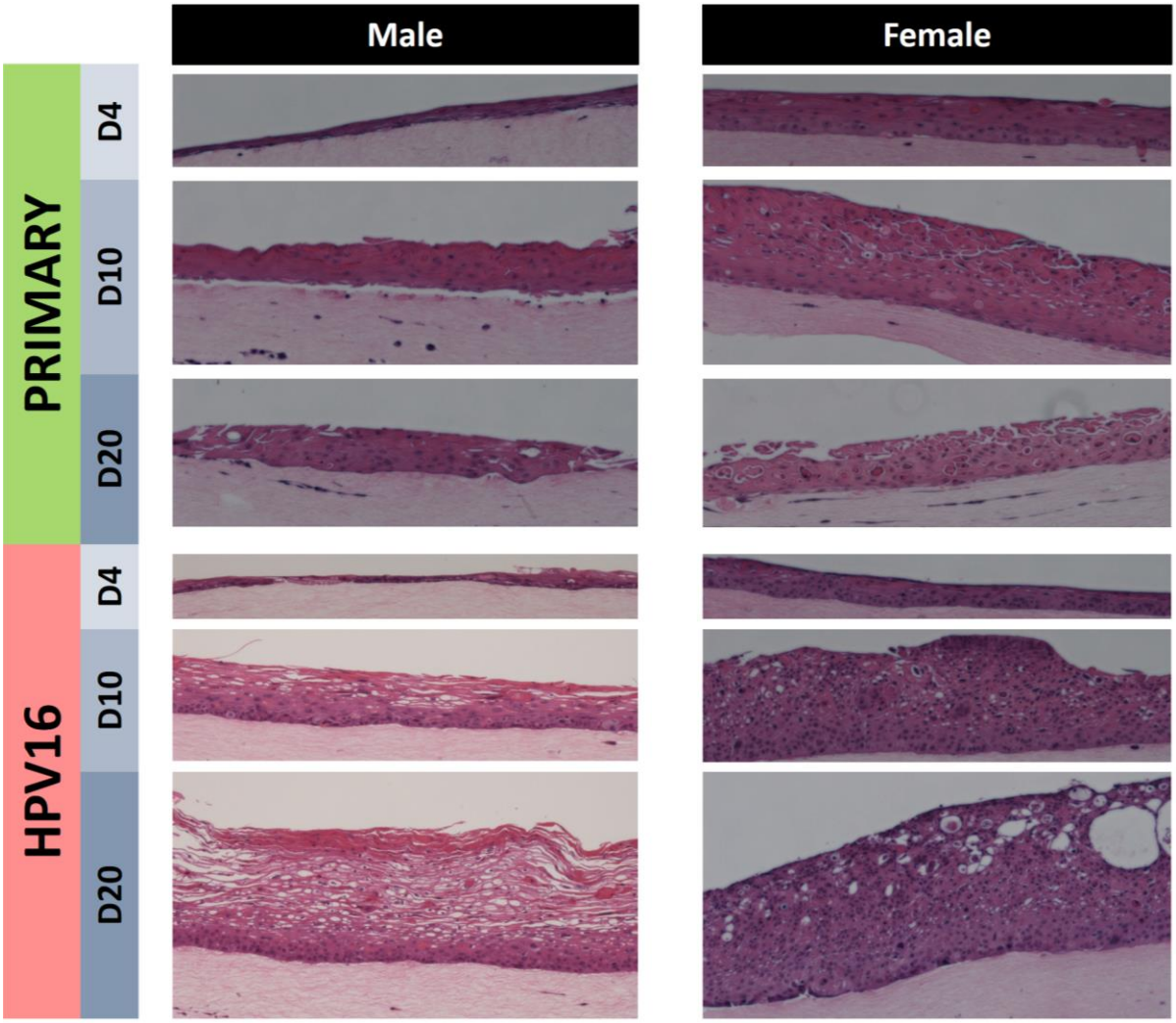

Figure 4.2. Hematoxylin and eosin stains of raft tissue. Hematoxylin and eosin (H&E) stains of non-infected and HPV16 infected tonsil raft tissue at different time points.

Changes in tonsil methylome with HPV16 infection

Before analyzing our data separately in males and females, we first combined the data from both sexes to analyze the general trends occurring in the methylome regardless of sex. Genome-wide average methylation was analyzed across approximately 2 million CpG sites and 20 million non-CpG cites (CH sites, where H = A, C, or T). Results showed that the level of genome-wide average methylation of CpG sites remains stable between 40% and 50% regardless of whether the samples are monolayer or raft cultures, and

whether they are infected or non-infected with HPV16 (Figure 4.3). While the number of genome-wide CH sites are much more abundant than CpG sites, their average level of methylation was significantly lower and also remained stable between 0.5% and 2% regardless of whether the samples are monolayer or raft cultures, and whether they are infected or non-infected with HPV16 (Figure 4.3). These results suggest that HPV infection, and tissue differentiation status does not affect the genome-wide average rate of methylation in both CpG and non-CpG contexts. Given that the total methylation levels remain unchanged in the different experimental groups, we then investigated whether there are specific sites of differential methylation with HPV16 infection over the time course of d4, d10, and d20.

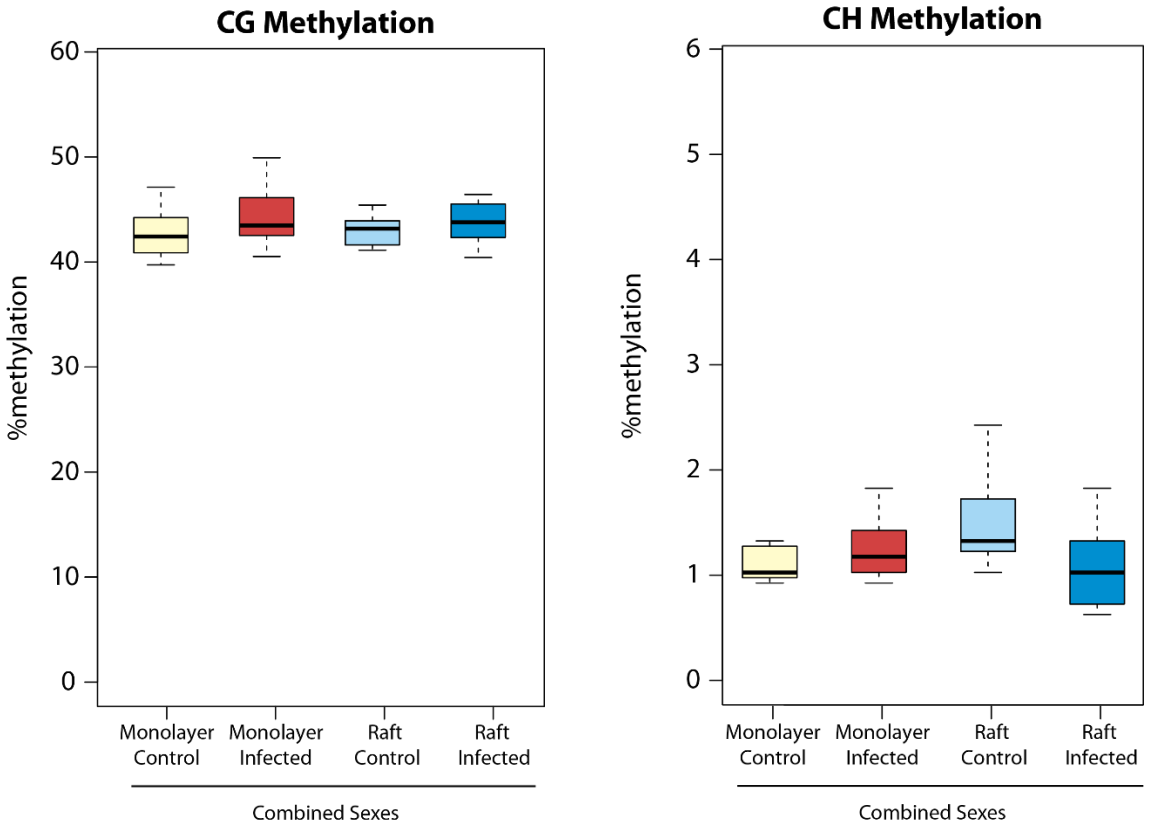

Figure 4.3. Genome-wide CG and CH methylation rates in monolayer and raft cultures of HPV16-infected and non-infected control tonsil keratinocytes.

Methylome analysis comparing HPV16 infected and non-infected human tonsil keratinocytes at each time point of raft culture (d4, d10, d20) showed that there was an overall total of 270,453 HPV16 differentially methylated CpGs (HDMCGs) throughout the three time points (Figure 4.4). Of these HDMCGs, only 43,432 sites were common among the three time points while the majority of them were specific to one or two time points. As an example, of the 110,779 HDMCGs occurring on d4, 41,025 of them

are not observed on d10 and 56,928 of them are not observed in d20, and 30,606 of them are unique to d4 (not observed in either d10 and d20). Similarly, 88,923 HDMCGs and 40,360 HDMCGs are unique to d10 and d20 rafts. When considering that this data is coming from the same exact set of raft tissue, just at different time points, it is striking how dynamic the methylome is over the time course. In other words, the same set of raft tissues seem to have a significant degree of methylation patterns that are unique to each time point with HPV infection.

At this point, it is unclear whether these dynamic changes over the time course is driven by the different stages of tissue differentiation or the different stages of the viral life-cycle occurring at the different time points. Another aspect that is unclear is whether these dynamic changes are induced by the host immune response against HPV16 infection, or if these changes are caused by the virus as it attempts to dampen the host immune response and manipulate the cellular machinery for viral replication and assembly. Considering that the tonsil keratinocytes are persistently infected with HPV16 and that they produce high levels of progeny virions in raft culture, it is likely that the dynamic changes in the host methylome is induced by the virus rather than by the host immune response. Moreover, although not much is known about the effect of HPV infection and the effect of viral proteins on TET proteins that facilitate demethylation, a few studies have reported that the viral oncoprotein E7 increases the expression and activity of DNMT1 (84, 85), and increased copy number and expression of DNMT3B has been observed in cervical cancer samples (86). These studies also suggest that the dynamic methylome changes are induced by the virus as it attempts to dampen host immune response and manipulate host machinery for viral replication and production.

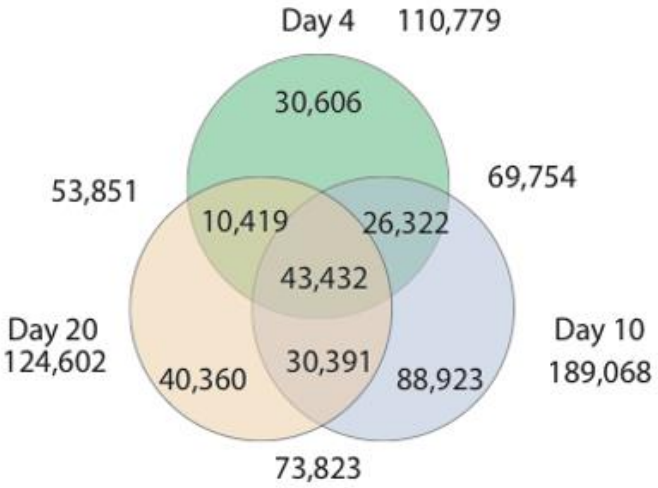

Figure 4.4. HPV16 differentially methylated CpGs (HDMCGs) of tonsil keratinocyte raft cultures at d4, d10, d20.

Sex-specific changes in tonsil methylome with HPV16 infection

Similar to what was observed in the overall (sex-combined) analysis of monolayer and raft cultures (Figure 4.3), the percentage of CpG methylation (Figure 4.5) and non-CpG methylation (Figure 4.6) remained stable between monolayer and raft cultures, HPV16 infected and non-infected samples, and male and female tonsil keratinocytes. These results indicate that tissue differentiation, HPV infection, and sex does not affect the overall level of methylation. This, however, does not tell us whether sex has an effect on differential methylation patterns with HPV16 infection, and therefore, we next analyzed the distribution of sex-specific and sex-common HDMCGs in monolayer and raft cultures.

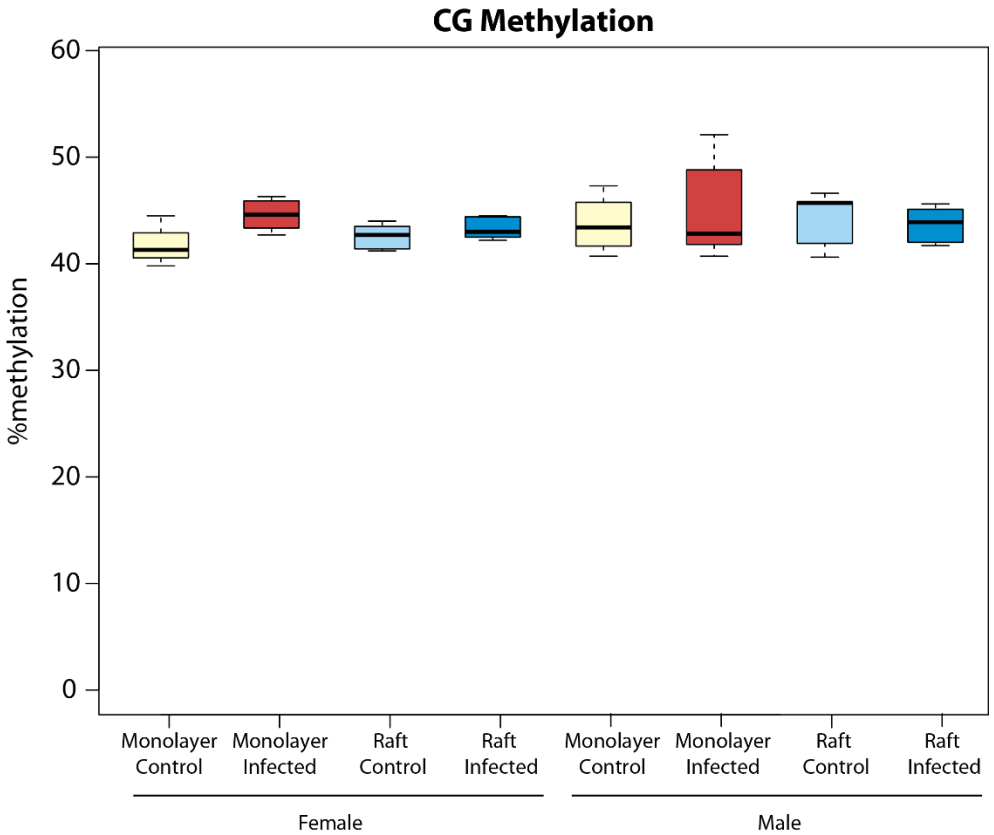

Figure 4.5. Genome-wide CG methylation rates in monolayer and raft cultures of HPV16-infected and non-infected control tonsil keratinocytes, separated by sex.

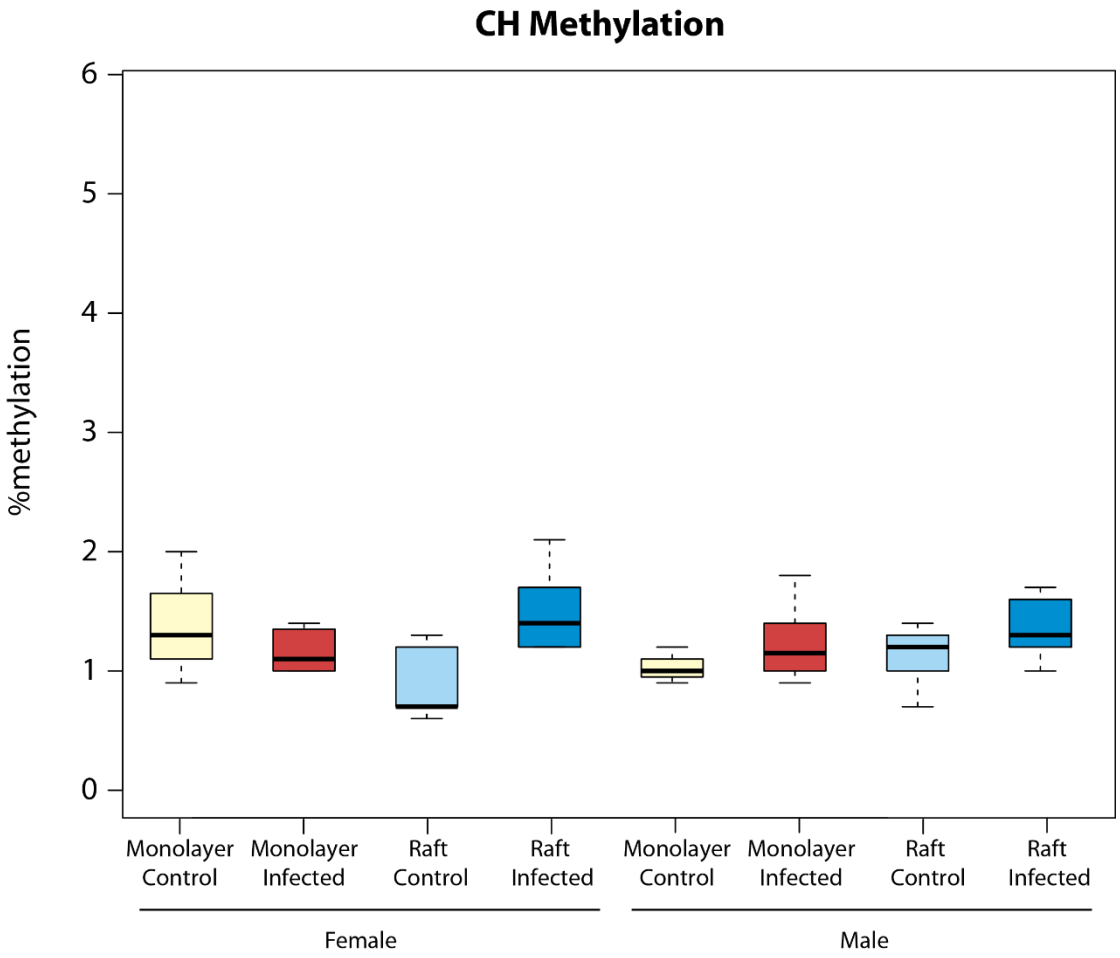

Figure 4.6. Genome-wide CH methylation rates in monolayer and raft cultures of HPV16-infected and non-infected control tonsil keratinocytes, separated by sex.

Methylome analysis of monolayer cultures of tonsil keratinocytes showed that there were a total of 10,318 HDMCGs in females and 17,461 HDMCGs in males (Figure 4.7). These changes included 1,698 HDMCGs that were commonly hypermethylated, and 2,634 HDMCGs that were commonly hypomethylated between the two sexes. The total number of sex-common HDMCGs was significantly higher than expected by chance. Interestingly, while the 4,332 sex-common HDMCGs were either hypermethylated (hyperHDMCGs) or hypomethylated (hypoHDMCGs) in the same direction, only three sex-common HDMCGs had methylation patterns in the opposite direction between the two sexes. The overall number of sex-specific HDMCGs was much higher in males (6,256 hyperHDMCGs and 6,873 hypoHDMCGs) than in females (2,197 hyperHDMCGs and 3,789 hypoHDMCGs). HDMCGs in the X chromosome were observed in both a sex-common and sex-specific pattern, and none of the sex-common HDMCGs were modulated in the opposite direction.

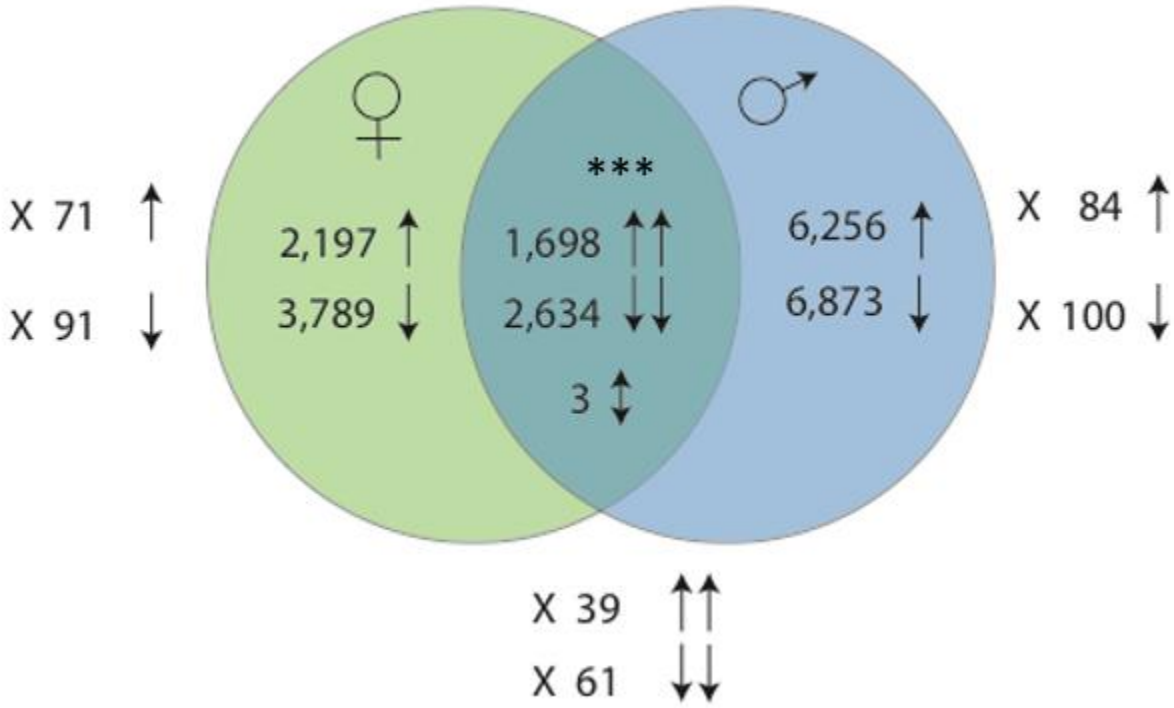

Figure 4.7. HPV16 differentially methylated CpGs (HDMCGs) of tonsil keratinocyte monolayer cultures in males and females.

In contrast to the total number of HDMCGs in monolayer culture which was 23,447 including both sex-common and sex-specific HDMCGs, the total number of HDMCGs in raft cultures was much greater ranging from 207,254 to 329,043 at the different time points (Figure 4.8). Female-specific HDMCGs increased from 70,307 to 108,420 from d4 to d10, and increased again to 125,922 on d20. Male-specific HDMCGs also increased from 101,043 to 151,660 from d4 to d10, but decreased almost 2-fold on d20 to 79,422. Sex-common HDMCGs followed the trend of male-specific HDMCGs by increasing from 35,904 to 68,963 from d4 to d10, and then decreasing to 44,015 on d20. Similar to what was found in monolayer HDMCGs, the total number of sex-common HDMCGs in raft cultures were significantly higher than what is expected by chance. Moreover, within the sex-common HDMCGs, the number of sites that had differential methylation in the same direction (hypo- or hyper- methylation) was significantly greater than what is expected by chance. The number of sex-specific HDMCGs are noticeably greater in males than in females on d4 and d10. However, due to the consistent increase of HDMCGs over time in females and a sudden drastic decrease of HDMCGs on d20 in males, females had a greater number of HDMCGs on d20 than males. HDMCGs in the X chromosome followed this general trend: the number of HDMCGs consistently increased over time in females while the number increased from d4 to d10, and then

drastically decreased on d20 in males. Also, the number of X chromosome HDMCGs was greater in males on d4 and d10, and greater in females on d20.

Overall, these results suggest that while HPV16 is mainly modulating the methylation patterns of the host in a sex-specific manner, there is still a significant proportion of the methylome change that is shared between the two sexes. Considering this in the context of the epidemiological sex bias in HPV-associated HNSCCs can help shed light on what the sex-common and sex-specific methylome changes mean. Epidemiological studies have shown higher prevalence of HPV infection in males than in females suggesting that there is a sex-bias or sex-specificity during initial infection of HPV, which could include virus attachment, entry, and intracellular trafficking to establish and infection. However, in this study, since we used tonsil keratinocytes that are already persistently infected with HPV16, our study design and results cannot be used to interpret sex differences in the initial infection stages. In our study, both male and female cell lines were persistently infected with the same virus, and upon 20 days of raft culture, tissue from both sexes gave high titers of progeny virions. Also, the tissue morphology of both sexes over the time course was indistinguishable (Figure 4.2). Therefore, the sex-common HDMCGs may be involved in supporting the various stages of the HPV life-cycle (post-establishment of persistent infection) as these are common and indistinguishable between the two sexes. On the other hand, the sex specific HDMCGs may refer to how the two sexes respond to HPV infection, and how the viral proteins affect normal cellular physiology that eventually leads to sex differences in oropharyngeal cancer incidence.

When looking at the direction of HDMCGs, there are consistently greater numbers of hypoHDMCGs than hyperHDMCGs in female-specific HDMCGs throughout the time course. Similarly, there were greater numbers of hypoHDMCGs than hyperHDMCGs on d4 and d10 in male-specific HDMCGs, but this was reversed on d20. The sex-common HDMCGs followed the trend of female-specific HDMCGs by having greater levels of hypoHDMCGs than hyperHDMCGs throughout the time course. Interestingly, the number of sex-common HDMCGs with opposite methylation patterns (the same site being hypermethylated in one sex and hypomethylated in the other) was significantly higher in raft tissue compared to monolayer cultures (Figures 4.7 and 4.8). While there were only three sex-common HDMCGs with opposite methylation patterns in monolayers representing merely 0.007% of sex-common HDMCGs, those in raft cultures ranged between 7,526 and 13,642 over the time course representing 19.8% to 25.6% of the sex-common HDMCGs (Figure 4.8). This suggests that tissue differentiation and/or progression of the HPV life-cycle accentuates the sex-specific response to HPV infection. In other words, sex-specific responses are not as strong during the initial stages of infection (attachment, entry, intracellular trafficking of viral genome to the nucleus) that occurs in monolayer cultures.

In females, there were greater levels of hypoHDMCGs than hyperHDMCGs on the X chromosome throughout the time course, reflecting the general pattern of female-specific HDMCGs in the autosomes. In stark contrast, there were greater levels of hyperHDMCGs than hypoHDMCGs in the male X chromosome consistently throughout the time course, which does not reflect the general pattern of male-specific HDMCGs (Figure 4.8). This suggests that progression of viral life-cycle and/or tissue differentiation causes preferential hypomethylation of the X chromosome in females and hypermethylation in males. These distinct methylation patterns in males and females may have an association with sex-bias in oral HPV infection prevalence, especially when considering that the X chromosome contains many immune-related genes.

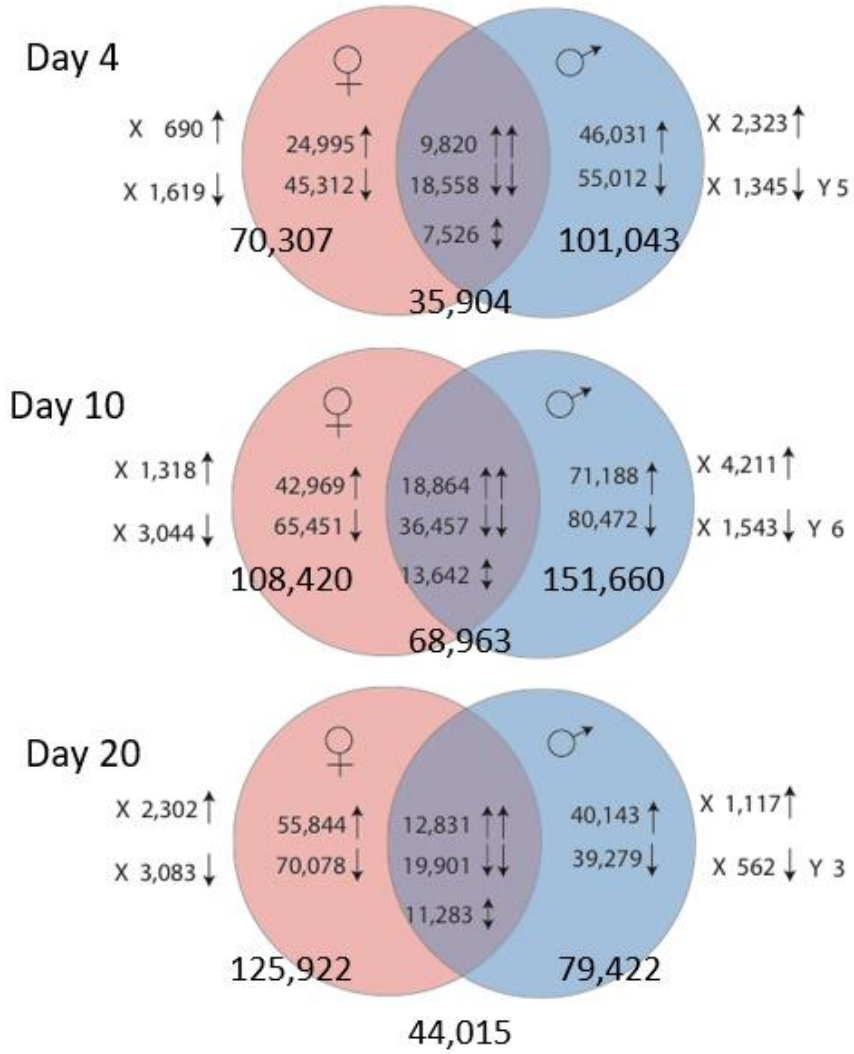

Figure 4.8. Venn diagrams of HDMCGs of raft tissue in males and females on d4, d10, and d20.

Venn diagrams of sex-specific HDMCGs over the time course (d4, d10, d20) illustrates the dynamic host methylome over the course of epidermal differentiation and HPV life-cycle (Figure 4.9). As already shown in Figure 4.8, the temporal progression of increasing HDMCGs from d4 to d10, and then a decrease from d10 to d20 can be observed in male-specific HDMCGs. In female-specific HDMCGs, the levels consistently increase throughout the time course. In sex-specific HDMCGs, there are a core set of sites that are differentially methylated throughout the time course: 10,643 and 13,007 sites in female-specific and male-specific HMDCGs, respectively. However, most of the HMDCGs are specific to a certain timepoint, similar to what was observed in the overall (sex-combined) analysis of HDMCGs over the time course (Figure 4.4). For example, in female rafts, 36,406 CpG sites were differentially methylated at d4 specifically, and the same set of rafts had 64,789 new set of differentially methylated CpG sites that were specific to d10, and again a separate set of 81,356 differentially methylated CpG sites specific to d 20. This shows that the host methylome is going through a dynamic change throughout the different stages of epidermal differentiation and the HPV life-cycle, and that each of these stages have their own unique biomolecular landscape.

Similar to what was discussed above for the sex-combined analysis of HDMCGs over the time course (Figure 4.4), it is likely that the dynamic changes of the methylome is caused by the virus dampening the host immune response and manipulating the host machinery to produce progeny virions, since the cell lines used in this study were persistently infected and produce high titers of progeny virions, and previous studies have reported increased DNA methyltransferase activity with HPV infection (84–86).

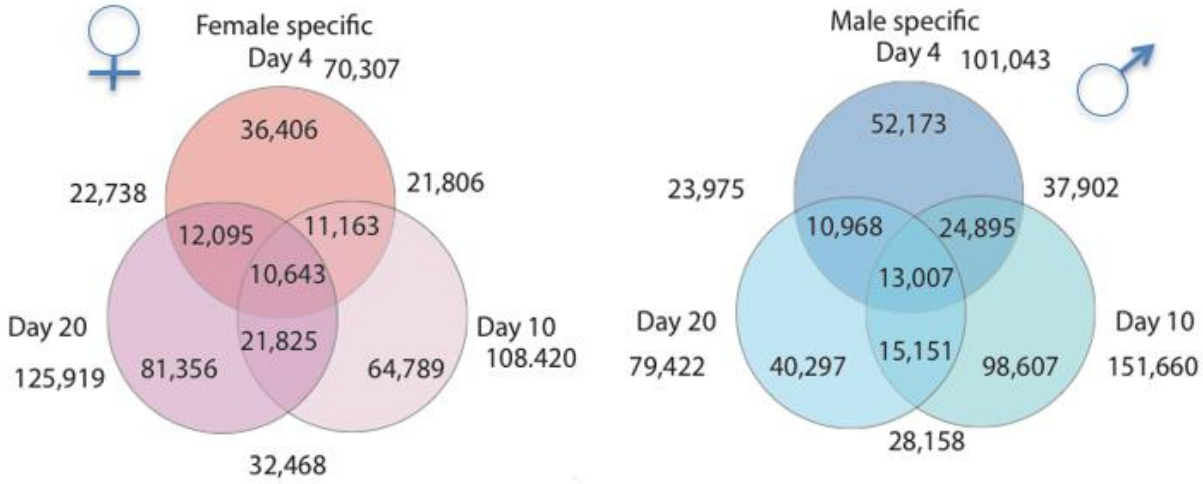

Figure 4.9. Venn diagrams of sex-specific HDMCGs of raft tissues over the time course.

We next conducted a principal component analysis (PCA) on all of our raft methylome data sets. The analysis takes into account all of the CpG sites, their location, and the

methylation percentage at each site for each cell line in order to compare the overall methylation patterns and visualize how similar or how different they are to each other. In the PCA plot (Figure 4.10), the distance between any two points is inversely proportionate to the similarity between the two methylome data that the two points represent. In other words, the methylome data sets that are closer to each other on the PCA plot have more similar methylation patterns to each other than data sets that are farther apart.

Interestingly, all of the control rafts from both sexes at all time points clustered together as shown in blue circles in Figure 4.10. This indicates that the overall methylation pattern of the host genome remains similar among individual samples regardless of sex, and between different stages of tissue growth and differentiation (d4, d10, d20) when there is no HPV16 infection. Therefore, there does not seem to be sex-bias or differentiation-dependent patterns of overall methylation patterns in non-infected tonsil tissue. In contrast, with HPV16 infection (red circles) each cell line diverged away from the cluster of non-infected samples (blue circles), indicating that HPV16 infection does in fact cause significant changes in methylation patterns in the host. What stands out is that the three time points (d4, d10, d20) for each infected cell line still cluster together. This suggests that while HPV16 infection causes significant changes in the host methylome, these changes remain stable throughout tissue differentiation and different stages of the HPV life cycle.

The degree to which HPV16 infection affects the host methylation pattern was variable among the different cell lines as shown by the variable distances between the non-infected cluster and each of the infected clusters. No apparent sex-specific trends could be observed but the female 16HTLK clusters were closer to each other than the male 16HTLK clusters, which included two cell lines (M19, M28) that were the farthest away from the non-infected control cluster. Overall, these results suggest that there is a host-specific response to HPV16 infection that is not sex-specific, but remains stable throughout tissue differentiation and progression of the HPV life cycle. The fact that HPV16 infection causes unique changes in methylation pattern in each host indicates that each host responds to the infection in a highly heterogeneous manner. Since most HPV infections are naturally resolved and only a small fraction of infections eventually develop into cancer, how the methylome of each host responds to HPV infection may be associated with each individual's risk of developing cancer.

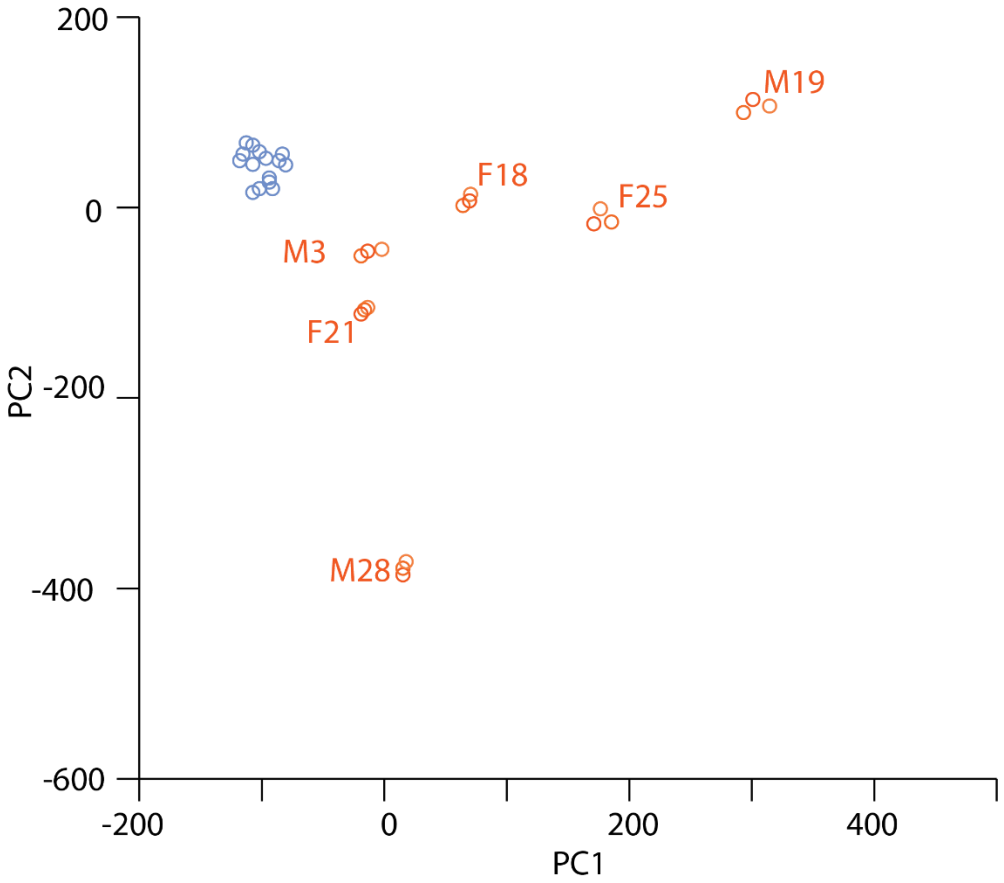

Figure 4.10. PCA analysis. PCA analysis of control (non-infected) rafts (blue) and infected rafts (red) over the time course. All male and female control rafts at all time points (d4, d10, d20) were clustered together, and therefore, was not labeled. The three time points (d4, d10, d20) of each HPV16 infected cell line clustered together, and therefore, was not labelled. M: male 16HTLK cell lines, F: female 16HTLK cell lines.

Visual mapping of HDMCGs across the genome revealed that hyperHDMCGs and hypoHDMCGs are distributed throughout the autosomes and the X chromosome for both sex-common and sex-specific HDMCGs in both monolayer and raft cultures (Figures 4.11 and 4.12). Macroscopically, the HDMCG distribution across the genome did not reveal any trend or specific pattern. However, zooming in to view each individual HDMCG shows that specific regions of specific genes are targeted by both sex-common and sex-specific HDMCGs (Figure 4.13).

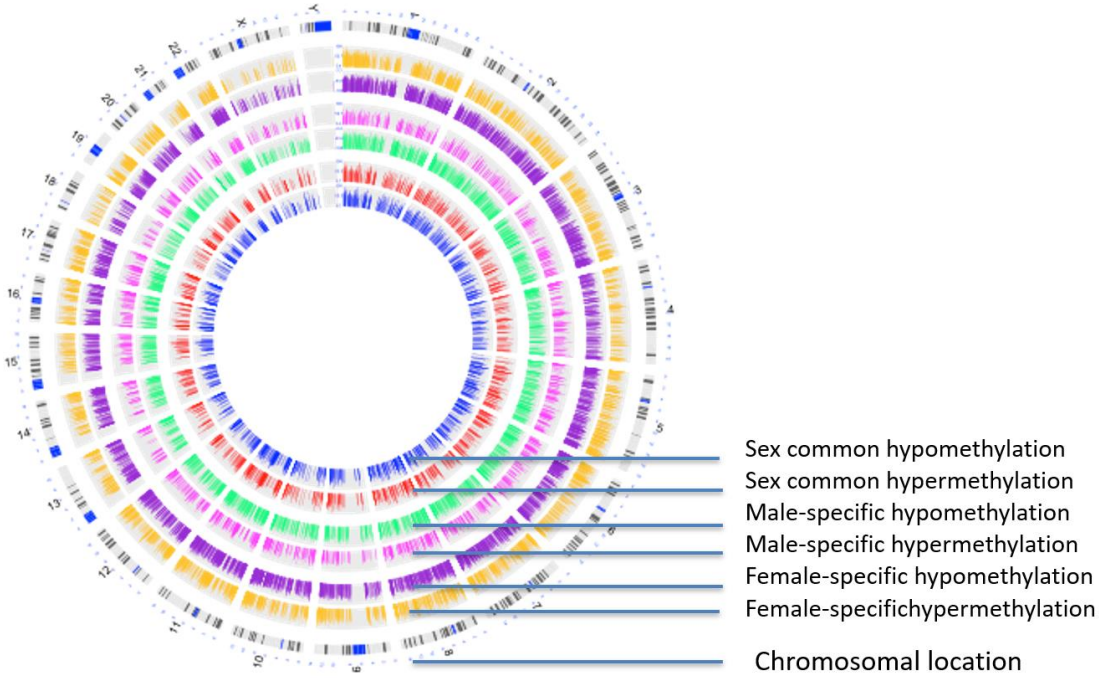

Figure 4.11. Circus plot of monolayer HDMCGs throughout the genome.

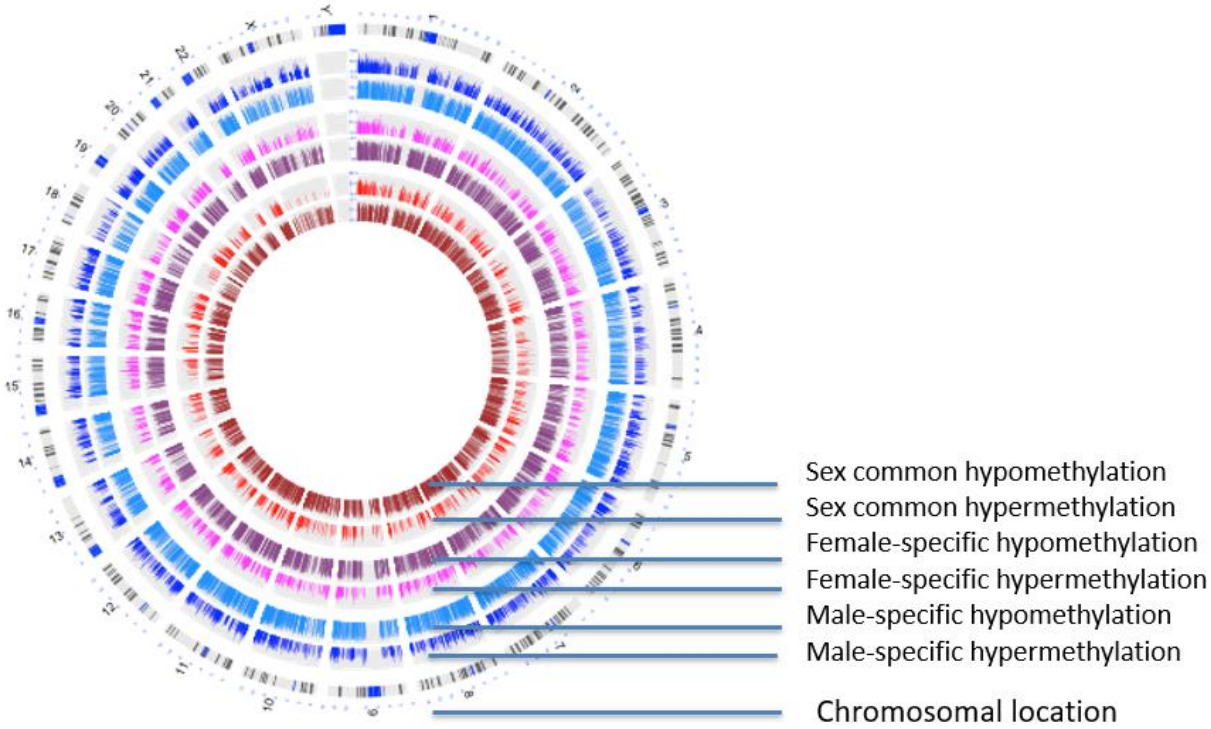

Figure 4.12. Circus plot of raft culture HDMCGs throughout the genome.

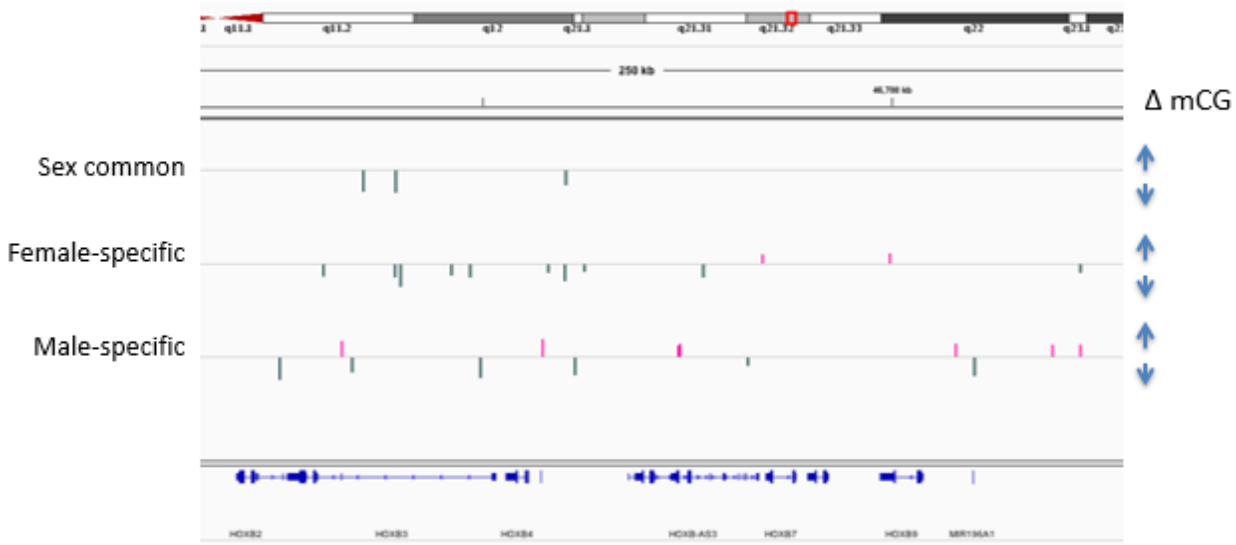

Figure 4.13. Example of sex-specific and sex-common HDMCGs.

When analyzing the distribution of HDMCGs in the context of genomic regions, the intronic regions were overrepresented while promoter regions were underrepresented. (Figure 4.14). Also, the distribution of HDMCGs in CpG islands (CGIs) were significantly underrepresented while those in CGI shores were overrepresented (Figure 4.15). These trends remained consistent in male-specific, female-specific, sex-combined HDMCGs, as well as in HDMCGs of each time point. Considering that the majority of human gene promoters contain CGIs, it is not surprising that underrepresentation HDMCGs in CGIs is concomitant with underrepresentation of HDMCGs in promoter regions. Similarly, concomitant overrepresentation of HDMCGs in intronic regions and CGI shores reflects the fact that many CGI shores overlap with gene bodies (Figure 1.9). What is interesting is that while promoters and CGIs contain approximately 45% of the targeted CpG sites that were analyzed (reflecting the fact that CGIs, by definition, are CpG-ense), only around 25-30% and 10-15% of HDMCGs were located in promoters and CGIs, respectively. This suggests that the virus is purposefully avoiding differential methylation of CGIs, but rather preferentially targets differential methylation of gene bodies as a way to modulate host gene expression. Since methylation and demethylation of gene promoters are one of the most studied and established epigenetic mechanisms, most previous studies of HNSCCs have focused on methylation patterns of gene promoters and overlooked methylation patterns in the gene body. Our study shows that the majority of HDMCGs occur in the gene body (exons and introns) as shown in Figure 4.14, and therefore, it is likely that modulation of host gene expression

via methylation changes in the gene body plays a significant role in facilitating HPV infection and progression of the viral life cycle.

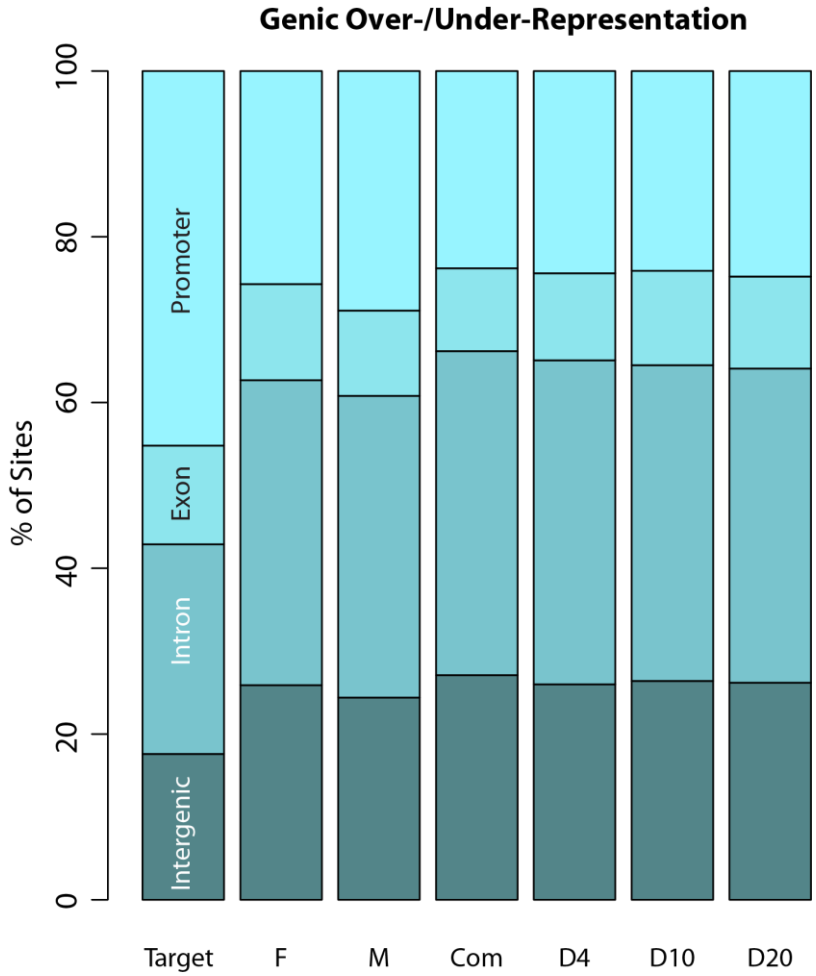

Figure 4.14. Distribution of HDMCGs in genomic regions. Target: all CpG sites targeted and analyzed in our data; F: female-specific HDMCGs common to all time points; M: male-specific HDMCGs common to all time points; Com: sex-combined HDMCGs common to all time points; D4: sex-common HDMCGs on D4; D10: sex-common HDMCGs on D10; D20: sex-common HDMCGs on D20.

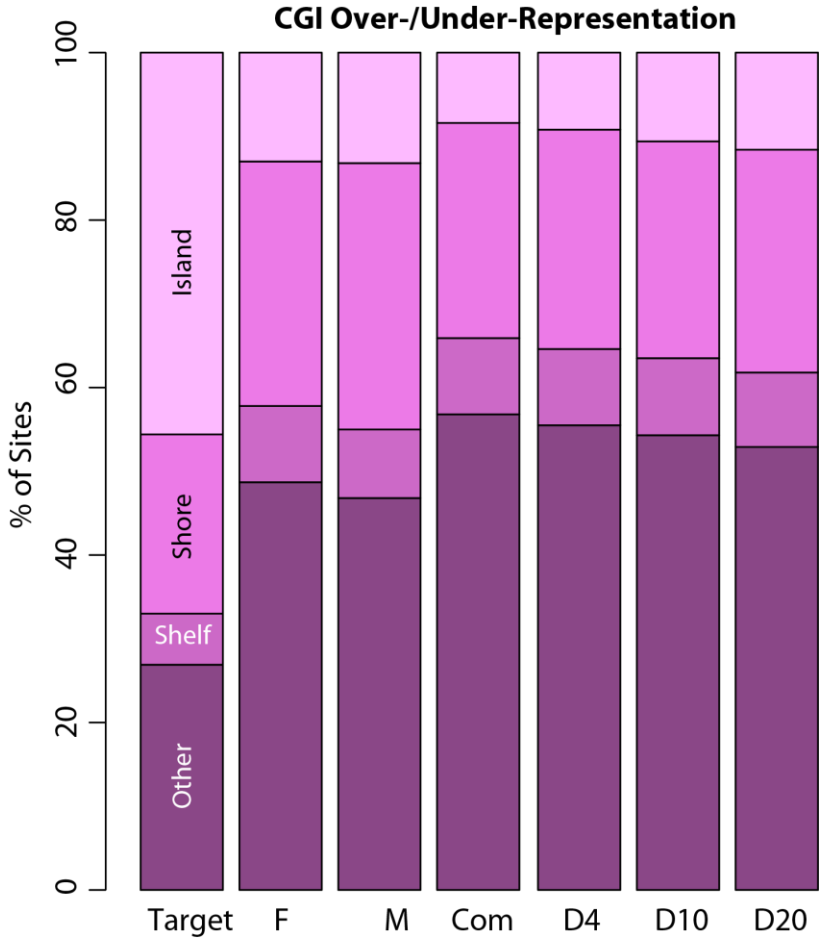

Figure 4.15. Distribution of HDMCGs in CpG islands, shores, shelves, and other regions. Target: all CpG sites targeted and analyzed in our data; F: female-specific HDMCGs common to all time points; M: male-specific HDMCGs common to all time points; Com: sex-combined HDMCGs common to all time points; D4: sex-common HDMCGs on D4; D10: sex-common HDMCGs on D10; D20: sex-common HDMCGs on D20.

Discussion

The overall higher levels of HDMCGs in males than in females in both monolayer and raft cultures (except in d20 raft tissue) suggests that HPV16 infection induces a greater disruption of the host methylome in males than in females. When considering this in the context of epidemiological studies that show higher rates of oral HPV infection and oropharyngeal cancers in males (92, 102), higher levels of HDMCGs in males could be interpreted as the virus being able to more efficiently alter the molecular environment of male hosts to its advantage in order to establish a successful infection.

The fact that female-specific HDMCGs consistently increase over the time course of d4, d10, d20 while male-specific HDMCGs significantly increase from d4 to d10, but dramatically decrease from d10 to d20 suggests that the levels and patterns of sex-specific HDMCGs are dependent on the tissue differentiation status or the HPV life-cycle. Since the raft tissue experience gradual differentiation over time, increasing female-specific HDMCGs over the time course may indicate that tissue differentiation could assist the virus exploit the host's molecular environment in females. In contrast, the dramatic drop in male-specific HDMCGs at d20 suggests that the virus is better at manipulating the host environment at earlier stages of raft culture when the tissue is less differentiated.

Since the HPV life-cycle is dependent on epidermal differentiation, these changes of sex-specific HDMCGs over time can also be interpreted in the context of the HPV life-cycle. The higher levels of male-specific HDMCGs at d4 and d10 suggests that the virus disrupts the host methylome to a greater degree in males during early stages of the viral life-cycle when genome replication and expression of all viral genes happen at maximal levels. Measuring and comparing the total number of viral genomes at d4 and d10 in males and females may help explain the effect of the different methylation patterns between the two sexes on viral replication. On the other hand, higher levels of female-specific HDMCGs at d20 suggests that the female methylome is disrupted to a greater degree in females during the late stages of the viral life-cycle as the viral particles are assembled and viral capsid maturation occurs. Therefore, it is possible that progeny virions from female tonsil tissue are less stable and less infectious than progeny virions from male tissue. In future experiments, we can test infectivity of progeny virions with HaCat cell infectivity assays, and progeny virion capsid stability with Optiprep density gradient centrifugation assays.

The effect of tissue differentiation and progression of the HPV life-cycle on HDMCG levels can also be seen in the significant increase in total HDMCGs in raft tissue when compared to monolayer cultures (Figures 4.4 and 4.8). In particular, the number of HDMCGs with opposite methylation patterns between the sexes is dramatically increased in raft tissue compared to monolayer cultures, suggesting that tissue differentiation and viral life-cycle progression amplify the sex-specific effects in HPV16 infection. Moreover, comparing HDMCGs over the time course of d4, d10, and 20 revealed that the majority of HDMCGs are specific to each time point, suggesting that the methylome goes through dynamic changes throughout tissue differentiation and viral life-cycle. Currently, it is unclear whether this increase in HDMCG level is solely attributed to tissue differentiation or progression of the HPV life-cycle, or whether it is an effect of both of them. PCA analysis of control and infected raft tissues showed that d4, d10, and d20 tissue of the same cell line cluster together, whether or not it is infected with HPV16. This indicates that the overall general methylation pattern does not change much throughout the different stages of tissue differentiation, which

suggests that HPV infection may have a greater effect on methylome changes than tissue differentiation. Analysis of the methylome at different stages of tissue differentiation without HPV infection could shed light onto how much tissue differentiation contributes to changes in the methylome.

The X chromosome is highly enriched in immune-related genes (106, 250). In our study, we observed greater levels of hypoHDMCGs than hyperHDMCGs on the X chromosome of females while there were greater levels of hyperHDMCGs than hypoHDMCGs on the X chromosome of males throughout the time course (Figure 4.8). Since epidemiological studies show higher rates of HPV infection and associated lesions in males than females, it can be suspected that the hypomethylation pattern of the X chromosome in females happen in promoter regions of immune response genes, which increase their expression and help clear the infection. In contrast, the hypermethylation pattern of the X chromosome in males may suppress the expression of immune response genes, subsequently resulting in immune evasion and successful HPV infection. Therefore, the sex bias that exists in oral HPV infection and oropharyngeal cancer incidence may be a result of a balancing act between the host's effort to epigenetically activate the immune response against the virus, and virus's effort to hijack the cellular methylation machinery to epigenetically suppress host immune response.

Our study shows the general pattern of HDMCGs in males and females throughout different time points. In future studies, the methylation patterns should be analyzed at the level of individual genes in order to identify specific pathways that are affected by DNA methylation. This will also help us understand whether the changes in the host methylome is caused by the host immune system trying to clear the virus, or by the virus trying to evade host immunity and manipulate host machinery for viral replication and progeny virion production. It is most likely that there is a certain degree of balance and interplay between these two forces. Moreover, the significant number of sex-specific HDMCGs in our data and the higher prevalence of oral infections and HNSCCs in males suggest that the landscape of balance and interplay between the two forces will look different in males and females.

CHAPTER 5: The effect of antiretroviral treatment on HPV infection

Experimental design

Epidemiological studies suggest association of ART with increased risk of HPV associated diseases including oral warts and anal cancer (121, 135, 143–147), while its association with cervical cancer is less clear (121, 148–150). So far, not much is known about the biology and mechanism through which ART drugs can affect HPV infection. Previous studies have focused on the effect of ART on non-infected primary cells of human gingival tissue (133, 134, 141, 142). Here, we study the effect of ART on HPV16 infected cells of various tissue types including tonsil, cervical, and anal tissue.

In this study, tonsillar, cervical, and anal human keratinocytes were electroporated with the HPV16 genome and passaged until they were persistently infected with HPV16. Each of these persistently infected cell lines are referred to as 16HTLK (tonsillar), 16HCK (cervical), and 16HAK (anal). These cell lines were used to create raft cultures and were treated with Amprenavir and Kaletra at three different concentrations (Cmax and two concentrations below Cmax) from d8 to d20 of culture, when the tissue were harvested for analysis (Figure 5.1). While Cmax represents the maximal drug concentration in the patient's serum, the two concentrations below Cmax were used since the actual concentration of the drug reaching each anatomical site is likely below the concentration in the blood. Our end-goal is to analyze the effect of ART drugs on the methylome of the three different types of tissue, but first, we examine the effect of ART on viral replication and progeny virion production.

Figure 5.1. ART drug study design.

The effect of Amprenavir and Kaletra on 16HTLK

The total number of viral genomes, which includes genomes that are both encapsidated and not encapsidated, and viral titer (as measured by the number of encapsidated genomes) were measured as shown in Figure 5.2. In 16HTLK raft tissue, the number of total genomes were significantly higher than the viral titers regardless of ART treatment and concentration, which reflects the numerous viral genomes in the tissue that have not yet been encapsidated (Figure 5.2).

Since the vehicle control (ethanol) group had significantly decreased viral titer compared to the no-treatment control, no further conclusions could be made from this data (Figure 5.3).

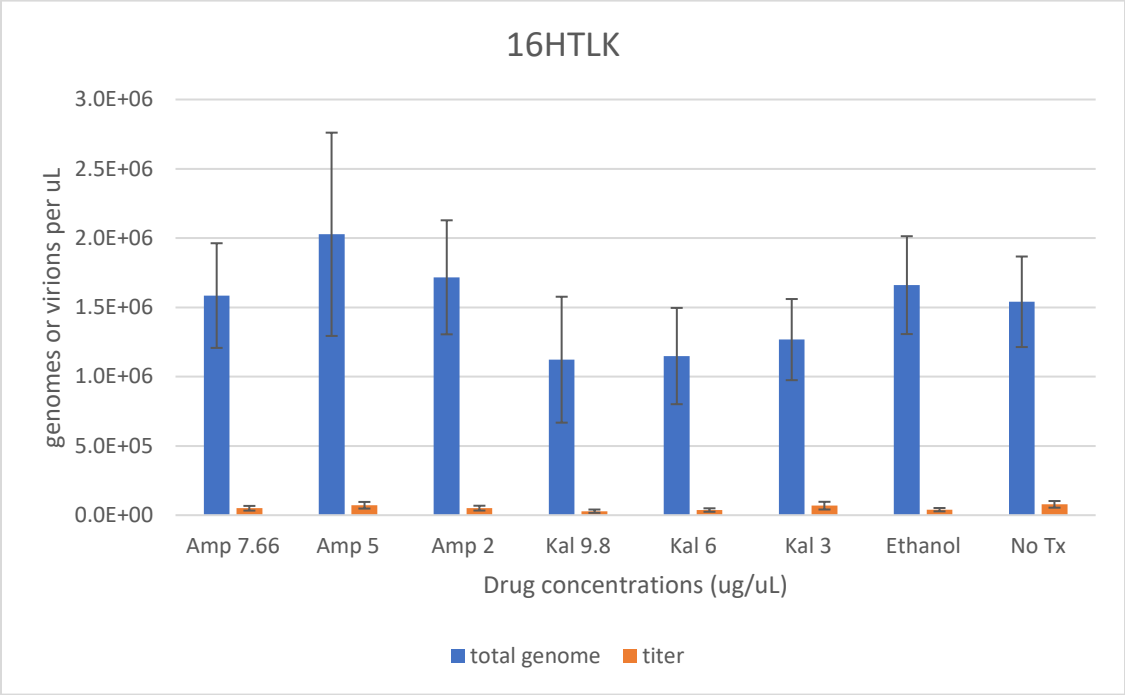

Figure 5. 2. Total genome and viral titer of 16HTLK raft tissue treated with Amprenavir or Kaletra (n=6).

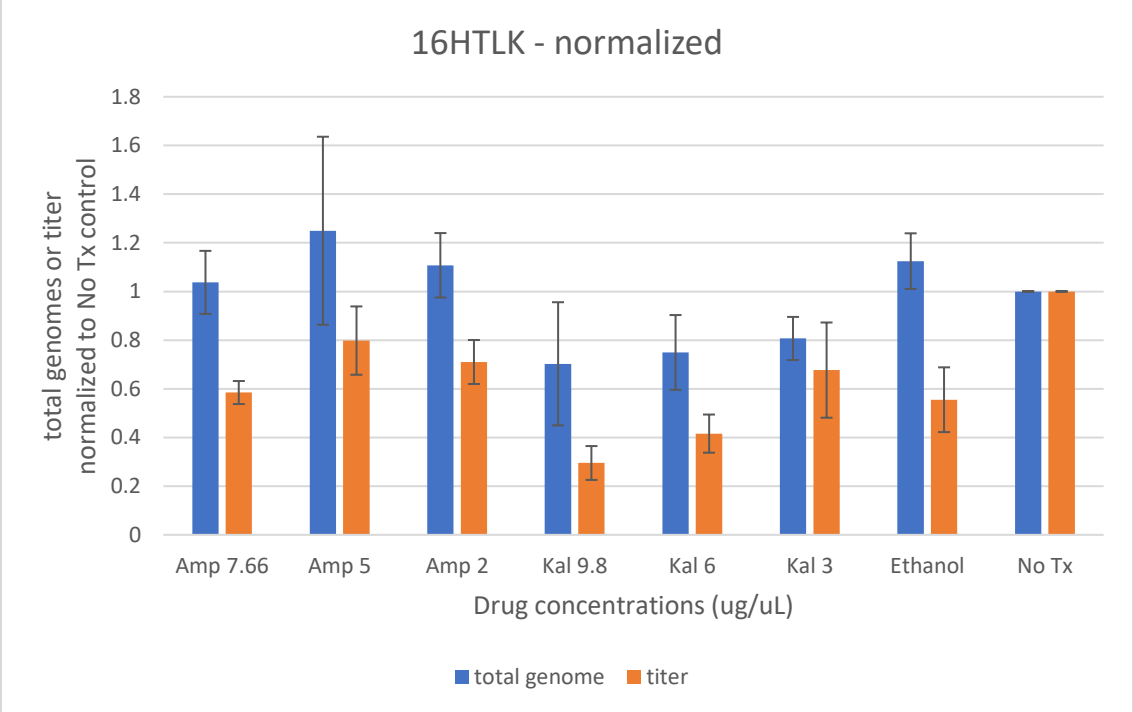

Figure 5. 3. Total genome and viral titer of 16HTLK raft tissue normalized to no treatment (No Tx) control (n=6).

The effect of Amprenavir and Kaletra on 16HCK

Similar to what was observed in 16HTLK raft tissue, the number of total genomes was significantly higher than the number of virions in 16HCK regardless of the concentration of Amprenavir and Kaletra (Figure 5.4). While treatment with Amprenavir decreased total viral genomes and virion production in general, both total genomes and viral titer increased with decreasing concentrations of Amprenavir treatment (Figure 5.5). A similar trend was observed with Kaletra treatment, but both total viral genomes and viral titer were reduced to a greater degree than when treated with Amprenavir.

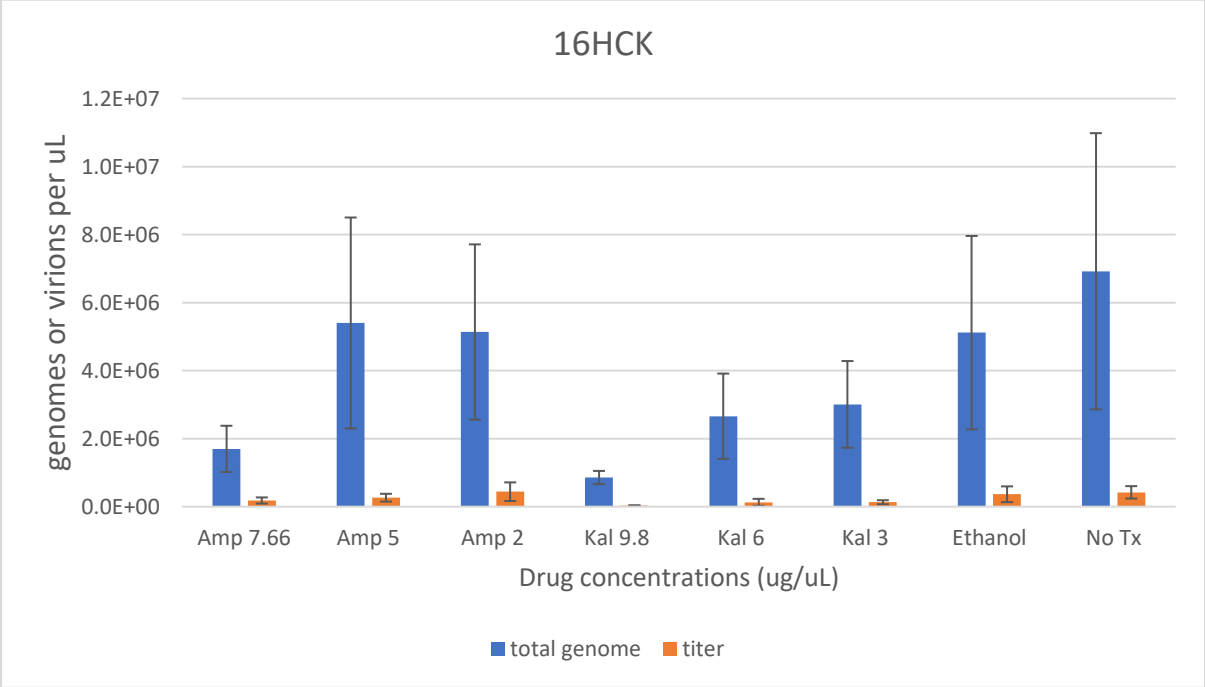

Figure 5. 4. Total genome and viral titer of 16HCK raft tissue treated with Amprenavir or Kaletra (n=3).

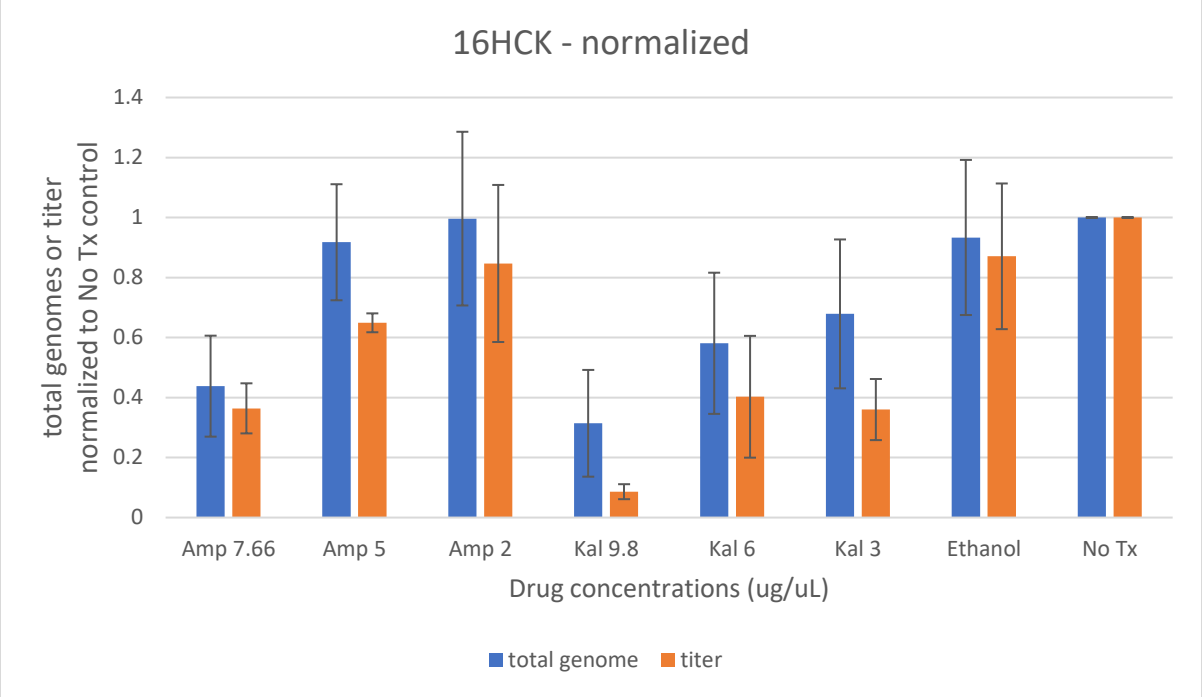

Figure 5. 5. Total genome and viral titer of 16HCK raft tissue normalized to no treatment (No Tx) control (n=3).

The effect of Amprenavir and Kaletra on 16HAK

Consistent with what was observed in 16HTLK and 16HCK, the number of total genomes was significantly higher than the number of virions in 16HAK regardless of the concentration of Amprenavir and Kaletra (Figure 5.6). Interestingly, treatment with Amprenavir had no significant effect on total viral genomes and viral titer, and did not show any trends of dose-dependence (Figure 5.7). Moreover, treatment with Kaletra at the two higher concentrations increased viral titers, but the great variability among the cell lines renders the significance of this finding unclear (Figure 5.7).

The normalized values of total viral genomes and viral titer was comparable to each other throughout most treatment groups, indicating that the drug treatments affected viral replication and viral assembly to a similar degree across the different drug concentrations. This contrasts what was observed in 16HCK tissue where normalized total genome was generally higher than normalized viral titer, suggesting that virus assembly was affected to a greater degree than viral replication.

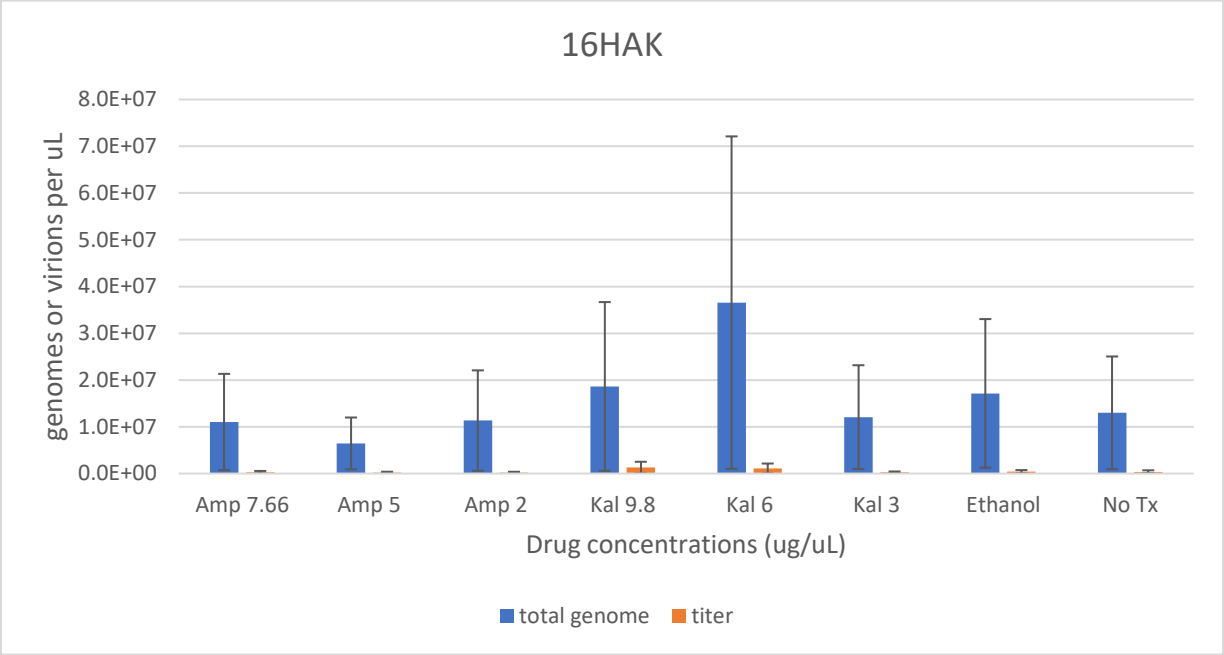

Figure 5. 6. Total genome and viral titer of 16HAK raft tissue treated with Amprenavir or Kaletra (n=3).

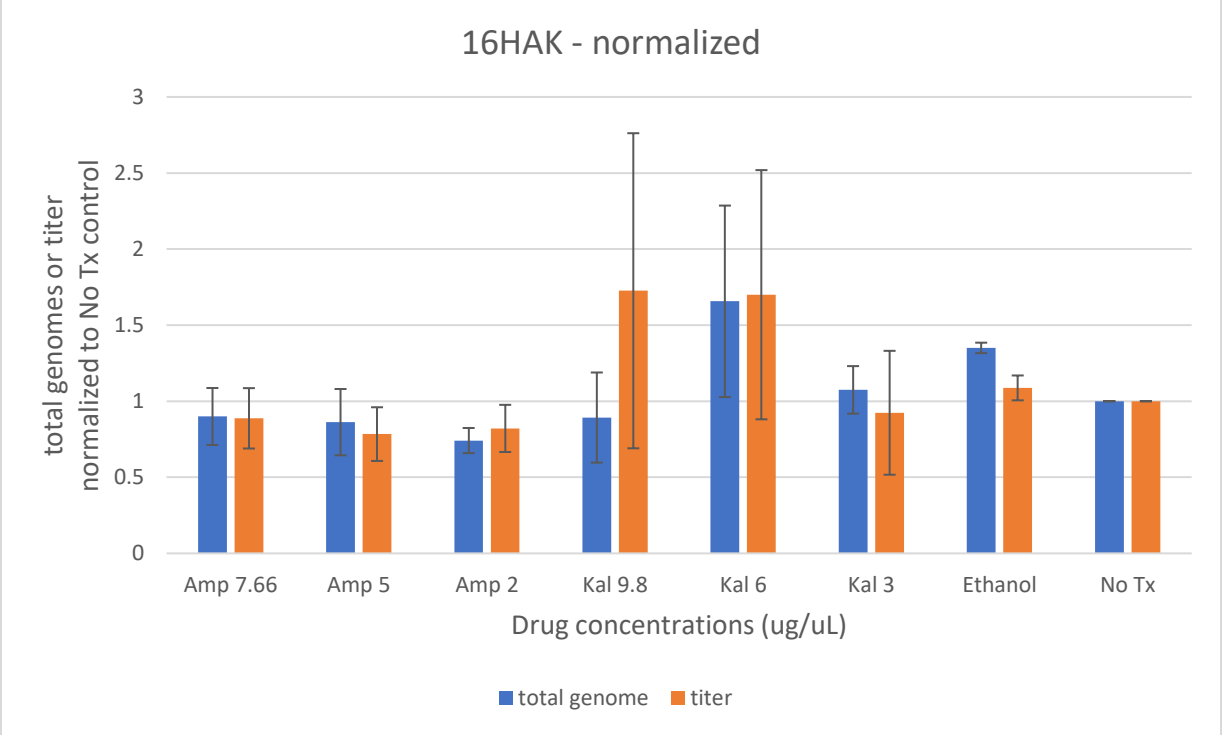

Figure 5. 7. Figure 5. 5. Total genome and viral titer of 16HAK raft tissue normalized to no treatment (No Tx) control (n=3).

Discussion

Epidemiological studies have reported that ART use increases the risk of developing HPV-associated lesions including oral warts and anal cancer (121, 135, 143–147). In vitro studies have also suggested that ART drugs can dysregulate oral tissue to make it more susceptible to HPV infection (133, 134, 141, 142). However, our study shows that treatment of HPV16 infected tissue with Amprenavir and Kaletra generally decreases the virion production in cervical tissue. This suggests that the increased risk of HPV-associated lesions with ART is due to its effect on initial infection, rather than its contribution to the progression of the HPV life-cycle after an infection is already established. Since the cell lines used for this study were already persistently infected with HPV16 before treatment with the drugs, it was not possible to test whether initial HPV infection was affected with treatment. In order to test whether ART affects initial infection in future studies, non-infected primary keratinocytes should be treated with ART drugs first before being infected with the virus.

In the 16HTLK experiment, it is interesting how the viral titer was significantly decreased with ethanol (vehicle control)—a trend that was not observed in 16HCK and 16HAK (Figure 5.3). This is particularly intriguing because alcohol consumption is associated with elevated risk of developing HPV-negative HNSCCs. The considerable decrease in 16HTLK viral titer with ethanol treatment may be explained by the inherent susceptibility of oral tissue to alcohol exposure. Ethanol may have had a significant effect on the molecular environment of the tonsil keratinocytes and subsequently affected the production of HPV virions in these cells. Since ethanol was used as a vehicle for drug delivery (the drugs were dissolved in ethanol before use), it is possible that the results from the 16HTLK experiment (Figure 5.3) is distorted. In order to avoid the possibly significant off-target effect of ethanol, a different vehicle for the drug should be considered in future studies.

In general, Amprenavir and Kaletra treatment decreased viral titer (Figures 5.5, and 5.7). Across the experiments in the different tissue types, the only experimental groups that showed noticeable increase in viral titer was the 16HAK tissue treated with the two higher concentrations of Kaletra (Figure 5.7). This result aligns with epidemiological studies that showed increased risk of anal cancer in patients taking protease inhibitor (PI)-based ART regimens (121, 145–147). No studies have yet established a correlation between ART and oropharyngeal cancer or cervical cancer. Therefore, previous

epidemiological studies and our results together suggest that ART's effect on promoting HPV infection and associated lesions may be specific to anal tissue.

In 16HCK raft tissue, the viral titer is affected to a greater degree than the number of total genomes (Figure 5.5). This suggests that the ART drugs interfere with viral assembly and maturation to a greater degree than they do viral genome replication. In order to further investigate the effect of Amprenavir and Kaletra on viral maturation, Optiprep density gradient centrifugation could be used to quantify the proportion of fully mature and stable viral capsids in each treatment group. Testing the infectivity of virions produced in each treatment group will also provide further insight on how ART drugs affect HPV production.

CHAPTER 6: Discussion

HPV infection is the world's most common sexually transmitted infection, and is responsible for approximately 5% of all cancers worldwide including virtually all cases of cervical cancer, and the majority of anal, vaginal, penile, and oropharyngeal cancers. For this reason, the biology of HPV infections and their progression to cancer has been studied extensively for decades. With the recent introduction of highly effective vaccines, most HPV infections have now become preventable. However, vaccination rates in many countries are below 50%, and vaccines cannot treat already infected individuals. Moreover, currently the only available treatment options are waiting for the infections to naturally resolve, or physically removing the infected tissue via surgical excision or ablation. Since infected tissues can be asymptomatic and cytologically normal at early stages of infection, identifying infected tissue is challenging unless the lesions have developed into the neoplastic stages, which can take years. Therefore, the extended period of the asymptomatic stages of infection and lack of antiviral treatments contributes to the persistent global burden of HPV-associated malignancies. Many questions remain unanswered in the biology of HPV infection. In our studies, we use genomics and epigenomics to reveal unknown pathways and mechanisms of HPV infection, which may ultimately lead to identification of novel therapeutic targets and development of the first antiviral treatment for HPV infection.

Genomics, and in particular, the study of global gene expression changes allows us to observe the overall change of expression profile and can help identify individual genes and biological pathways that are affected. In our study, we used microarray analysis to measure and analyze changes in the cervical transcriptome with HPV16 infection. While previous transcriptome studies have focused on the cancerous stages of HPV16 infection when progeny virion production is significantly decreased, we examined for the first time transcriptome changes occurring at early stages in tissue producing high levels of progeny virions. Through this analysis, we identified gene categories and biological pathways significantly affected by HPV16 infection. We also identified novel genes that have never been associated with HPV infection before, such as the late cornified envelope (LCE) genes. Most interestingly, we showed a set of genes that were significantly downregulated in our analysis, but were significantly upregulated in previous studies of HPV-associated cancers (Table 3.4), highlighting that early productive stages of HPV infection and cancerous stages of infection are distinct disease states with different molecular environments that need to be studied and treated within their own separate contexts. Future studies that examine the biology of this switch

between early productive stages and cancerous stages could help us understand the exact mechanisms of tumorigenesis caused by HPV, which could also help identify potential therapeutic targets. For example, while SERPINB4 was downregulated 48-fold in our model of productive infection, it is overexpressed in various types of cancer including cervical cancer, and has been widely studied as a cancer biomarker. Overexpression of SERPINB4 in our model of early productive infection and examining how this affects viral replication, assembly, and progeny production may help explain why the virus is downregulating this gene at early stages. On the other hand, using shRNA to inhibit the expression of SERPINB4 in cancer cell lines and observing how that affects the proliferative and invasive properties could elucidate why SERPINB4 is upregulated in cancerous stages and how it contributes to tumor progression and maintenance. Clinically, findings from these studies may have implications on when to use certain treatments at different stages of the disease. For example, a drug that increases the expression of SERPINB4 may be effective in treating early stages of infection, whereas the same drug may accelerate disease progression when used during the cancerous stages of infection. We can also model tumor progression with our organotypic raft culture system by continuously passaging the HPV infected cell lines and putting them up on raft culture every few passages. Using this model, we can observe the transition from downregulation to upregulation of SERPINB4, and by comparing it to the change in expression of viral proteins, proliferation markers, and differentiation markers, we could examine the changing molecular environment throughout the different stages of infection. Similarly, carrying out these studies with other genes that go through this switch from downregulated to upregulated expression pattern with disease progression (Table 3.4) will help elucidate which factors contribute to disease progression and tumorigenesis.

Our study also utilized epigenomics to study how methylome the host methylome is affected by HPV16 infection in tonsil keratinocytes. Again, our study is the first to examine the entire host methylome in HPV infection during early stages of infection when high levels of progeny virions are produced. In particular, we compared differential methylation with HPV16 infection throughout the genome at three time points that represent different stages of tissue differentiation and HPV life cycle. There is a strong sex-bias in oral HPV infection and incidence of HPV-associated oropharyngeal cancers, with the prevalence in males being significantly higher than that in females. Therefore, we grouped our analysis by sex in order to study the sex-specific effects of HPV infection on the methylome. Our results showed that the methylome experiences dynamic temporal changes throughout different stages of tissue differentiation and HPV life cycle. Moreover, a significant number of sex-specific changes were observed with HPV16 infection throughout the time course suggesting that epigenetic regulation of

gene expression may contribute to the sex differences in oral HPV infection and oropharyngeal cancer incidence. Interestingly, PCA analysis showed that the overall methylation patterns are similar among non-infected cell lines regardless of sex, and different states of tissue differentiation (Figure 4.10). In contrast, HPV infection caused a divergence in methylation patterns among different cell lines, suggesting that the virus adapts to each environment and manipulates the host's methylome in a manner that is specific and unique to each host. In future studies, we can express certain viral genes in primary cells and conduct PCA analysis to identify whether a single or a group of viral factors are responsible for this divergence in methylation pattern that occurs with infection. Similarly, we can study the effect of antiviral agents on the methylome of persistently infected cell lines to see whether this divergence can be reversed when certain viral pathways are inhibited. Moreover, conducting PCA analysis on the transcriptome data we have on HPV16 infection of tonsil tissue will reveal whether the divergence of individual cell lines brought out by HPV infection is also occurring in global gene expression patterns.

In the future, we would also like to analyze which specific genes and pathways were affected by differential methylation and cross-analyze the methylome data with transcriptome data to examine whether the methylome patterns are consistent with gene expression patterns. For example, in our microarray study of tonsil tissue, one of the top downregulated genes with HPV16 infection was SAA1 (serum amyloid A1). Analyzing the methylation pattern of SAA1 including the promoter region and gene body, and linking it back to the microarray data will allow us to determine whether the virus is downregulating this gene by changing the gene's methylation pattern. We can also study the effect of methylation and demethylation of specific CpG sites. While manipulation of DNA methylation was traditionally achieved with non-specific global methylation inhibitors, recent advancements in precision gene editing have led to the development of targeted methylation and demethylation of specific DNA sequences using the CRISPR machinery (251, 252). By reversing hyper- or hypo-methylated HDMCGs with targeted methylation or demethylation, and studying how this affects virus production, maturation, infectivity, and intracellular trafficking will help us understand how methylation pattern changes at specific sites or within specific genes affects the viral life-cycle. Conducting these analyses in sex-specific and sex-common genes and pathways will help us further understand the role of methylation changes in the sex bias of HPV infection.

Sex bias is not unique to oropharyngeal cancers amongst HPV-associated malignancies. As shown in Figure 1.1, sex bias also exists in anal cancer, except that in this case, cancer incidence is significantly higher in females than in males. Similar to oropharyngeal

cancers, not much is known on why this strong sex bias exists in anal cancer. Future studies of sex-specific methylome changes in anal tissue and comparing it to the tonsil tissue data will help elucidate mechanisms through which males and females respond differently to HPV infection.

Interestingly, differential methylation was underrepresented in promoter regions and overrepresented in intronic regions, indicating that the virus affects gene regulation more frequently through differential methylation in gene bodies rather than in promoter regions. These findings contrast previous studies that have mainly focused on the methylation status of promoter regions in HPV infection. Although it has been shown that methylation of the gene body correlates with increased gene expression (Figure 1.9), not much is known about the exact mechanism. Previous studies have reported that DNA methylation of gene bodies correlate with histone modification and enhancer activity (253, 254). Therefore, analyzing DNA looping and enhancer activity, histone modification, and chromosome structure will help us understand the effect of differential DNA methylation in HPV infection, and between males and females.

Our study of the effect of ART drugs on different types of HPV16 infected tissue suggested that different tissue types can respond differently to ART. In particular, progeny virion production increased only in anal keratinocytes, which is interesting because the only type of HPV-associated cancer that have been linked to ART is anal cancer. We hope to further examine the effect of ART on the different types of tissue by testing infectivity of progeny virions, and conducting methylome analysis.

The combination of organotypic raft cultures that produces high levels of progeny virions, and utilization of genomics and epigenomics tools have allowed us to pose and explore questions that have never been asked before. Our findings may help identify novel targets for antiviral therapy, and also help elucidate the molecular mechanisms that cause sex differences in HPV infection and associated cancers.

References

1. Dunne EF, Unger ER, Sternberg M, McQuillan G, Swan DC, Patel SS, Markowitz LE, H W, NV R, TA T, RL W, H T, LE M, JM W, FX B, AB M, EL F, LA K, LL V, PE G, PE G, CL P, SD V, BV S, E K, G C, F X, PE C, IG D, JA K, JW S, PE G, GS O, FR L, S B, KM S. 2007. Prevalence of HPV Infection Among Females in the United States. JAMA 297:813.
2. Sanjosé S, Díaz M, Castellsagué X, Clifford G, Bruni L. 2007. Worldwide prevalence and genotype distribution of cervical HPV in women with normal cytology. Lancet Infect Dis 7:453–459.
3. de Martel C, Plummer M, Vignat J, Franceschi S. 2017. Worldwide burden of cancer attributable to HPV by site, country and HPV type. Int J Cancer 141:664–670.
4. De Martel C, Ferlay J, Franceschi S, Vignat J, Bray F, Forman D, Plummer M. 2012. Global burden of cancers attributable to infections in 2008: A review and synthetic analysis. Lancet Oncol 13:607–615.
5. Bruni L, Diaz M, Barrionuevo-Rosas L, Herrero R, Bray F, Bosch FX, de Sanjosé S, Castellsagué X. 2016. Global estimates of human papillomavirus vaccination coverage by region and income level: a pooled analysis. Lancet Glob Heal 4:e453-63.
6. Rimer B, Harper H, Witte O. 2014. Accelerating HPV vaccine uptake: urgency for action to prevent cancer; a report to the President of the United States from the President's Cancer Panel. Bethesda, MD Natl Cancer Inst.
7. Douglas J. 2016. Papillomavirus, p. 2219–2223. *In* Goldman-Cecil Medicine, 25th ed. Elsevier.
8. Conway MJ, Alam S, Ryndock EJ, Cruz L, Christensen ND, Roden RBS, Meyers C. 2009. Tissue-spanning redox gradient-dependent assembly of native human papillomavirus type 16 virions. J Virol 83:10515–10526.
9. Scheffner M, Werness BA, Huibregtse JM, Levine AJ, Howley PM. 1990. The E6 oncoprotein encoded by human papillomavirus types 16 and 18 promotes the degradation of p53. Cell 63:1129–36.
10. Werness BA, Levine AJ, Howley PM. 1990. Association of human papillomavirus types 16 and 18 E6 proteins with p53. Science 248:76–9.
11. Dyson N, Howley PM, Münger K, Harlow E. 1989. The human papilloma virus-16 E7 oncoprotein is able to bind to the retinoblastoma gene product. Science 243:934–7.
12. Boyer SN, Wazer DE, Band V. 1996. E7 protein of human papilloma virus-16 induces degradation of retinoblastoma protein through the ubiquitin-proteasome pathway. Cancer Res 56:4620–4.
13. Gonzalez SL, Stremlau M, He X, Basile JR, Münger K. 2001. Degradation of the retinoblastoma tumor suppressor by the human papillomavirus type 16 E7

oncoprotein is important for functional inactivation and is separable from proteasomal degradation of E7. J Virol 75:7583–91.
14. Gu W, Putral L, Hengst K, Minto K, Saunders NA, Leggatt G, McMillan NAJ. 2006. Inhibition of cervical cancer cell growth in vitro and in vivo with lentiviral-vector delivered short hairpin RNA targeting human papillomavirus E6 and E7 oncogenes. Cancer Gene Ther 13:1023–32.
15. Hall AHS, Alexander KA. 2003. RNA interference of human papillomavirus type 18 E6 and E7 induces senescence in HeLa cells. J Virol 77:6066–9.
16. Lea JS, Sunaga N, Sato M, Kalahasti G, Miller DS, Minna JD, Muller CY. 2007. Silencing of HPV 18 Oncoproteins With RNA Interference Causes Growth Inhibition of Cervical Cancer Cells. Reprod Sci 14:20–28.
17. Pim D, Broniarczyk J, Bergant M, Playford MP, Banks L. 2015. A Novel PDZ Domain Interaction Mediates the Binding between Human Papillomavirus 16 L2 and Sorting Nexin 27 and Modulates Virion Trafficking. J Virol 89:10145–10155.
18. Popa A, Zhang W, Harrison MS, Goodner K, Kazakov T, Goodwin EC, Lipovsky A, Burd CG, DiMaio D. 2015. Direct Binding of Retromer to Human Papillomavirus Type 16 Minor Capsid Protein L2 Mediates Endosome Exit during Viral Infection. PLoS Pathog.
19. Bergant Mar S C M, Ozbun MA, Campos SK, Myers MP, Banks L, Bergant Marušič M, Ozbun MA, Campos SK, Myers MP, Banks L. 2012. Human Papillomavirus L2 Facilitates Viral Escape from Late Endosomes via Sorting Nexin 17. Traffic 13:455–467.
20. Stanley MA. 2012. Epithelial cell responses to infection with human papillomavirus. Clin Microbiol Rev 25:215–22.
21. Doorbar J, Quint W, Banks L, Bravo IG, Stoler M, Broker TR, Stanley MA. 2012. The Biology and Life-Cycle of Human Papillomaviruses. Vaccine 30:F55–F70.
22. Bosch FX, Burchell AN, Schiffman M, Giuliano AR, de Sanjose S, Bruni L, Tortolero-Luna G, Kjaer SK, Muñoz N. 2008. Epidemiology and Natural History of Human Papillomavirus Infections and Type-Specific Implications in Cervical Neoplasia. Vaccine.
23. S SMCPJJRAW. 2007. Human papillomavirus and cervical cancer. TT -. Lancet.
24. Baseman JG, Koutsky L thera A. 2005. The epidemiology of human papillomavirus infections. J Clin Virol.
25. Woodman C., Collins S., Young C., Young LS. 2007. The natural history of cervical HPV infection: unresolved issues - ProQuest. Nat Rev Cancer 7:11–22.
26. Flint P, Haughey B, Lund V, Niparko J, Robbins K, Regan Thomas J, Lesperance M. 2015. Human Papillomavirus, p. 1080. *In* Cummings Otolaryngology - Head and Neck Surgery, 6th ed. Elsevier.
27. McLaughlin-Drubin ME, Meyers C. 2005. Propagation of infectious, high-risk HPV in organotypic “raft” culture, p. 171–186. *In* Human Papillomaviruses. Humana Press, New Jersey.
28. Meyers C. 1996. Organotypic (raft) epithelial tissue culture system for the

differentiation-dependent replication of papillomavirus. Methods Cell Sci 18:201–210.
29. Meyers C, Frattini MG, Hudson JB, Laimins LA. 1992. Biosynthesis of human papillomavirus from a continuous cell line upon epithelial differentiation. Science 257:971–973.
30. Detmar M, Hirakawa S. 2018. Vascular Biology, p. 1775–1785. *In* Dermatology. Elsevier.
31. Andrei G, Duraffour S, Van den Oord J, Snoeck R. 2010. Epithelial raft cultures for investigations of virus growth, pathogenesis and efficacy of antiviral agents. Antiviral Res 85:431–449.
32. Gehris R. 2018. Dermatology, p. 275–340. *In* Zitelli and Davis' Atlas of Pediatric Physical Diagnosis. Elsevier.
33. Ferlay J, Shin HR, Bray F, Forman D, Mathers C, Parkin DM. 2010. Estimates of worldwide burden of cancer in 2008: GLOBOCAN 2008. Int J Cancer 127:2893–2917.
34. Cripe TP, Haugen TH, Turk JP, Tabatabai F, Schmid PG, Dürst M, Gissmann L, Roman A, Turek LP, Turek LP. 1987. Transcriptional regulation of the human papillomavirus-16 E6-E7 promoter by a keratinocyte-dependent enhancer, and by viral E2 trans-activator and repressor gene products: implications for cervical carcinogenesis. EMBO J 6:3745–53.
35. Sang B-C, Barbosa MS. 1992. Increased E6/E7 transcription in HPV 18-immortalized human keratinocytes results from inactivation of E2 and additional cellular events. Virology 189:448–455.
36. Wong YF, Cheung TH, Tsao GS, Lo KW, Yim SF, Wang VW, Heung MM, Chan SC, Chan LK, Ho TW, Wong KW, Li C, Guo Y, Chung TK, Smith DI. 2006. Genome-wide gene expression profiling of cervical cancer in Hong Kong women by oligonucleotide microarray. Int J Cancer 118:2461–2469.
37. Sopov I, Sorensen T, Magbagbeolu M, Jansen L, Beer K, Kuhne-Heid R, Kirchmayr R, Schneider A, D??rst M. 2004. Detection of cancer-related gene expression profiles in severe cervical neoplasia. Int J Cancer 112:33–43.
38. Gius D, Funk MC, Chuang EY, Feng S, Huettner PC, Nguyen L, Bradbury CM, Mishra M, Gao S, Buttin BM, Cohn DE, Powell MA, Horowitz NS, Whitcomb BP, Rader J. 2007. Profiling microdissected epithelium and stroma to model genomic signatures for cervical carcinogenesis accommodating for covariates. Cancer Res 67:7113–7123.
39. Rosty C, Sheffer M, Tsafrir D, Stransky N, Tsafrir I, Peter M, de Crémoux P, de La Rochefordière A, Salmon R, Dorval T, Thiery JP, Couturier J, Radvanyi F, Domany E, Sastre-Garau X. 2005. Identification of a proliferation gene cluster associated with HPV E6/E7 expression level and viral DNA load in invasive cervical carcinoma. Oncogene 24:7094–7104.
40. Pyeon D, Newton MA, Lambert PF, Den Boon JA, Sengupta S, Marsit CJ, Woodworth CD, Connor JP, Haugen TH, Smith EM, Kelsey KT, Turek LP, Ahlquist P.

2007. Fundamental differences in cell cycle deregulation in human papillomavirus-positive and human papillomavirus-negative head/neck and cervical cancers. Cancer Res 67:4605–4619.

41. Narayan G, Bourdon V, Chaganti S, Arias-Pulido H, Nandula S V, Rao PH, Gissmann L, Dürst M, Schneider A, Pothuri B, Mansukhani M, Basso K, Chaganti RSK, Murty V V. 2007. Gene dosage alterations revealed by cDNA microarray analysis in cervical cancer: identification of candidate amplified and overexpressed genes. Genes Chromosomes Cancer 46:373–84.
42. Chen Y, Miller C, Mosher R, Zhao X, Deeds J, Morrissey M, Bryant B, Yang D, Meyer R, Cronin F, Gostout BS, Smith-mccune K, Schlegel R. 2003. Identification of cervical cancer markers by cDNA and tissue microarrays. CANCER Res 63:1927–1935.
43. Zhai Y, Kuick R, Nan B, Ota I, Weiss SJ, Trimble CL, Fearon ER, Cho KR. 2007. Gene expression analysis of preinvasive and invasive cervical squamous cell carcinomas identifies HOXC10 as a key mediator of invasion. Cancer Res 67:10163–10172.
44. Fu Wong Y, Selvanayagam ZE, Wei N, Porter J, Vittal R, Hu R, Lin Y, Liao J, Weichung Shih J, Hong Cheung T, Wing Kit Lo K, Fan Yim S, Kai Yip S, Tse Ngong D, Siu N, Kit Ying Chan L, Sing Chan C, Kong T, Kutlina E, McKinnon RD, Denhardt DT, Chin K-V, Kwok Hung Chung T. 2003. Expression genomics of cervical cancer: molecular classification and prediction of radiotherapy response by DNA microarray. Clin Cancer Res 9:5486–92.
45. Wan F, Miao X, Quraishi I, Kennedy V, Creek KE, Pirisi L. 2008. Gene expression changes during HPV-mediated carcinogenesis: A comparison between an in vitro cell model and cervical cancer. Int J Cancer 123:32–40.
46. Klymenko T, Gu Q, Herbert I, Stevenson A, Iliev V, Watkins G, Pollock C, Bhatia R, Cuschieri K, Herzyk P, Gatherer D, Graham SV. 2017. RNASeq analysis of differentiated keratinocytes reveals a massive response to late events during human papillomavirus type 16 infection, including loss of epithelial barrier function. J Virol JVI.01001-17.
47. Arany I, Evans T, Tyring SK. 1998. Tissue specific HPV expression and downregulation of local immune responses in condylomas from HIV seropositive individuals. Sex Transm Infect 74:349–53.
48. Bedell MA, Hudson JB, Golub TR, Turyk ME, Hosken M, Wilbanks GD, Laimins LA. 1991. Amplification of human papillomavirus genomes in vitro is dependent on epithelial differentiation. J Virol 65:2254–60.
49. Garner-Hamrick PA, Fostel JM, Chien W-M, Banerjee NS, Chow LT, Broker TR, Fisher C. 2004. Global effects of human papillomavirus type 18 E6/E7 in an organotypic keratinocyte culture system. J Virol 78:9041–50.
50. Duffy CL, Phillips SL, Klingelhutz AJ. Microarray analysis identifies differentiation-associated genes regulated by human papillomavirus type 16 E6.
51. Parkin DM, Bray F, Ferlay J, Pisani P. 2005. Global Cancer Statistics, 2002. CA Cancer J Clin.

52. 2017. Head and Neck Cancers. Natl Cancer Inst.
53. Marur S, D'Souza G, Westra WH, Forastiere AA. 2010. HPV-associated head and neck cancer: a virus-related cancer epidemic. Lancet Oncol 11:781–9.
54. Klussmann JP, Weissenborn SJ, Wieland U, Dries V, Kolligs J, Jungehuelsing M, Eckel HE, Dienes HP, Pfister HJ, Fuchs PG. 2001. Prevalence, distribution, and viral load of human papillomavirus 16 DNA in tonsillar carcinomas. Cancer.
55. Chaturvedi AK, Engels EA, Anderson WF, Gillison ML, Hopkins J. Incidence Trends for Human Papillomavirus-Related and-Unrelated Oral Squamous Cell Carcinomas in the United States. J Clin Oncol 26:612–619.
56. Mehanna H, Beech T, Nicholson T, El-Hariry I, McConkey C, Paleri V, Roberts S. 2013. Prevalence of human papillomavirus in oropharyngeal and nonoropharyngeal head and neck cancer-systematic review and meta-analysis of trends by time and region. Head Neck 35:747–755.
57. Ang KK, Harris J, Wheeler R, Weber R, Rosenthal DI, Nguyen-Tân F, Westra WH, Chung CH, Jordan RC, Lu C, Kim H, Axelrod R, Silverman CC, Redmond KP, Gillison ML, Nguyen-Tân PF, Westra WH, Chung CH, Jordan RC, Lu C, Kim H, Axelrod R, Silverman CC, Redmond KP, Gillison ML. 2010. Human Papillomavirus and Survival of Patients with Oropharyngeal Cancer — NEJM. N Engl J Med.
58. Lindel K, Beer KT, Laissue J, Greiner RH, Aebersold DM. 2001. Human papillomavirus positive squamous cell carcinoma of the oropharynx. Cancer 92:805–813.
59. Butz K, Geisen C, Ullmann A, Spitkovsky D, Hoppe-Seyler F. 1996. Cellular responses of HPV-positive cancer cells to genotoxic anti-cancer agents: Repression ofE6/E7-oncogene expression and induction of apoptosis. Int J Cancer 68:506–513.
60. Bristow RG, Benchimol S, Hill RP. 1996. The p53 gene as a modifier of intrinsic radiosensitivity: implications for radiotherapy. Radiother Oncol 40:197–223.
61. Dahm-Daphi J. 2000. p53: Biology and Role for Cellular Radiosensitivity. Strahlentherapie und Onkol 176:278–285.
62. Lindquist D, Romanitan M, Hammarstedt L, Näsman A, Dahlstrand H, Lindholm J, Onelöv L, Ramqvist T, Ye W, Munck-Wikland E, Dalianis T. 2007. Human papillomavirus is a favourable prognostic factor in tonsillar cancer and its oncogenic role is supported by the expression of E6 and E7. Mol Oncol 1:350–355.
63. Gillison ML, Koch WM, Capone RB, Spafford M, Westra WH, Wu L, Zahurak ML, Daniel RW, Viglione M, Symer DE, Shah K V., Sidransky D. 2000. Evidence for a Causal Association Between Human Papillomavirus and a Subset of Head and Neck Cancers. J Natl Cancer Inst 92:709–720.
64. Liu Y, McKalip A, Herman B. 2000. Human papillomavirus type 16 E6 and HPV-16 E6/E7 sensitize human keratinocytes to apoptosis induced by chemotherapeutic agents: Roles of p53 and caspase activation. J Cell Biochem 78:334–349.
65. Liu Y, Xing H, Han X, Shi X, Liang F, Cheng G, Lu Y, Ma D. 2008. Apoptosis of HeLa

cells induced by cisplatin and its mechanism. J Huazhong Univ Sci Technol [Medical Sci 28:197–199.
66. 2018. Head and Neck Cancers. Centers Dis Control Prev.
67. Clark D. 2018. Epigenetics and Epigenomics, p. 691–710. *In* Molecular Biology, 3rd ed. Elsevier, London, UK.
68. Virani S, Colacino JA, Kim JH, Rozek LS. 2012. Cancer Epigenetics: A Brief Review. ILAR J 53:359–369.
69. Waters SA, Capraro A, Mcintyre KL, Graves JAM, Waters PD. 2018. The Methylome of Vertebrate Sex Chromosomes.
70. Duncan BK, Miller JH. 1980. Mutagenic deamination of cytosine residues in DNA. Nature.
71. Vu TH, Li T, Nguyen D, Nguyen BT, Yao XM, Hu JF, Hoffman AR. 2000. Symmetric and asymmetric DNA methylation in the human IGF2-H19 imprinted region. Genomics 64:132–43.
72. Jones PA, Laird PW. 1999. Cancer epigenetics comes of age. Nat Genet 21:163–7.
73. Cotton AM, Lam L, Affleck JG, Wilson IM, Peñaherrera MS, McFadden DE, Kobor MS, Lam WL, Robinson WP, Brown CJ. 2011. Chromosome-wide DNA methylation analysis predicts human tissue-specific X inactivation. Hum Genet 130:187–201.
74. Xiao F-H, He Y-H, Li Q-G, Wu H, Luo L-H, Kong Q-P. 2015. A genome-wide scan reveals important roles of DNA methylation in human longevity by regulating age-related disease genes. PLoS One 10:e0120388.
75. Edwards CA, Ferguson-Smith AC. 2007. Mechanisms regulating imprinted genes in clusters. Curr Opin Cell Biol 19:281–289.
76. Meehan R, Lewis J, Cross S, Nan X, Jeppesen P, Bird A. 1992. Transcriptional repression by methylation of CpG. J Cell Sci Suppl 16:9–14.
77. Lechner M, Fenton TR. 2016. The Genomics, Epigenomics, and Transcriptomics of HPV-Associated Oropharyngeal Cancer-Understanding the Basis of a Rapidly Evolving Disease.
78. Wilson AS, Power BE, Molloy PL. 2007. DNA hypomethylation and human diseases. Biochim Biophys Acta - Rev Cancer 1775:138–162.
79. Woodman CBJ, Collins SI, Young LS. 2007. The natural history of cervical HPV infection: unresolved issues. Nat Rev | CANCER 7.
80. Park I-S, Chang X, Loyo M, Wu G, Chuang A, Kim MS, Chae YK, Lyford-Pike S, Westra WH, Saunders JR, Sidransky D, Pai SI. 2011. Characterization of the methylation patterns in human papillomavirus type 16 viral DNA in head and neck cancers. Cancer Prev Res 4:207–217.
81. Thain A, Jenkins O, Clarke AR, Gaston K. 1996. CpG methylation directly inhibits binding of the human papillomavirus type 16 E2 protein to specific DNA sequences. J Virol.
82. Fernandez AF, Rosales C, Lopez-Nieva P, Graña O, Ballestar E, Ropero S, Espada J, Melo SA, Lujambio A, Fraga MF, Pino I, Javierre B, Carmona FJ, Acquadro F, Steenbergen RDM, Snijders PJF, Meijer CJ, Pineau P, Dejean A, Lloveras B, Capella

G, Quer J, Buti M, Esteban J-IL, Allende H, Rodriguez-Frias F, Castellsague X, Minarovits J, Ponce J, Capello D, Gaidano G, Cigudosa JC, Gomez-Lopez G, Pisano DG, Valencia A, Piris MA, Bosch FX, Cahir-McFarland E, Kieff E, Esteller M. 2009. The dynamic DNA methylomes of double-stranded DNA viruses associated with human cancer. Genome Res 19:438–451.

83. Santin AD, Zhan F, Bignotti E, Siegel ER, Cané S, Bellone S, Palmieri M, Anfossi S, Thomas M, Burnett A, Kay HH, Roman JJ, O 'brien TJ, Tian E, Cannon MJ, Shaughnessy J, Pecorelli S. 2005. Gene expression profiles of primary HPV16-and HPV18-infected early stage cervical cancers and normal cervical epithelium: identification of novel candidate molecular markers for cervical cancer diagnosis and therapy. Virology 331:269–291.
84. Laurson J, Khan S, Chung R, Cross K, Raj K. 2010. Epigenetic repression of E-cadherin by human papillomavirus 16 E7 protein. Carcinogenesis 31:918–926.
85. Burgers WA, Blanchon L, Pradhan S, Launoit Y de, Kouzarides T, Fuks F. 2007. Viral oncoproteins target the DNA methyltransferases. Oncogene 26:1650–1655.
86. Wilting S, Snijders P, Meijer G, Ylstra B, van den IJssel P, Snijders A, Albertson D, Coffa J, Schouten J, van de Wiel M, Meijer C, Steenbergen R. 2006. Increased gene copy numbers at chromosome 20q are frequent in both squamous cell carcinomas and adenocarcinomas of the cervix. J Pathol 209:220–230.
87. Kamio M, Yoshida T, Ogata H, Douchi T, Nagata Y, Inoue M, Hasegawa M, Yonemitsu Y, Yoshimura A. 2004. SOCS1 [corrected] inhibits HPV-E7-mediated transformation by inducing degradation of E7 protein. Oncogene 23:3107–15.
88. Sun S, Steinberg BM. 2002. PTEN is a negative regulator of STAT3 activation in human papillomavirus-infected cells. J Gen Virol 83:1651–8.
89. Paschos K, Allday MJ. 2010. Epigenetic reprogramming of host genes in viral and microbial pathogenesis. Trends Microbiol 18:439–447.
90. Lai H-C, Lin Y-W, Chang C-C, Wang H-C, Chu T-W, Yu M-H, Chu T-Y. 2007. Hypermethylation of two consecutive tumor suppressor genes, BLU and RASSF1A, located at 3p21.3 in cervical neoplasias. Gynecol Oncol 104:629–35.
91. Lechner M, Fenton T, West J, Wilson G, Feber A, Henderson S, Thirlwell C, Dibra HK, Jay A, Butcher L, Chakravarthy AR, Gratrix F, Patel N, Vaz F, O'Flynn P, Kalavrezos N, Teschendorff AE, Boshoff C, Beck S. 2013. Identification and functional validation of HPV-mediated hypermethylation in head and neck squamous cell carcinoma. Genome Med 5:15.
92. Chaturvedi AK, Graubard BI, Broutian T, Pickard RKL, Tong Z-Y, Xiao W, Kahle L, Gillison ML. 2015. NHANES 2009-2012 Findings: Association of Sexual Behaviors with Higher Prevalence of Oral Oncogenic Human Papillomavirus Infections in U.S. Men. Cancer Res 75:2468–77.
93. Souza GD', Wentz A, Kluz N, Zhang Y, Sugar E, Youngfellow RM, Guo Y, Xiao W, Gillison ML. 2016. Sex Differences in Risk Factors and Natural History of Oral Human Papillomavirus Infection. J Infect Dis ® 213:1893–1899.
94. Griesbeck M, Altfeld M. 2015. Sex differences in the manifestations of HIV-1

infectionSex and Gender Differences in Infection and Treatments for Infectious Diseases.
95. Neyrolles O, Quintana-Murci L. 2009. Sexual inequality in tuberculosis. PLoS Med 6:e1000199.
96. Klein SL. 2012. Sex influences immune responses to viruses, and efficacy of prophylaxis and treatments for viral diseases. BioEssays 34:1050–1059.
97. Boissier J, Chlichlia K, Digon Y, Ruppel A, Moné H. 2003. Preliminary study on sex-related inflammatory reactions in mice infected with Schistosoma mansoni. Parasitol Res 91:144–50.
98. Xia H-J, Zhang G-H, Wang R-R, Zheng Y-T. 2009. The influence of age and sex on the cell counts of peripheral blood leukocyte subpopulations in Chinese rhesus macaques. Cell Mol Immunol 6:433–40.
99. Melgert BN, Oriss TB, Qi Z, Dixon-McCarthy B, Geerlings M, Hylkema MN, Ray A. 2010. Macrophages: regulators of sex differences in asthma? Am J Respir Cell Mol Biol 42:595–603.
100. Klein SL, Jedlicka A, Pekosz A. 2010. The Xs and Y of immune responses to viral vaccines. Lancet Infect Dis 10:338–349.
101. Vom Steeg LG, Klein SL, Heitman J. 2016. SeXX Matters in Infectious Disease Pathogenesis Sex Versus Gender Differences Evidence of Male-Female Differences in Infectious Diseases.
102. Gillison ML, Chaturvedi AK, Anderson WF, Fakhry C. 2015. Epidemiology of Human Papillomavirus-Positive Head and Neck Squamous Cell Carcinoma. J Clin Oncol 33:3235–3242.
103. Smith EM, Ritchie JM, Summersgill KF, Klussmann JP, Lee JH, Wang D, Haugen TH, Turek LP. 2004. Age, sexual behavior and human papillomavirus infection in oral cavity and oropharyngeal cancers. Int J Cancer.
104. Gillison ML, D'Souza G, Westra W, Sugar E, Xiao W, Begum S, Viscidi R. 2008. Distinct risk factor profiles for human papillomavirus type 16-positive and human papillomavirus type 16-negative head and neck cancers. J Natl Cancer Inst.
105. Brooks YS, Ostano P, Jo S-H, Dai J, Getsios S, Dziunycz P, Hofbauer GFL, Cerveny K, Chiorino G, Lefort K, Dotto GP. 2014. Multifactorial ERβ and NOTCH1 control of squamous differentiation and cancer. J Clin Invest 124:2260–76.
106. Clocchiatti A, Cora E, Zhang Y, Dotto GP. 2016. Sexual dimorphism in cancer. Nat Rev Cancer 16:330–339.
107. Ouyang PY, Zhang LN, Lan XW, Xie C, Zhang WW, Wang QX, Su Z, Tang J, Xie FY. 2015. The significant survival advantage of female sex in nasopharyngeal carcinoma: A propensity-matched analysis. Br J Cancer.
108. Wisnivesky JP, Halm EA. 2007. Sex differences in lung cancer survival: Do tumors behave differently in elderly women? J Clin Oncol.
109. Tevfik Dorak M, Karpuzoglu E. 2012. Gender differences in cancer susceptibility: An inadequately addressed issue. Front Genet.
110. Lai J-J, Lai K-P, Zeng W, Chuang K-H, Altuwaijri S, Chang C. 2012. Androgen

receptor influences on body defense system via modulation of innate and adaptive immune systems: lessons from conditional AR knockout mice. Am J Pathol 181:1504–12.

111. Templeton AJ, McNamara MG, Šeruga B, Vera-Badillo FE, Aneja P, Ocaña A, Leibowitz-Amit R, Sonpavde G, Knox JJ, Tran B, Tannock IF, Amir E. 2014. Prognostic Role of Neutrophil-to-Lymphocyte Ratio in Solid Tumors: A Systematic Review and Meta-Analysis. JNCI J Natl Cancer Inst 106:dju124.
112. Yu C-P, Ho J-Y, Huang Y-T, Cha T-L, Sun G-H, Yu D-S, Chang F-W, Chen S-P, Hsu R-J. 2013. Estrogen inhibits renal cell carcinoma cell progression through estrogen receptor-β activation. PLoS One 8:e56667.
113. Passarelli MN, Phipps AI, Potter JD, Makar KW, Coghill AE, Wernli KJ, White E, Chan AT, Hutter CM, Peters U, Newcomb PA. 2013. Common single-nucleotide polymorphisms in the estrogen receptor β promoter are associated with colorectal cancer survival in postmenopausal women. Cancer Res 73:767–75.
114. Hartman J, Edvardsson K, Lindberg K, Zhao C, Williams C, Ström A, Gustafsson J-A. 2009. Tumor repressive functions of estrogen receptor beta in SW480 colon cancer cells. Cancer Res 69:6100–6.
115. Sareddy GR, Nair BC, Gonugunta VK, Zhang Q -g., Brenner A, Brann DW, Tekmal RR, Vadlamudi RK. 2012. Therapeutic Significance of Estrogen Receptor Agonists in Gliomas. Mol Cancer Ther 11:1174–1182.
116. Pinton G, Brunelli E, Murer B, Puntoni R, Puntoni M, Fennell DA, Gaudino G, Mutti L, Moro L. 2009. Estrogen receptor-beta affects the prognosis of human malignant mesothelioma. Cancer Res 69:4598–604.
117. Yakimchuk K, Iravani M, Hasni MS, Rhönnstad P, Nilsson S, Jondal M, Okret S. 2011. Effect of ligand-activated estrogen receptor β on lymphoma growth in vitro and in vivo. Leukemia 25:1103–10.
118. Langley CL, Benga-De E, Critchlow CW, Ndoye I, Mbengue-Ly MD, Kuypers J, Woto-Gaye G, Mboup S, Bergeron C, Holmes KK, Kiviat NB. 1996. HIV-1, HIV-2, human papillomavirus infection and cervical neoplasia in high-risk African women. AIDS 10:413–7.
119. Critchlow CW, Surawicz CM, Holmes KK, Kuypers J, Daling JR, Hawes SE, Goldbaum GM, Sayer J, Hurt C, Dunphy C. 1995. Prospective study of high grade anal squamous intraepithelial neoplasia in a cohort of homosexual men: influence of HIV infection, immunosuppression and human papillomavirus infection. AIDS 9:1255–62.
120. Brickman C, Palefsky JM. 2015. Human Papillomavirus in the HIV-Infected Host: Epidemiology and Pathogenesis in the Antiretroviral Era. Curr HIV/AIDS Rep 12:6–15.
121. Palefsky J. Human papillomavirus-related disease in people with HIV.
122. Chaturvedi AK, Madeleine MM, Biggar RJ, Engels EA. 2009. Risk of Human Papillomavirus–Associated Cancers Among Persons With AIDS. JNCI J Natl Cancer Inst 101:1120–1130.

123. Ceccarelli M, Venanzi Rullo E, Facciolà A, Madeddu G, Cacopardo B, Taibi R, Rita Pinzone M, Picerno I, di Rosa M, Visalli G, Condorelli F, Nunnari G, Francesco Pellicanò G. 2018. Head and neck squamous cell carcinoma and its correlation with human papillomavirus in people living with HIV: a systematic review.
124. Thorsteinsson K, Storgaard M, Katzenstein TL, Ladelund S, Rönsholt FF, Johansen IS, Pedersen G, Gaardsting A, Nielsen LN, Bonde J, Lebech A-M. 2018. Prevalence of cervical, oral, and anal human papillomavirus infection in women living with HIV in Denmark – The SHADE cohort study. J Clin Virol 105:64–71.
125. Kim RH, Yochim JM, Kang MK, Shin K-H, Christensen R, Park N-H. 2008. HIV-1 Tat enhances replicative potential of human oral keratinocytes harboring HPV-16 genome. Int J Oncol 33:777–82.
126. Barillari G, Palladino C, Bacigalupo I, Leone P, Falchi M, Ensoli B. 2016. Entrance of the Tat protein of HIV-1 into human uterine cervical carcinoma cells causes upregulation of HPV-E6 expression and a decrease in p53 protein levels. Oncol Lett 12:2389–2394.
127. Fletcher C. 2018. Overview of antiretroviral agents used to treat HIV. UpToDate.
128. Gulick RM. 2016. ANTIRETROVIRAL THERAPY OF HUMAN IMMUNODEFICIENCY VIRUS ANTIRETROVIRAL THERAPY OF HUMAN IMMUNODEFICIENCY VIRUS AND ACQUIRED IMMUNODEFICIENCY SYNDROME, p. 2287–2292. *In* Goldman-Cecil Medicine, 25th ed. Elsevier.
129. Borrás-Blasco J, Navarro-Ruiz A, Borrás C, Casterá E. 2008. Adverse cutaneous reactions associated with the newest antiretroviral drugs in patients with human immunodeficiency virus infection. J Antimicrob Chemother 62:879–88.
130. Lopinavir and ritonavir: Drug information. UpToDate.
131. AGENERASE.
132. Mittmann N, Knowles SR, Koo M, Shear NH, Rachlis A, Rourke SB. 2012. Incidence of toxic epidermal necrolysis and Stevens-Johnson syndrome in an HIV cohort: An observational, retrospective case series study. Am J Clin Dermatol 13:49–54.
133. Israr M, Mitchell D, Alam S, Dinello D, Kishel JJ, Meyers C. 2011. The HIV protease inhibitor lopinavir/ritonavir (Kaletra) alters the growth, differentiation and proliferation of primary gingival epithelium. HIV Med 12:145–156.
134. Israr M, Mitchell D, Alam S, Dinello D, Kishel JJ, Meyers C. 2010. Effect of the HIV protease inhibitor amprenavir on the growth and differentiation of primary gingival epithelium. Antivir Ther 15:253–265.
135. Greenspan D, Canchola AJ, MacPhail LA, Cheikh B, Greenspan JS. 2001. Effect of highly active antiretroviral therapy on frequency of oral warts. Lancet 357:1411–1412.
136. Scully C, Diz Dios P. 2001. Orofacial effects of antiretroviral therapies. Oral Dis 7:205–10.
137. Goodgame JC, Pottage JC, Jablonowski H, Hardy WD, Stein A, Fischl M, Morrow P, Feinberg J, Brothers CH, Vafidis I, Nacci P, Yeo J, Pedneault L. 2000. Amprenavir in combination with lamivudine and zidovudine versus lamivudine and zidovudine

alone in HIV-1-infected antiretroviral-naive adults. Amprenavir PROAB3001 International Study Team. Antivir Ther 5:215–25.

138. Rotunda A, Hirsch RJ, Scheinfeld N, Weinberg JM. 2003. Severe cutaneous reactions associated with the use of human immunodeficiency virus medications. Acta Derm Venereol 83:1–9.
139. Flint SR, Tappuni A, Leigh J, Schmidt-Westhausen A-M, MacPhail L. 2006. (B3) Markers of immunodeficiency and mechanisms of HAART therapy on oral lesions. Adv Dent Res 19:146–51.
140. Lee CA, Mistry D, Sharma R, Coatesworth AP. 2006. Rhinological, laryngological, oropharyngeal and other head and neck side effects of drugs. J Laryngol Otol 120:e6.
141. Mitchell D, Israr M, Alam S, Dinello D, Kishel J, Jia R, Meyers C. HIV nucleoside reverse transcriptase inhibitors efavirenz and tenofovir change the growth and differentiation of primary gingival epithelium.
142. Mitchell D, Israr M, Alam S, Kishel J, Dinello D, Associates OS, Meyers C. Effect of HIV nucleoside reverse transcriptase inhibitor, Zidovudine, on the growth and differentiation of primary gingival epithelium.
143. King MD, Reznik DA, O'Daniels CM, Larsen NM, Osterholt D, Blumberg HM. 2002. Human papillomavirus-associated oral warts among human immunodeficiency virus-seropositive patients in the era of highly active antiretroviral therapy: an emerging infection. Clin Infect Dis 34:641–8.
144. Cameron JE, Mercante D, O'Brien M, Gaffga AM, Leigh JE, Fidel PL, Hagensee ME. 2005. The impact of highly active antiretroviral therapy and immunodeficiency on human papillomavirus infection of the oral cavity of human immunodeficiency virus-seropositive adults. Sex Transm Dis 32:703–9.
145. Chao C, Leyden WA, Xu L, Horberg MA, Klein D, Towner WJ, Quesenberry CP, Abrams DI, Silverberg MJ. 2012. Exposure to antiretroviral therapy and risk of cancer in HIV-infected persons. AIDS 26:2223–2231.
146. Bruyand M, Ryom L, Shepherd L, Fatkenheuer G, Grulich A, Reiss P, de Wit S, d´Arminio Monforte A, Furrer H, Pradier C, Lundgren J, Sabin C, D:A:D study group. 2015. Cancer Risk and Use of Protease Inhibitor or Nonnucleoside Reverse Transcriptase Inhibitor–Based Combination Antiretroviral Therapy. JAIDS J Acquir Immune Defic Syndr 68:568–577.
147. Mbang PA, Kowalkowski MA, Amirian ES, Giordano TP, Richardson PA, Hartman CM, Chiao EY. 2015. Association between Time on Protease Inhibitors and the Incidence of Squamous Cell Carcinoma of the Anus among U.S. Male Veterans. PLoS One 10:e0142966.
148. Patel P, Hanson DL, Sullivan PS, Novak RM, Moorman AC, Tong TC, Holmberg SD, Brooks JT, Adult and Adolescent Spectrum of Disease Project and HIV Outpatient Study Investigators. 2008. Incidence of types of cancer among HIV-infected persons compared with the general population in the United States, 1992-2003. Ann Intern Med 148:728–36.

149. Biggar RJ, Chaturvedi AK, Goedert JJ, Engels EA, HIV/AIDS Cancer Match Study. 2007. AIDS-Related Cancer and Severity of Immunosuppression in Persons With AIDS. JNCI J Natl Cancer Inst 99:962–972.
150. Franceschi S, Lise M, Clifford GM, Rickenbach M, Levi F, Maspoli M, Bouchardy C, Dehler S, Jundt G, Ess S, Bordoni A, Konzelmann I, Frick H, Dal Maso L, Elzi L, Furrer H, Calmy A, Cavassini M, Ledergerber B, Keiser O, Swiss HIV Cohort Study. 2010. Changing patterns of cancer incidence in the early- and late-HAART periods: the Swiss HIV Cohort Study. Br J Cancer 103:416–22.
151. Borges ÁH. 2017. Combination antiretroviral therapy and cancer risk. Curr Opin HIV AIDS 12:12–19.
152. Bower M, Mazhar D, Stebbing J. 2006. Should Cervical Cancer Be an Acquired Immunodeficiency Syndrome–Defining Cancer? J Clin Oncol 24:2417–2419.
153. McLaughlin-Drubin ME, Wilson S, Mullikin B, Suzich J, Meyers C. 2003. Human papillomavirus type 45 propagation, infection, and neutralization. Virology 312:1–7.
154. Meyers C, Mayer TJ, Ozbun MA. 1997. Synthesis of infectious human papillomavirus type 18 in differentiating epithelium transfected with viral DNA. J Virol 71:7381–7386.
155. Ozbun MA, Meyers C. 1997. Characterization of late gene transcripts expressed during vegetative replication of human papillomavirus type 31b. J Virol 71:5161–72.
156. Eden E, Navon R, Steinfeld I, Lipson D, Yakhini Z. 2009. GOrilla: a tool for discovery and visualization of enriched GO terms in ranked gene lists. BMC Bioinformatics 10:48.
157. Supek F, Bošnjak M, Škunca N, Šmuc T. 2011. Revigo summarizes and visualizes long lists of gene ontology terms. PLoS One 6.
158. Szklarczyk D, Franceschini A, Wyder S, Forslund K, Heller D, Huerta-Cepas J, Simonovic M, Roth A, Santos A, Tsafou KP, Kuhn M, Bork P, Jensen LJ, Von Mering C. 2015. STRING v10: Protein-protein interaction networks, integrated over the tree of life. Nucleic Acids Res 43:D447–D452.
159. Biryukov J, Cruz L, Ryndock EJ, Meyers C. 2015. Native human papillomavirus production, quantification, and infectivity analysis, p. 317–331. *In* . Humana Press, New York, NY.
160. Meyers C, Alam S, Mane M, Hermonat PL. 2001. Altered biology of adeno-associated virus type 2 and human papillomavirus during dual infection of natural host tissue. Virology 287:30–39.
161. Peterson GL. 1977. A simplification of the protein assay method of Lowry et al. which is more generally applicable. Anal Biochem 83:346–356.
162. Hing B, Ramos E, Braun P, McKane M, Jancic D, Tamashiro KLK, Lee RS, Michaelson JJ, Druley TE, Potash JB. 2015. Adaptation of the targeted capture Methyl-Seq platform for the mouse genome identifies novel tissue-specific DNA methylation patterns of genes involved in neurodevelopment. Epigenetics

10:581–596.
163. Krueger F, Andrews SR. 2011. Bismark: a flexible aligner and methylation caller for Bisulfite-Seq applications. Bioinformatics 27:1571–1572.
164. Akalin A, Kormaksson M, Li S, Garrett-Bakelman FE, Figueroa ME, Melnick A, Mason CE. 2012. methylKit: a comprehensive R package for the analysis of genome-wide DNA methylation profiles. Genome Biol 13:R87.
165. Hochberg B. 1995. Controlling the False Discovery Rate: a Practical and Powerful Approach to Multiple Testing. J R Stat Soc.
166. Kang S Do, Chatterjee S, Alam S, Salzberg AC, Milici J, van der Burg SH, Meyers C. 2018. The Effect of Productive HPV16 Infection on Global Gene Expression of Cervical Epithelium. J Virol 92:JVI.01261-18.
167. Nees M, Geoghegan JM, Hyman T, Frank S, Miller L, Woodworth CD. 2001. Papillomavirus type 16 oncogenes downregulate expression of interferon-responsive genes and upregulate proliferation-associated and NF-kB-responsive genes in cervical keratinocytes. J Virol 75:4283–4296.
168. Lehoux M, Fradet-Turcotte A, Lussier-Price M, Omichinski JG, Archambault J. Inhibition of human papillomavirus DNA replication by an E1-derived p80/UAF1-binding peptide.
169. Huang TT, Nijman SMB, Mirchandani KD, Galardy PJ, Cohn MA, Haas W, Gygi SP, Ploegh HL, Bernards R, D'Andrea AD. 2006. Regulation of monoubiquitinated PCNA by DUB autocleavage. Nat Cell Biol 8:341–347.
170. Day T, Vaziri C. 2009. HPV E6 oncoprotein prevents recovery of stalled replication forks independently of p53 degradation. Cell Cycle.
171. Buitrago-Pérez A, Garaulet G, Vázquez-Carballo A, Paramio JM, García-Escudero R. 2009. Molecular signature of HPV-induced carcinogenesis: pRb, p53 and gene expression profiling. Curr Genomics 10:26–34.
172. Mendoza-Villanueva D, Diaz-Chavez J, Uribe-Figueroa L, Rangel-Escareão C, Hidalgo-Miranda A, March-Mifsut S, Jimenez-Sanchez G, Lambert P, Gariglio P. 2008. Gene expression profile of cervical and skin tissues from human papillomavirus type 16 E6 transgenic mice. BMC Cancer 8.
173. Vazquez-Ortiz G, Pina-Sanchez P, Vazquez K, Duenas A, Taja L, Mendoza P, Garcia JA, Salcedo M. 2005. Overexpression of cathepsin f, matrix metalloproteinases 11 and 12 in cervical cancer. BMC Cancer 5.
174. Yan L, Borregaard N, Kjeldsen L, Moses MA. 2001. The high molecular weight urinary matrix metalloproteinase (MMP) activity is a complex of gelatinase B/MMP-9 and neutrophil gelatinase-associated lipocalin (NGAL). Modulation of MMP-9 activity by NGAL. J Biol Chem 276:37258–65.
175. Yang J, Bielenberg DR, Rodig SJ, Doiron R, Clifton MC, Kung AL, Strong RK, Zurakowski D, Moses MA. 2009. Lipocalin 2 promotes breast cancer progression. Proc Natl Acad Sci U S A 106:3913–8.
176. Bauer M, Eickhoff JC, Gould MN, Mundhenke C, Maass N, Friedl A. 2008. Neutrophil gelatinase-associated lipocalin (NGAL) is a predictor of poor prognosis

in human primary breast cancer. Breast Cancer Res Treat 108:389–397.
177. Zhang H, Xu L, Xiao D, Xie J, Zeng H, Wang Z, Zhang X, Niu Y, Shen Z, Shen J, Wu X, Li E. 2007. Upregulation of neutrophil gelatinase-associated lipocalin in oesophageal squamous cell carcinoma: significant correlation with cell differentiation and tumour invasion. J Clin Pathol 60:555–61.
178. Friedl A, Stoesz SP, Buckley P, Gould MN. 1999. Neutrophil gelatinase-associated lipocalin in normal and neoplastic human tissues. Cell type-specific pattern of expression. Histochem J 31:433–441.
179. Santin AD, Zhan F, Bellone S, Palmieri M, Cane S, Bignotti E, Anfossi S, Gokden M, Dunn D, Roman JJ, O'Brien TJ, Tian E, Cannon MJ, Shaughnessy J, Pecorelli S. 2004. Gene expression profiles in primary ovarian serous papillary tumors and normal ovarian epithelium: Identification of candidate molecular markers for ovarian cancer diagnosis and therapy. Int J Cancer 112:14–25.
180. Hu L, Hittelman W, Lu T, Ji P, Arlinghaus R, Shmulevich I, Hamilton SR, Zhang W. 2009. NGAL decreases E-cadherin-mediated cell–cell adhesion and increases cell motility and invasion through Rac1 in colon carcinoma cells. Lab Investig 89:531–548.
181. Iannetti A, Pacifico F, Acquaviva R, Lavorgna A, Crescenzi E, Vascotto C, Tell G, Salzano AM, Scaloni A, Vuttariello E, Chiappetta G, Formisano S, Leonardi A. 2008. The neutrophil gelatinase-associated lipocalin (NGAL), a NF-kappaB-regulated gene, is a survival factor for thyroid neoplastic cells. Proc Natl Acad Sci U S A 105:14058–63.
182. Franceschini A, Lin J, Von Mering C, Jensen LJ. 2016. SVD-phy: Improved prediction of protein functional associations through singular value decomposition of phylogenetic profiles. Bioinformatics 32:1085–1087.
183. Kühne C, Banks L. 1998. E3-ubiquitin ligase/E6-AP links multicopy maintenance protein 7 to the ubiquitination pathway by a novel motif, the L2G box. J Biol Chem 273:34302–34309.
184. Das M, Prasad SB, Yadav SS, Govardhan HB, Pandey LK, Singh S, Pradhan S, Narayan G. 2013. Over expression of minichromosome maintenance genes is clinically correlated to cervical carcinogenesis. PLoS One 8.
185. Schneider H, Mule C, Pacho F. 2007. Biological function of laminin-5 and pathogenic impact of its deficiency. Eur J Cell Biol 86:701–717.
186. Amano S, Akutsu N, Ogura Y, Nishiyama T. 2004. Increase of laminin 5 synthesis in human keratinocytes by acute wound fluid, inflammatory cytokines and growth factors, and lysophospholipids. Br J Dermatol 151:961–970.
187. Radici L, Bianchi M, Crinelli R, Magnani M. 2013. Ubiquitin C gene: Structure, function, and transcriptional regulation. Adv Biosci Biotechnol 4:1057–1062.
188. Huh K-W, Demasi J, Ogawa H, Nakatani Y, Howley PM, Mü K. 2005. Association of the human papillomavirus type 16 E7 oncoprotein with the 600-kDa retinoblastoma protein-associated factor, p600.
189. White EA, Sowa ME, Tan MJA, Jeudy S, Hayes SD, Santha S, Münger K, Harper JW,

Howley PM. 2012. Systematic identification of interactions between host cell proteins and E7 oncoproteins from diverse human papillomaviruses. Proc Natl Acad Sci U S A 109:E260-7.

190. Karim R, Tummers B, Meyers C, Biryukov JL, Alam S, Backendorf C, Jha V, Offringa R, van Ommen GJB, Melief CJM, Guardavaccaro D, Boer JM, van der Burg SH. 2013. Human papillomavirus (HPV) upregulates the cellular deubiquitinase UCHL1 to suppress the keratinocyte's iunnate immune response. PLoS Pathog 9.
191. Karim R, Meyers C, Backendorf C, Ludigs K, Offringa R, van Ommen GJB, Melief CJM, van der Burg SH, Boer JM. 2011. Human papillomavirus deregulates the response of a cellular network comprising of chemotactic and proinflammatory genes. PLoS One 6.
192. Tummers B, Goedemans R, Pelascini LPL, Jordanova ES, van Esch EMG, Meyers C, Melief CJM, Boer JM, van der Burg SH. 2015. The interferon-related developmental regulator 1 is used by human papillomavirus to suppress NFκB activation. Nat Commun 6:6537.
193. Magnani M, Crinelli R, Bianchi M, Antonelli a. 2000. The ubiquitin-dependent proteolytic system and other potential targets for the modulation of nuclear factor-kB (NF-kB). Curr Drug Targets 1:387–99.
194. Ma W, Tummers B, van Esch EMG, Goedemans R, Melief CJM, Meyers C, Boer JM, van der Burg SH. 2016. Human papillomavirus downregulates the expression of IFITM1 and RIPK3 to escape from IFNγ- and TNFα-mediated antiproliferative effects and necroptosis. Front Immunol 7:496.
195. Eissa A, Amodeo V, Smith CR, Diamandis EP. 2011. Kallikrein-related peptidase-8 (KLK8) is an active serine protease in human epidermis and sweat and is involved in a skin barrier proteolytic cascade. J Biol Chem 286:687–706.
196. Huber M, Siegenthaler G, Mirancea N, Marenholz I, Nizetic D, Breitkreutz D, Mischke D, Hohl D. 2005. Isolation and characterization of human repetin, a member of the fused gene family of the epidermal differentiation complex. J Invest Dermatol 124:998–1007.
197. Liffers S-T, Maghnouj A, Munding JB, Jackstadt R, Herbrand U, Schulenborg T, Marcus K, Klein-Scory S, Schmiegel W, Schwarte-Waldhoff I, Meyer HE, Stühler K, Hahn SA. 2011. Keratin 23, a novel DPC4/Smad4 target gene which binds 14-3-3ε. BMC Cancer 11:137.
198. Mee JB, Cork MJ, Di Giovine FS, Duff GW, Groves RW. 2006. Interleukin-1: A key inflammatory mediator in psoriasis? Cytokine 33:72–78.
199. Ahmed ST, Darnell JE. 2009. Serpin B3/B4, activated by STAT3, promote survival of squamous carcinoma cells. Biochem Biophys Res Commun 378:821–5.
200. Iversen OJ, Lysvand H, Slupphaug G. 2017. Pso p27, a SERPINB3/B4-derived protein, is most likely a common autoantigen in chronic inflammatory diseases. Clin Immunol 174:10–17.
201. Duk JM, de Bruijn HW, Groenier KH, Hollema H, ten Hoor KA, Krans M, Aalders JG. 1990. Cancer of the uterine cervix: sensitivity and specificity of serum squamous

cell carcinoma antigen determinations. Gynecol Oncol 39:186–194.
202. Shimada H, Nabeya Y, Okazumi S, Matsubara H, Shiratori T, Gunji Y, Kobayashi S, Hayashi H, Ochiai T. 2003. Prediction of survival with squamous cell carcinoma antigen in patients with resectable esophageal squamous cell carcinoma. Surgery 133:486–94.
203. Takeshima N, Hirai Y, Katase K, Yano K, Yamauchi K, Hasumi K. 1998. The value of squamous cell carcinoma antigen as a predictor of nodal metastasis in cervical cancer. Gynecol Oncol 68:263–6.
204. Catanzaro JM, Sheshadri N, Pan J-AA, Sun Y, Shi C, Li J, Powers RS, Crawford HC, Zong W-XX. 2014. Oncogenic Ras induces inflammatory cytokine production by upregulating the squamous cell carcinoma antigens SerpinB3/B4. Nat Commun 5.
205. Kishi T, Grass L, Soosaipillai A, Scorilas A, Harbeck N, Schmalfeldt B, Dorn J, Mysliwiec M, Schmitt M, Diamandis EP. 2003. Human kallikrein 8, a novel biomarker for ovarian carcinoma. Cancer Res 63:2771–2774.
206. Borgoño CA, Kishi T, Scorilas A, Harbeck N, Dorn J, Schmalfeldt B, Schmitt M, Diamandis EP. 2006. Human kallikrein 8 protein is a favorable prognostic marker in ovarian cancer. Clin Cancer Res 12:1487–1493.
207. Pettus JR, Johnson JJ, Shi Z, Davis JW, Koblinski J, Ghosh S, Liu Y, Ravosa MJ, Frazier S, Stack MS. 2009. Multiple kallikrein (KLK 5, 7, 8, and 10) expression in squamous cell carcinoma of the oral cavity. Histol Histopathol 24:197–207.
208. Cane' S, Bignotti E, Bellone S, Palmieri M, De Las Casas L, Roman JJ, Pecorelli S, Cannon MJ, O'Brien T, Santin AD. 2004. The novel serine protease tumor-associated differentially expressed gene-14 (KLK8/Neuropsin/Ovasin) is highly overexpressed in cervical cancer. Am J Obstet Gynecol 190:60–66.
209. Ryu K-Y, Maehr R, Gilchrist CA, Long MA, Bouley DM, Mueller B, Ploegh HL, Kopito RR. 2007. The mouse polyubiquitin gene UbC is essential for fetal liver development, cell-cycle progression and stress tolerance. EMBO J 26:2693–2706.
210. Kalinin A, Marekov LN, Steinert PM. 2001. Assembly of the epidermal cornified cell envelope. J Cell Sci 114:3069–3070.
211. Brown DR, Bryan JT. Abnormalities of cornified cell envelopes isolated from human papillomavirus type 11-infected genital epithelium.
212. Lundstrom A, Egelrud T. 1991. Stratum corneum chymotryptic enzyme: A proteinase which may be generally present in the stratum corneum and with a possible involvement in desquamation. Acta Derm Venereol 71:471–474.
213. Egelrud T, Lundström A. 1991. A chymotrypsin-like proteinase that may be involved in desquamation in plantar stratum corneum. Arch Dermatol Res 283:108–112.
214. Egelrud T, Hofer PA, Lundström A. 1988. Proteolytic degradation of desmosomes in plantar stratum corneum leads to cell dissociation in vitro. Acta Derm Venereol 68:93–7.
215. Yamasaki K. 2006. Kallikrein-mediated proteolysis regulates the antimicrobial effects of cathelicidins in skin. FASEB J 20:2068–2080.

216. Petty RD, Kerr KM, Murray GI, Nicolson MC, Rooney PH, Bissett D, Collie-Duguid ESR. 2006. Tumor transcriptome reveals the predictive and prognostic impact of lysosomal protease inhibitors in non-small-cell lung cancer. J Clin Oncol 24:1729–1744.
217. Catanzaro JM, Guerriero JL, Liu J, Ullman E, Sheshadri N, Chen JJ, Zong W-XX. 2011. Elevated expression of squamous cell carcinoma antigen (SCCA) is associated with human breast carcinoma. PLoS One 6:e19096.
218. Pontisso P, Calabrese F, Benvegnù L, Lise M, Belluco C, Ruvoletto MG, Marino M, Valente M, Nitti D, Gatta A, Fassina G, Fassina G, De Falco S, Marino M, Valente M, Nitti D, Gatta A, Fassina G. 2004. Overexpression of squamous cell carcinoma antigen variants in hepatocellular carcinoma. Br J Cancer 90:833–7.
219. de Koning PJA, Kummer JA, de Poot SAH, Quadir R, Broekhuizen R, McGettrick AF, Higgins WJ, Devreese B, Worrall DM, Bovenschen N. 2011. Intracellular serine protease inhibitor SERPINB4 inhibits granzyme M-induced cell death. PLoS One 6:e22645.
220. Sun Y, Sheshadri N, Zong W-XX. 2016. SERPINB3 and B4: From biochemistry to biology. Semin Cell Dev Biol.
221. Mitsuishi K, Nakamura T, Sakata Y, Yuyama N, Arima K, Sugita Y, Suto H, Izuhara K, Ogawa H. 2005. The squamous cell carcinoma antigens as relevant biomarkers of atopic dermatitis. Clin Exp Allergy 35:1327–1333.
222. Takeda A, Higuchi D, Takahashi T, Ogo M, Baciu P, Goetinck PF, Hibino T. 2002. Overexpression of serpin squamous cell carcinoma antigens in psoriatic skin. J Invest Dermatol 118:147–154.
223. Kuwae K, Matsumoto-Miyai K, Yoshida S, Sadayama T, Yoshikawa K, Hosokawa K, Shiosaka S. 2002. Epidermal expression of serine protease, neuropsin (KLK8) in normal and pathological skin samples. J Clin Pathol Mol Pathol 55:235–241.
224. Calabrese F, Lunardi F, Balestro E, Marulli G, Perissinotto E, Loy M, Nannini N, Valente M, Saetta M, Agostini C, Rea F. 2012. Serpin B4 isoform overexpression is associated with aberrant epithelial proliferation and lung cancer in idiopathic pulmonary fibrosis. Pathology 44:192–198.
225. Shinoda Y, Kozaki K, Imoto I, Obara W, Tsuda H, Mizutani Y, Shuin T, Fujioka T, Miki T, Inazawa J. 2007. Association of KLK5 overexpression with invasiveness of urinary bladder carcinoma cells. Cancer Sci 98:1078–1086.
226. Yousef GM, Polymeris ME, Yacoub GM, Scorilas A, Soosaipillai A, Popalis C, Fracchioli S, Katsaros D, Diamandis EP. 2003. Parallel overexpression of seven kallikrein genes in ovarian cancer. Cancer Res 63:2223–2227.
227. Planque C, de Monte M, Guyetant S, Rollin J, Desmazes C, Panel V, Lemarié E, Courty Y. 2005. KLK5 and KLK7, two members of the human tissue kallikrein family, are differentially expressed in lung cancer. Biochem Biophys Res Commun 329:1260–1266.
228. Yousef GM, Scorilas A, Kyriakopoulou LG, Rendl L, Diamandis M, Ponzone R, Biglia N, Giai M, Roagna R, Sismondi P, Diamandis EP. 2002. Human kallikrein gene 5

(KLK5) expression by quantitative PCR: An independent indicator of poor prognosis in breast cancer. Clin Chem 48:1241–1250.

229. Ogawa K, Utsunomiya T, Mimori K, Tanaka F, Inoue H, Nagahara H, Murayama S, Mori M. 2005. Clinical significance of human kallikrein gene 6 messenger RNA expression in colorectal cancer. Clin Cancer Res 11:2889–93.
230. Marimuthu A, Chavan S, Sathe G, Sahasrabuddhe NA, Srikanth SM, Renuse S, Ahmad S, Radhakrishnan A, Barbhuiya MA, Kumar R V., Harsha HC, Sidransky D, Califano J, Pandey A, Chatterjee A. 2013. Identification of head and neck squamous cell carcinoma biomarker candidates through proteomic analysis of cancer cell secretome. Biochim Biophys Acta - Proteins Proteomics 1834:2308–2316.
231. Yousef GM, Borgoño CA, Popalis C, Yacoub GM, Polymeris M-E, Soosaipillai A, Diamandis EP. 2004. In-silico analysis of kallikrein gene expression in pancreatic and colon cancers. Anticancer Res 24:43–51.
232. Darling MR, Tsai S, Jackson-Boeters L, Daley TD, Diamandis EP. 2008. Human kallikrein 8 expression in salivary gland tumors. Head Neck Pathol 2:169–174.
233. Planque C, Li L, Zheng Y, Soosaipillai A, Reckamp K, Chia D, Diamandis EP, Goodglick L. 2008. A multiparametric serum kallikrein panel for diagnosis of non-small cell lung carcinoma. Clin Cancer Res 14:1355–62.
234. White NMA, Mathews M, Yousef GM, Prizada A, Fontaine D, Ghatage P, Popadiuk C, Dawson L, Doré JJE. 2009. Human kallikrein related peptidases 6 and 13 in combination with CA125 is a more sensitive test for ovarian cancer than CA125 alone. Cancer Biomarkers 5:279–287.
235. Wu Z-S, Wu Q, Yang J-H, Wang H-Q, Ding X-D, Yang F, Xu X-C. 2008. Prognostic significance of MMP-9 and TIMP-1 serum and tissue expression in breast cancer. Int J Cancer 122:2050–2056.
236. Riedel F, Götte K, Schwalb J, Hörmann K. 2000. Serum levels of matrix metalloproteinase-2 and -9 in patients with head and neck squamous cell carcinoma. Anticancer Res 20:3045–9.
237. Morgia G, Falsaperla M, Malaponte G, Madonia M, Indelicato M, Travali S, Mazzarino MC. 2005. Matrix metalloproteinases as diagnostic (MMP-13) and prognostic (MMP-2, MMP-9) markers of prostate cancer. Urol Res 33:44–50.
238. Yen C-Y, Chen C-H, Chang C-H, Tseng H-F, Liu S-Y, Chuang L-Y, Wen C-H, Chang H-W. 2009. Matrix metalloproteinases (MMP) 1 and MMP10 but not MMP12 are potential oral cancer markers. Biomarkers 14:244–249.
239. Deraz EM, Kudo Y, Yoshida M, Obayashi M, Tsunematsu T, Tani H, Siriwardena SBSM, Kiekhaee MR, Qi G, Iizuka S, Ogawa I, Campisi G, Muzio L Lo, Abiko Y, Kikuchi A, Takata T. 2011. MMP-10/stromelysin-2 promotes invasion of head and neck cancer. PLoS One 6:e25438.
240. Mathew R, Khanna R, Kumar R, Mathur M, Shukla NK, Ralhan R. 2002. Stromelysin-2 overexpression in human esophageal squamous cell carcinoma: potential clinical implications. Cancer Detect Prev 26:222–228.

241. Rochefort H, Cavailles V, Augereau P, Capony F, Maudelonde T, Touitou I, Garcia M. 1989. Overexpression and hormonal regulation of pro-cathepsin D in mammary and endometrial cancer. J Steroid Biochem 34:177–182.
242. Athanassiadou P, Sakellariou V, Petrakakou E, Athanassiades P, Zerva C, Liossi A, Michalas S. 1998. Cathepsin D immunoreactivity in ovarian cancer: Correlation with prognostic factors. Pathol Oncol Res 4:103–107.
243. Santamaría I, Velasco G, Cazorla M, Fueyo A, Campo E, López-Otín C. 1998. Cathepsin L2, a novel human cysteine proteinase produced by breast and colorectal carcinomas. Cancer Res 58:1624–30.
244. Ozbun MA, Meyers C. 1998. Human papillomavirus type 31b E1 and E2 transcript expression correlates with vegetative viral genome amplification. Virology.
245. Ozbun MA, Meyers C. 1998. Temporal usage of multiple promoters during the life cycle of human papillomavirus type 31b. J Virol.
246. Ozbun M a, Meyers C. 1999. Two novel promoters in the upstream regulatory region of human papillomavirus type 31b are negatively regulated by epithelial differentiation. J Virol.
247. Conway MJ, Alam S, Christensen ND, Meyers C. 2009. Overlapping and independent structural roles for human papillomavirus type 16 L2 conserved cysteines. Virology.
248. Conway MJ, Cruz L, Alam S, Christensen ND, Meyers C. 2011. Differentiation-dependent interpentameric disulfide bond stabilizes native human papillomavirus type 16. PLoS One.
249. Conway MJ, Cruz L, Alam S, Christensen ND, Meyers C. 2011. Cross-neutralization potential of native human papillomavirus N-terminal L2 epitopes. PLoS One.
250. Fish EN. 2008. The X-files in immunity: Sex-based differences predispose immune responses. Nat Rev Immunol.
251. Vojta A, Dobrinić P, Tadić V, Bočkor L, Korać P, Julg B, Klasić M, Zoldoš V. 2016. Repurposing the CRISPR-Cas9 system for targeted DNA methylation. Nucleic Acids Res 44:5615–5628.
252. Xu X, Tao Y, Gao X, Zhang L, Li X, Zou W, Ruan K, Wang F, Xu GL, Hu R. 2016. A CRISPR-based approach for targeted DNA demethylation. Cell Discov.
253. Schmidl C, Klug M, Boeld TJ, Andreesen R, Hoffmann P, Edinger M, Rehli M. 2009. Lineage-specific DNA methylation in T cells correlates with histone methylation and enhancer activity. Genome Res 19:1165–74.
254. Ikegami K, Ohgane J, Tanaka S, Yagi S, Shiota K. 2009. Interplay between DNA methylation, histone modification and chromatin remodeling in stem cells and during development. Int J Dev Biol 53:203–214.

VITA

Sa Do "John" Kang
Telephone: 919-699-9747
Email: sadokang88@gmail.com

EDUCATION

M.D. candidate
The Pennsylvania State University College of Medicine — Expected 2021

Ph.D. in Biomedical Sciences
The Pennsylvania State University, Pennsylvania — 2019

B.E. in Biomedical Engineering
Duke University — 2012

PUBLICATIONS

1. **Kang Sa Do**, Chatterjee S, Alam S, Salzberg AC, Milici J, van der Burg SH, Meyers C. 2018. The Effect of Productive HPV16 Infection on Global Gene Expression of Cervical Epithelium. J Virol 92:JVI.01261-18.

2. Jamiolkowski RM, **Kang Sa Do**, Rodriguez AK, Haseltine JM, Galinat LJ, Jantzen AE, Carlon TA, Darrabie MD, Arciniegas AJ, Mantilla JG, Haley NR, Noviani M, Allen JD, Stabler T V, Frederiksen JW, Alzate O, Keil LG, Liu S, Lin F-H, Truskey GA, Achneck HE. 2015. Increased yield of endothelial cells from peripheral blood for cell therapies and tissue engineering. Regen Med 10:447–460.

3. **Kang Sa Do**, Carlon T a, Jantzen AE, Lin F-H, Ley MM, Allen JD, Stabler T V, Haley NR, Truskey G a, Achneck HE. 2013. Isolation of functional human endothelial cells from small volumes of umbilical cord blood. Ann Biomed Eng 41:2181–2192.